Ricerca di Settori Oscuri e di Fotoni Oscuri che decadono in jet leptonici con l'esperimento ATLAS

Bernardo Ricci

IFAE 2024, Firenze

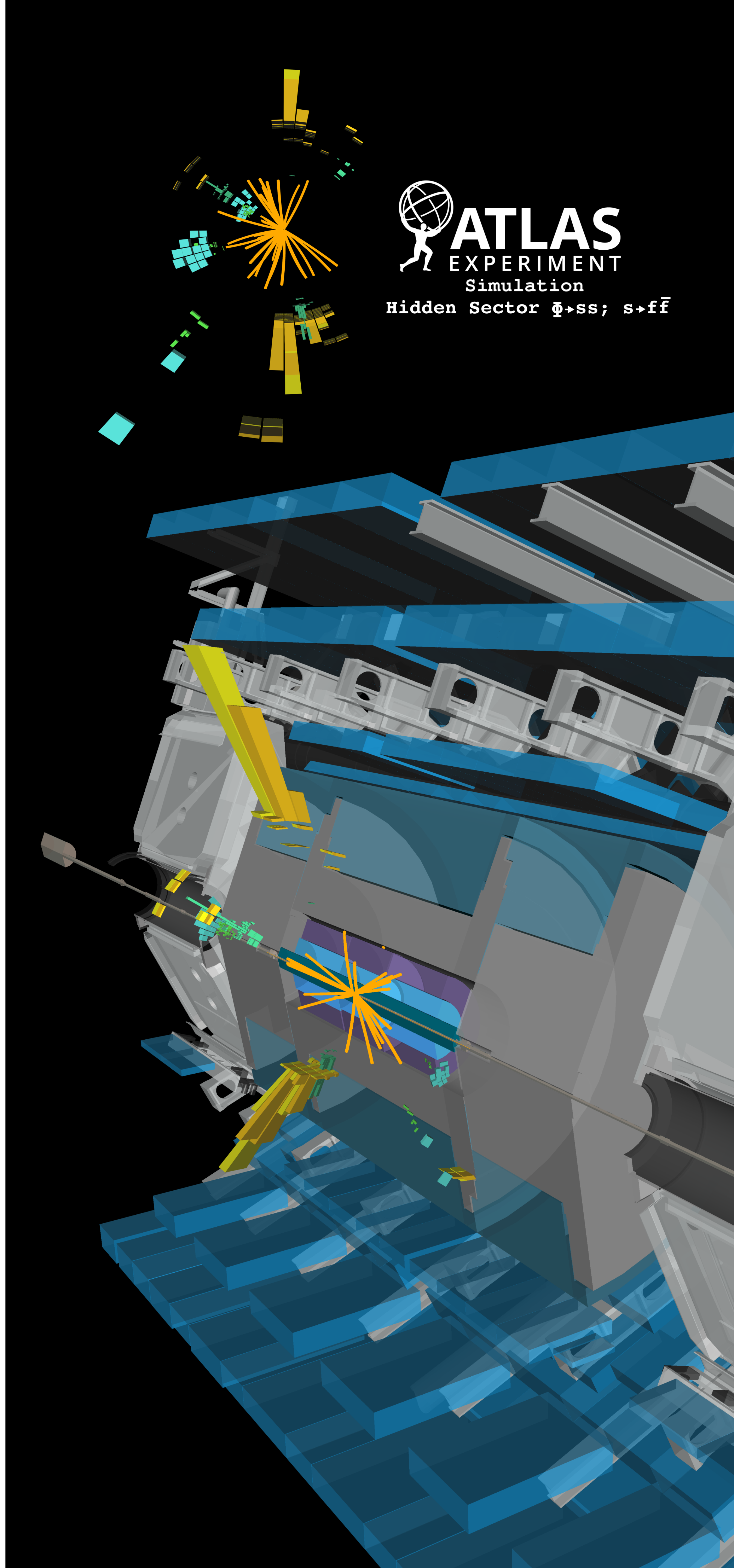

Settori Oscuri attraverso i portali

- Possibilità investigata: la Materia Oscura può essere costituita da un intero **Settore Oscuro** di particelle
- Modello minimale di Settore Oscuro: $U(1)_d$ spontaneamente rotto da un meccanismo di Higgs Oscuro —> interazione a corto raggio, il **Fotone Oscuro** γ_d può essere massivo e decadere
- Assunzione minima: è necessaria l'esistenza di un portale vettore (ϵ) tra il Settore Oscuro e il Modello Standard

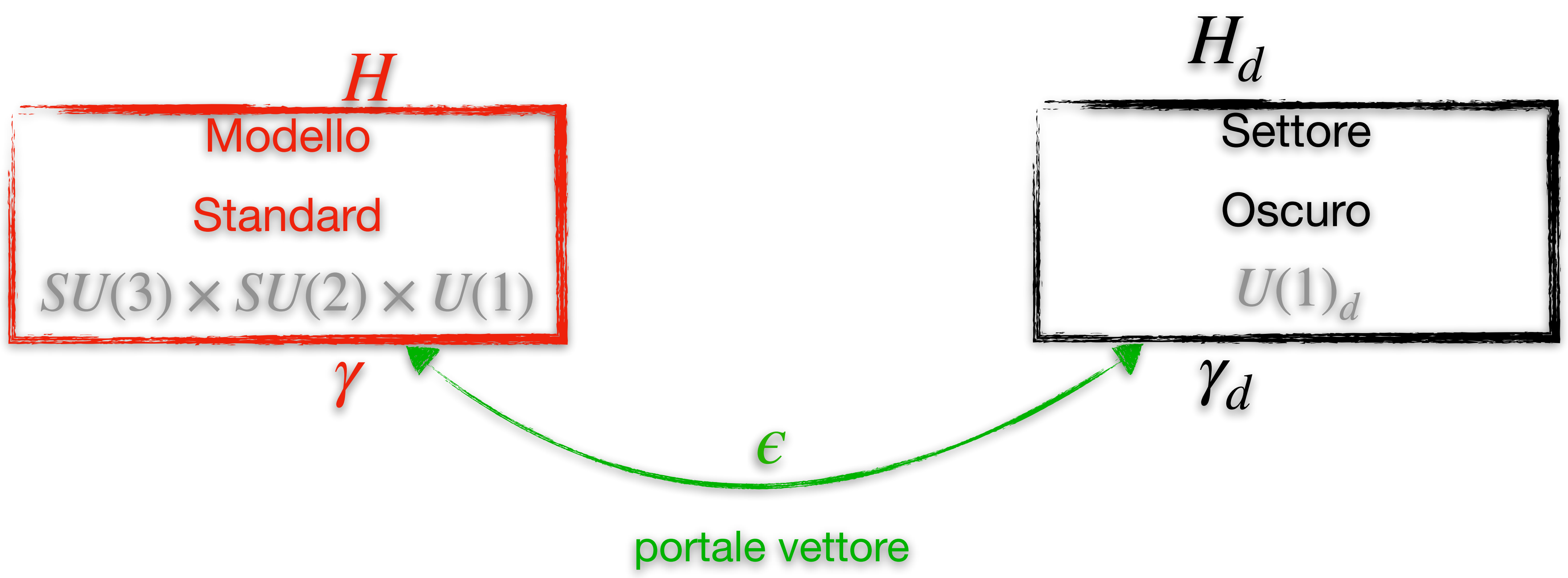

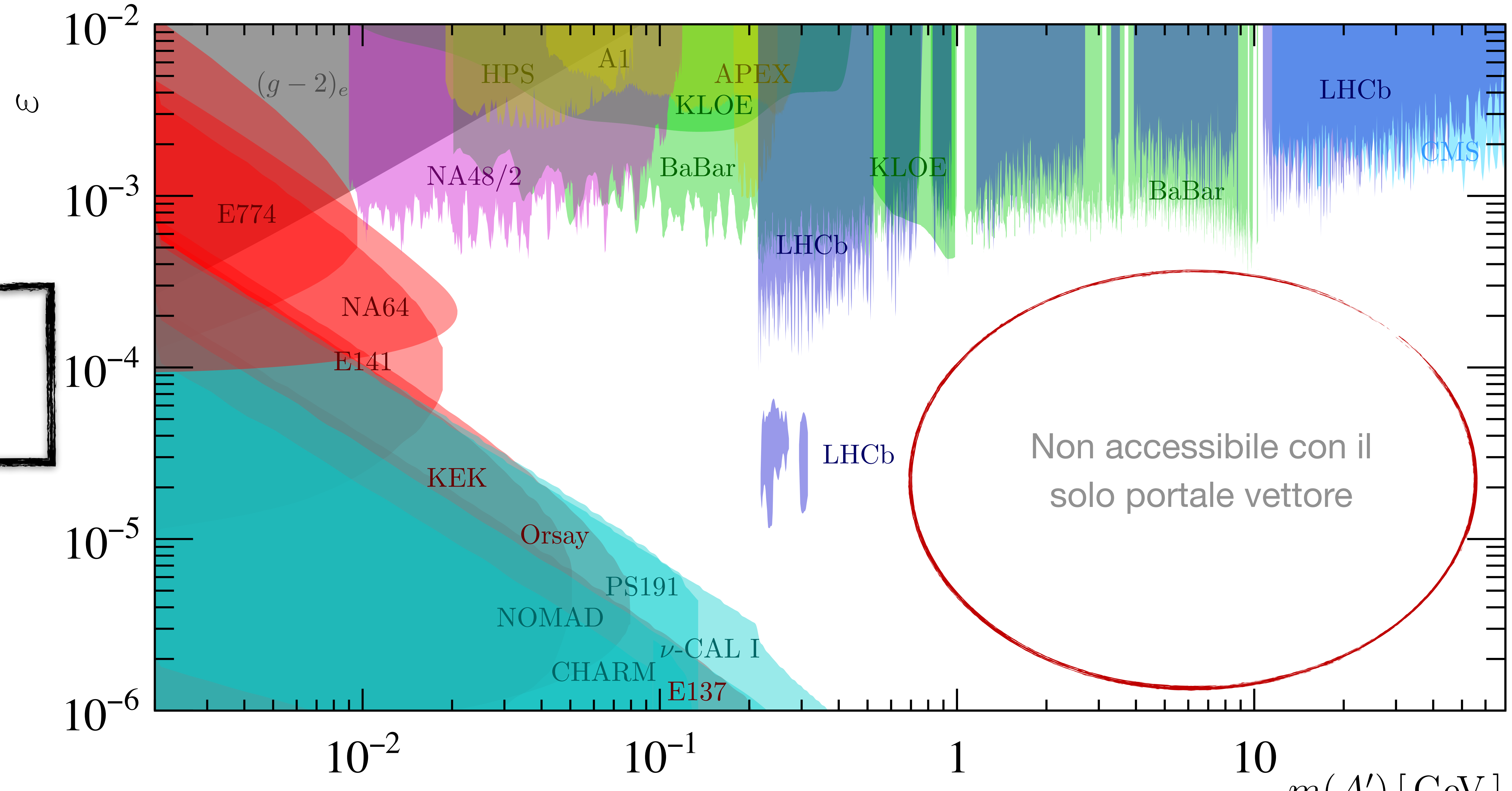

https://arxiv.org/abs/1801.04847

Settori Oscuri attraverso i portali

- Possibilità investigata: la Materia Oscura può essere costituita da un intero **Settore Oscuro** di particelle
- Modello minimale di Settore Oscuro: $U(1)_d$ spontaneamente rotto da un meccanismo di Higgs Oscuro —> interazione a corto raggio, il **Fotone Oscuro** γ_d può essere massivo e decadere
- Assunzione minima: è necessaria l'esistenza di un portale vettore (ϵ) tra il Settore Oscuro e il Modello Standard
- Il $BR(H \rightarrow und) < 11\%$ —> Il bosone di Higgs può decadere in particelle del Settore Oscuro attraverso il portale di Higgs

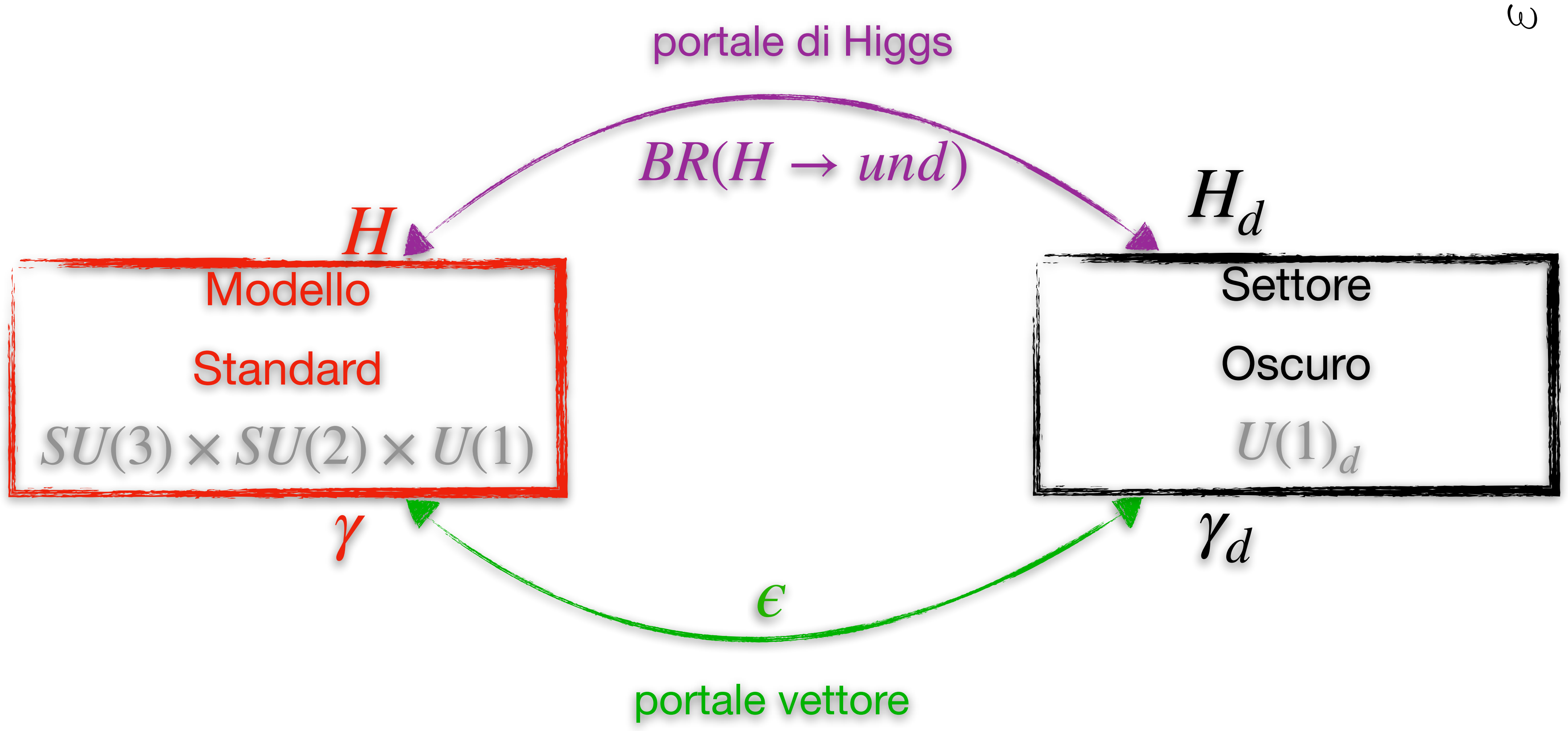

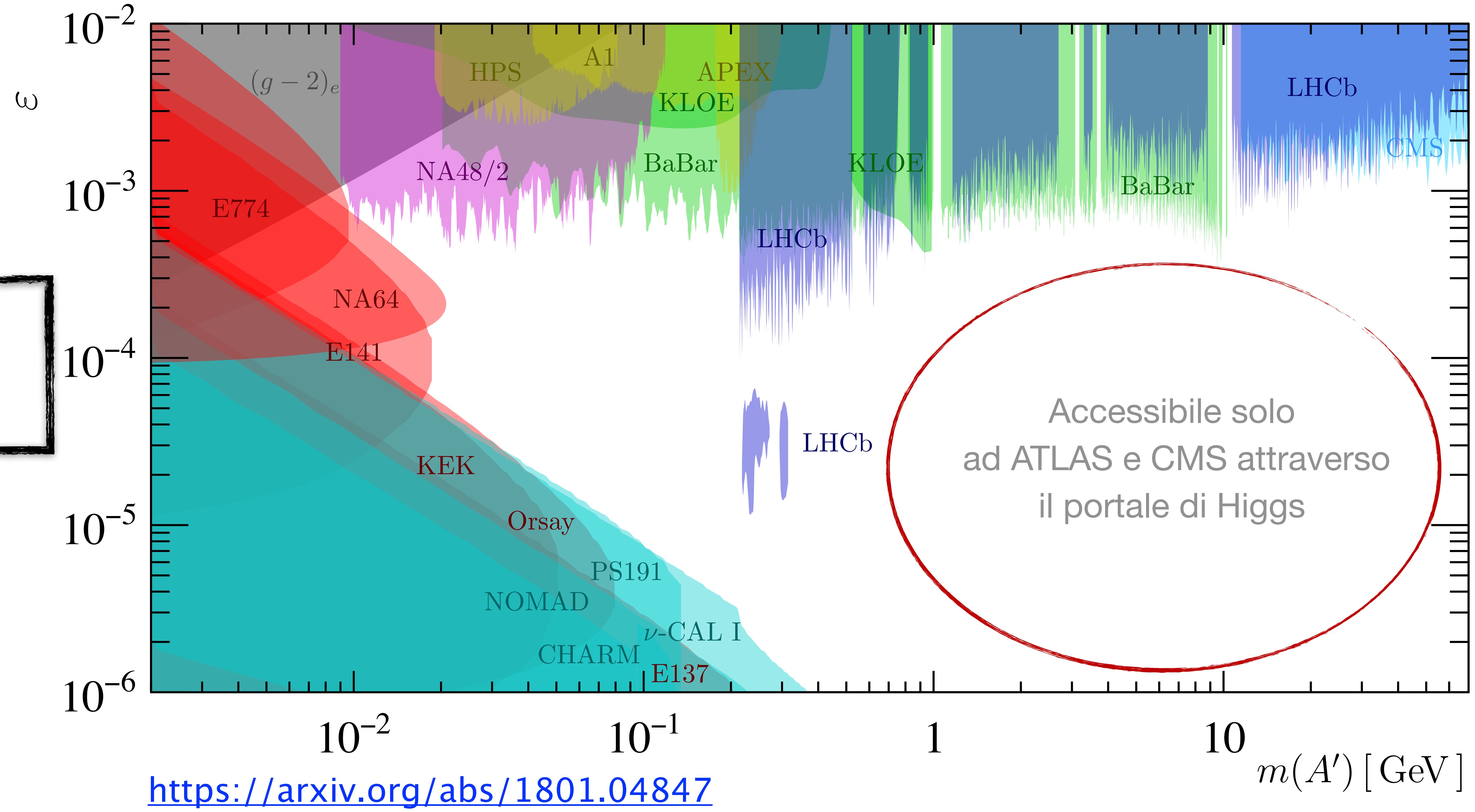

https://arxiv.org/abs/1801.04847

ATLAS è un rivelatore di particelle 'multifunzione' impiegato al Large Hadron Collider (LHC) al CERN
Durante il Run 2 di LHC (2015-2018) ATLAS ha raccolto collisioni p-p corrispondenti ad un'energia nel centro di massa pari a $\sqrt{s}$ = 13 TeV.

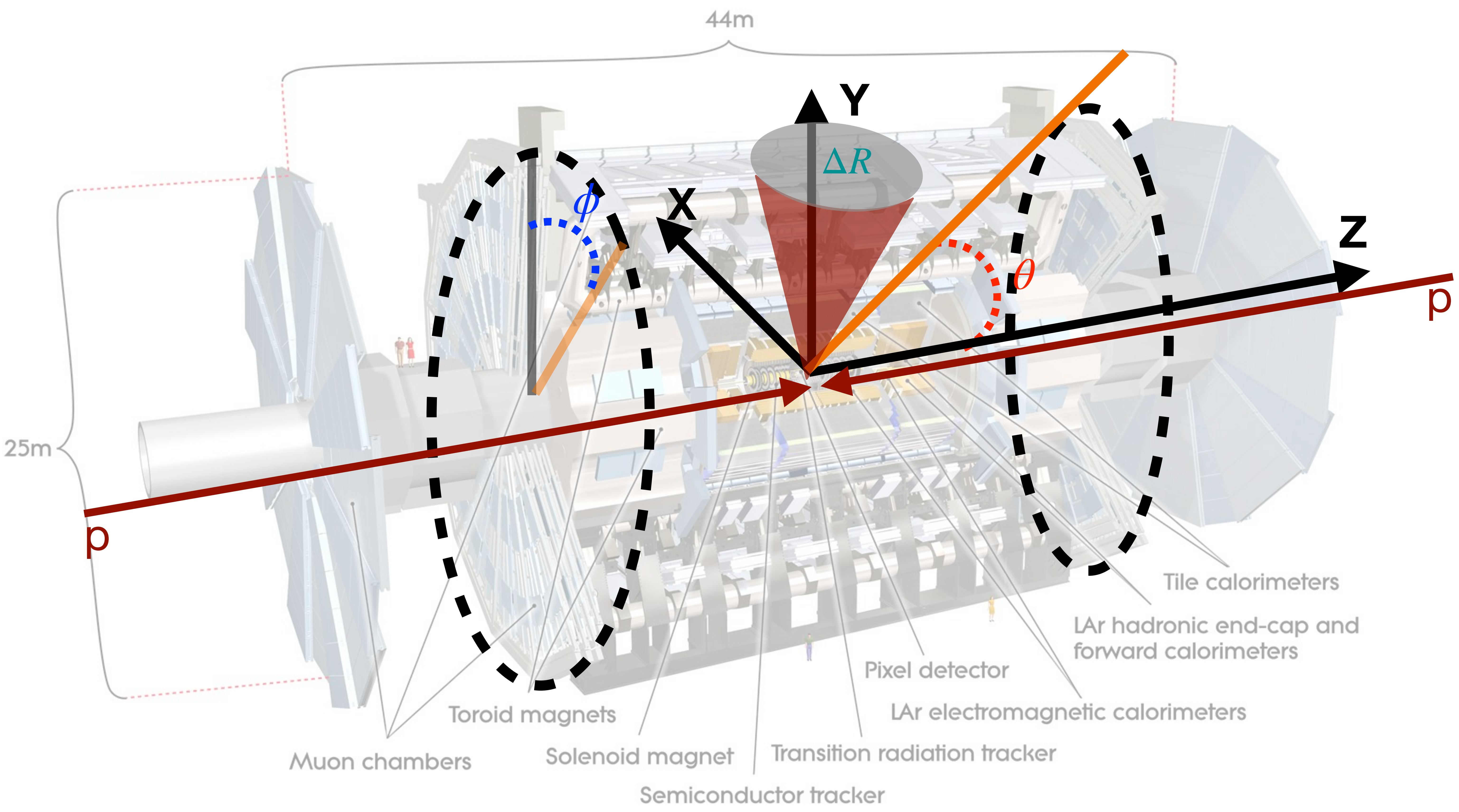

Pseudorapidità

$$\eta = -\ln(\tan\frac{\theta}{2})$$

Distanza tra due oggetti

$$\Delta R = \sqrt{\Delta\eta^2 + \Delta\phi^2}$$

Momento trasverso

$$p_{\mathrm{T}} = \sqrt{p_x^2 + p_y^2}$$

ATLAS è un rivelatore di particelle 'multifunzione' impiegato al Large Hadron Collider (LHC) al CERN
Durante il Run 2 di LHC (2015-2018) ATLAS ha raccolto collisioni p-p corrispondenti ad un'energia nel centro di massa pari a $\sqrt{s}$ = 13 TeV.

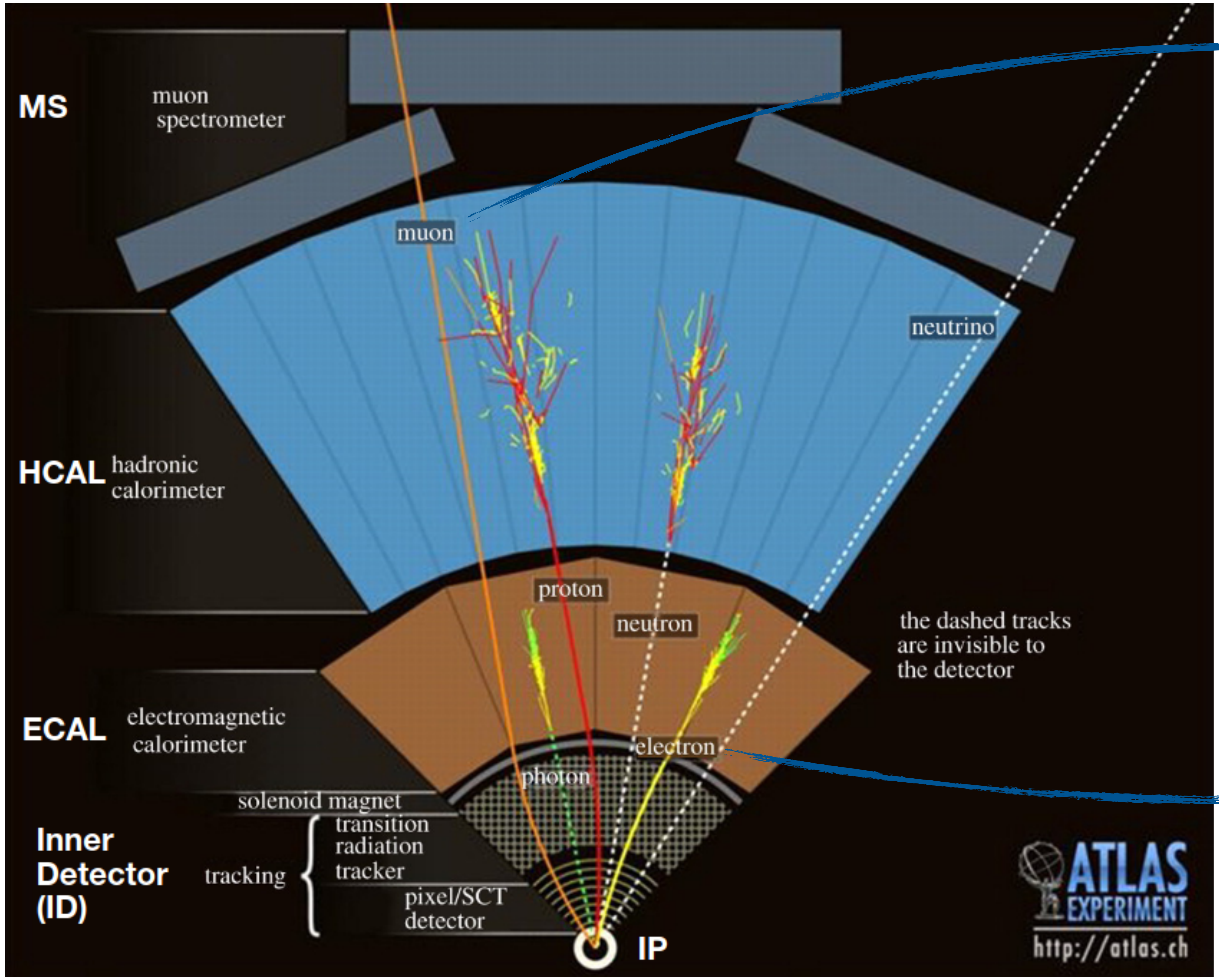

Muoni: ID + MS

Elettroni: ID + ECAL

Decadimenti “prompt” del Fotone Oscuro

<u>**Analisi in corso**</u>: decadimento prompt —> Il Fotone Oscuro decade nell’ID

Parametri liberi del Settore Oscuro:

$$\tau_{\gamma_d} \propto \left(\frac{10^{-4}}{\epsilon}\right)^2 \left(\frac{100MeV}{m_{\gamma_d}}\right)$$

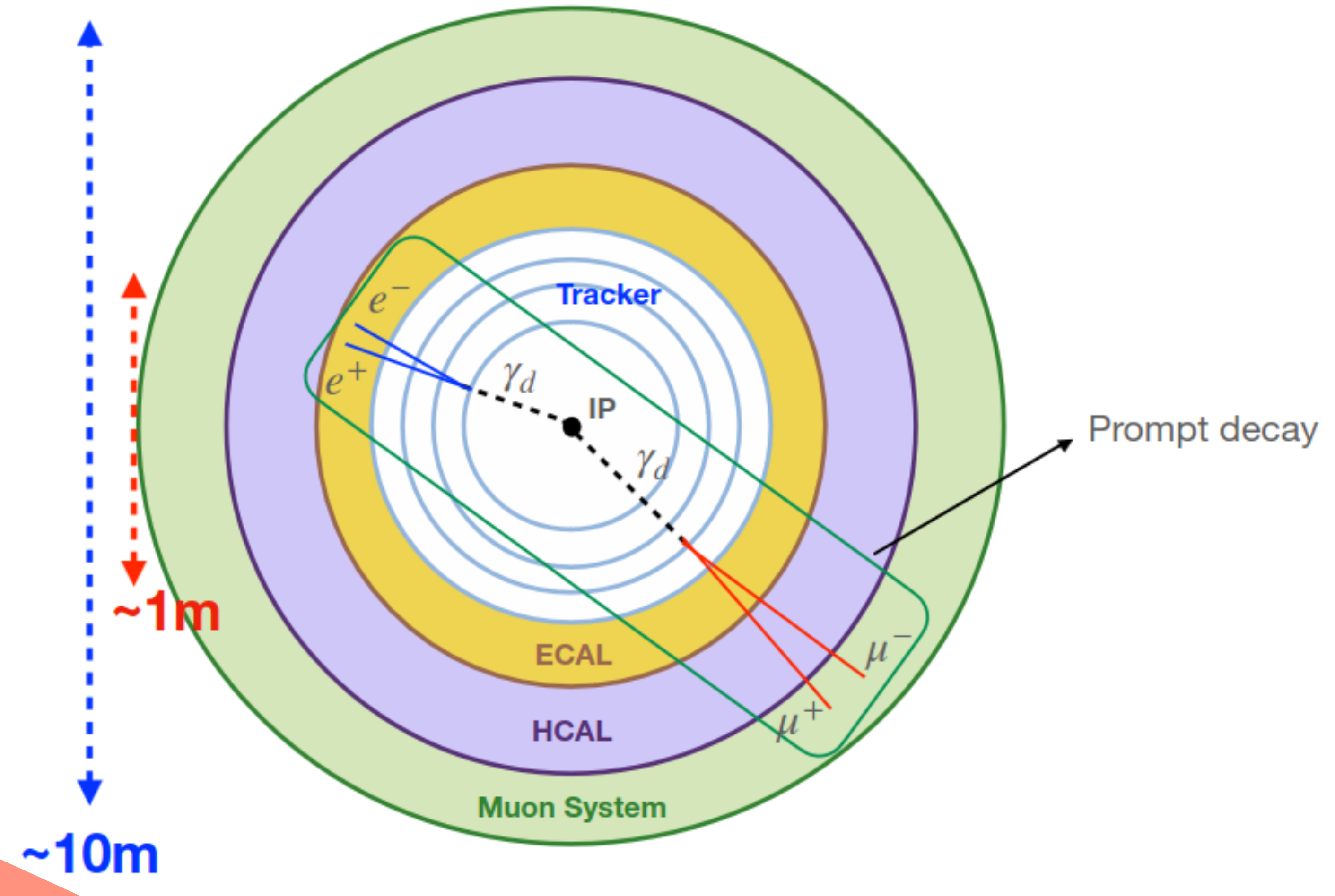

- $BR(H \to und)$ influisce sul numero di eventi
- ϵ influisce su dove decade il Fotone Oscuro ($\tau_{\gamma_d} \propto \epsilon^{-2}$)
- m_{γ_d} determina il BR del γ_d in particelle del Modello Standard

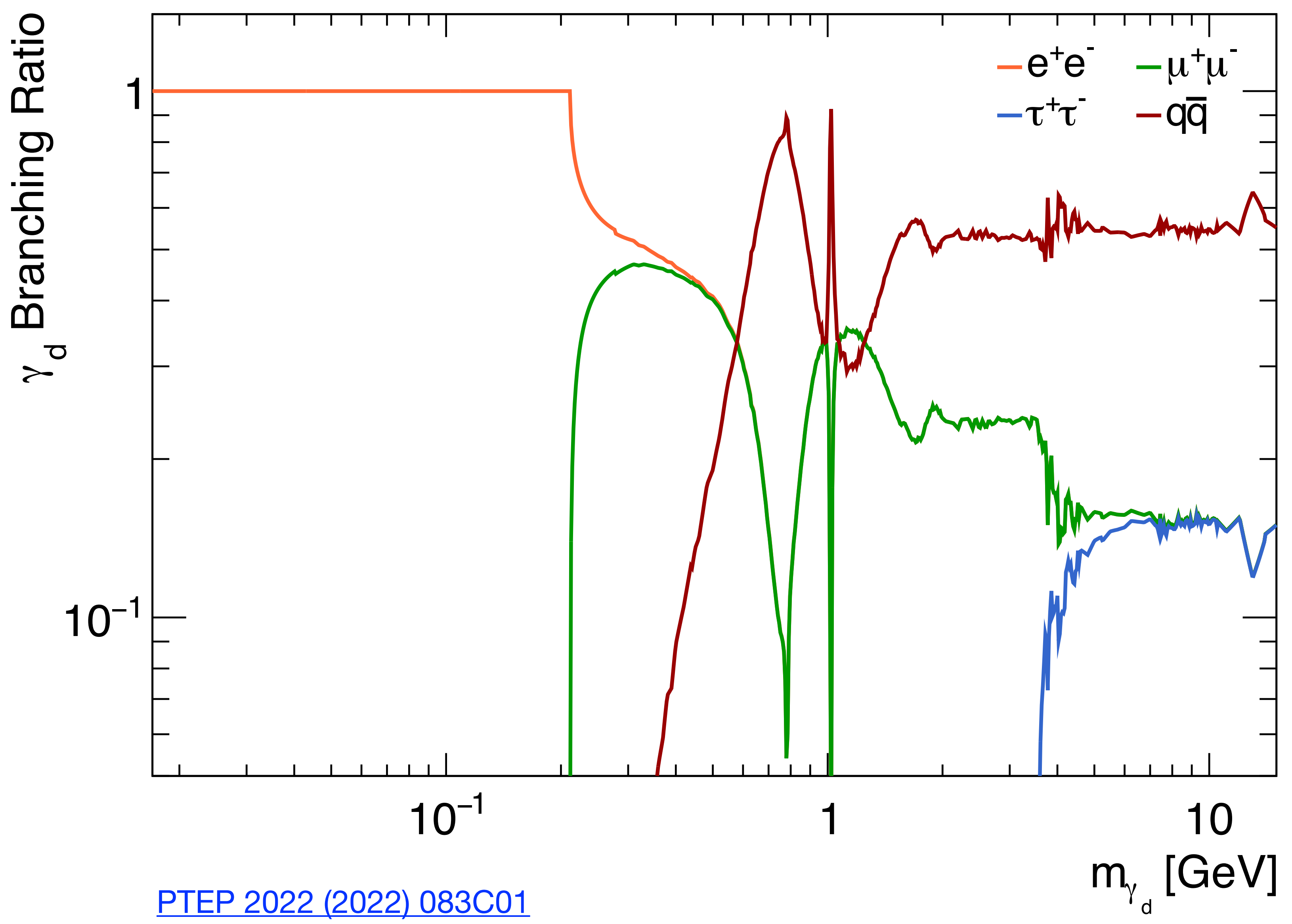

PTEP 2022 (2022) 083C01

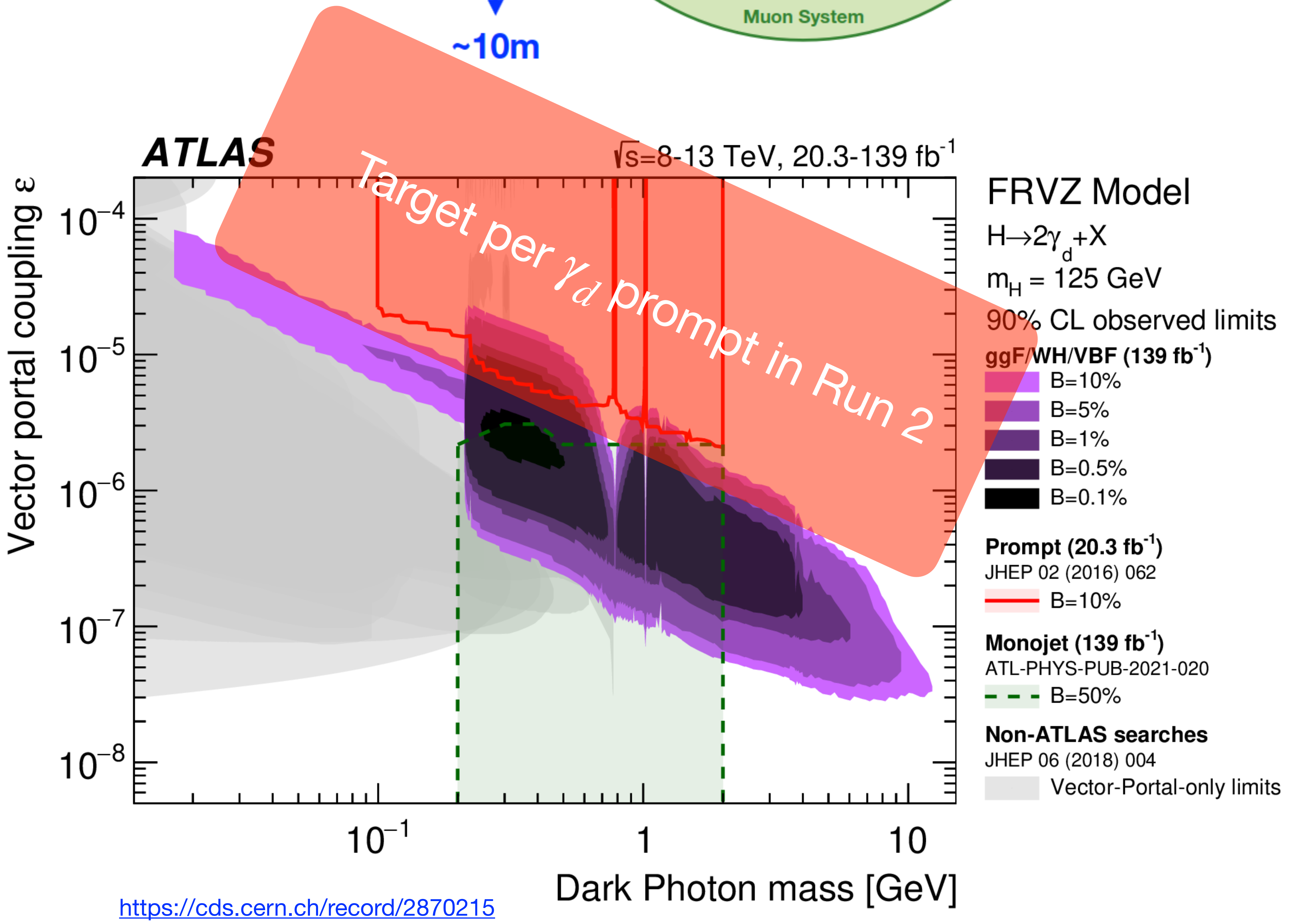

https://cds.cern.ch/record/2870215

FRVZ e HAHM

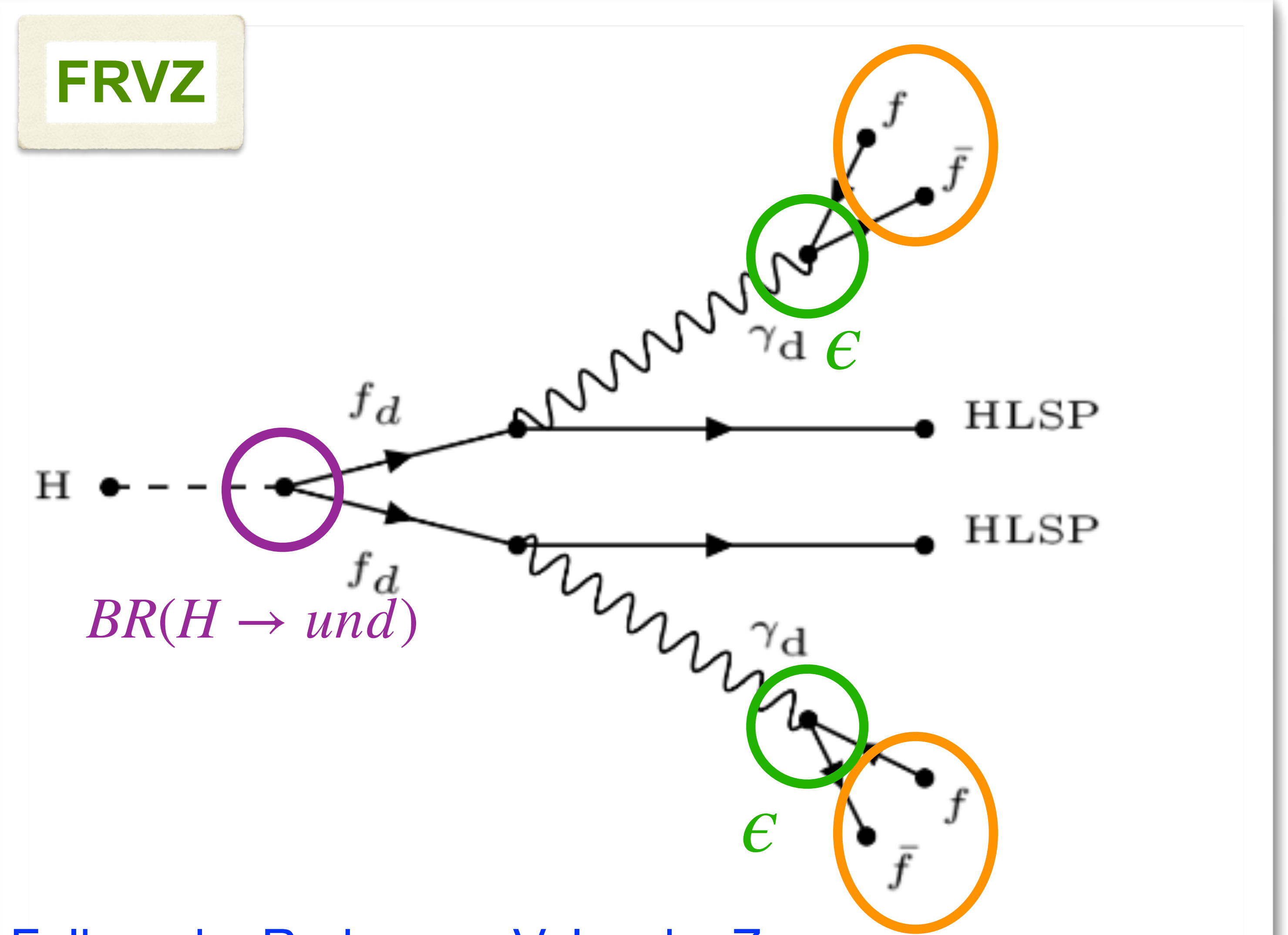

[Falkowsky-Ruderman-Volansky-Zupan]()

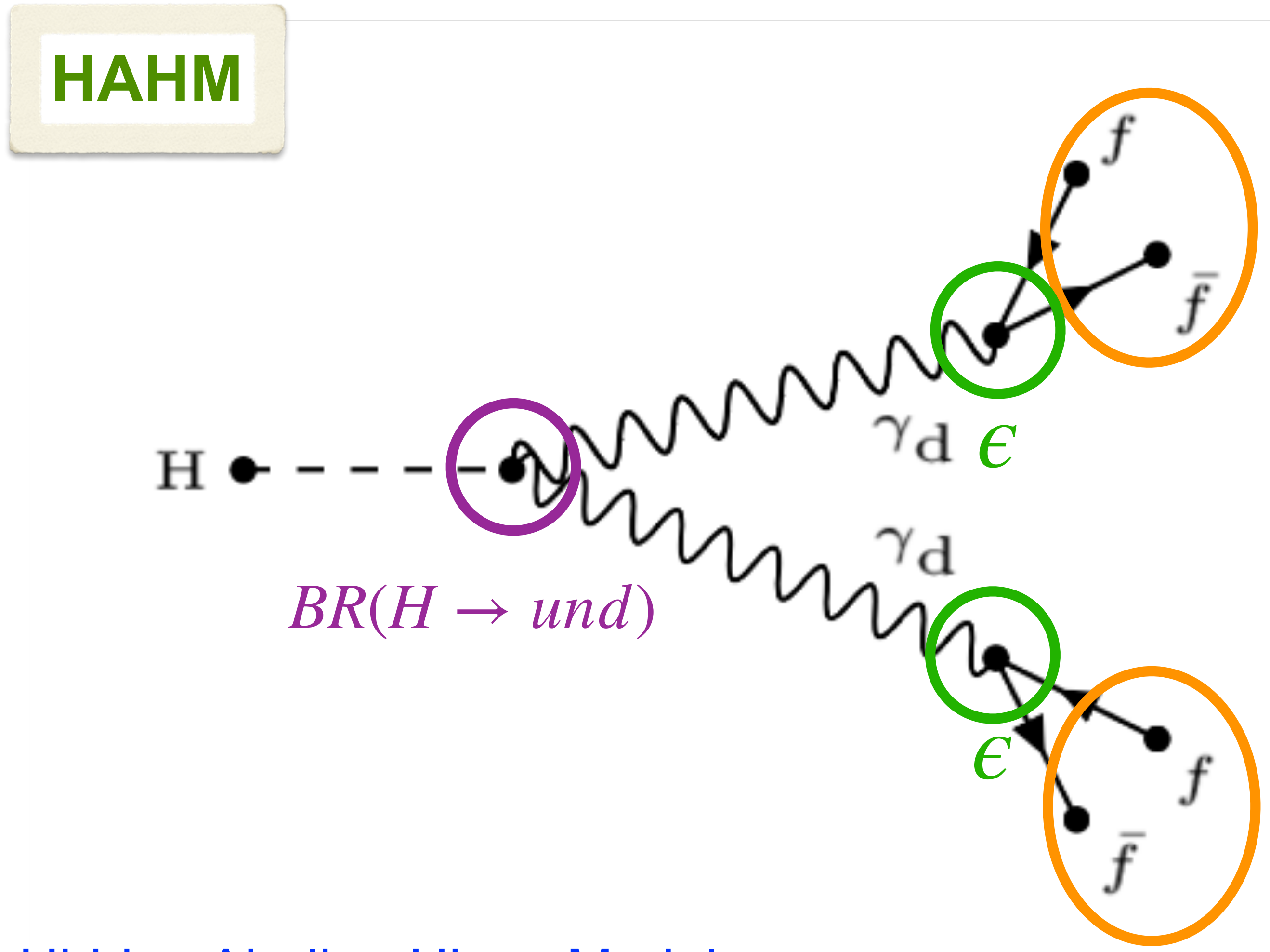

[Hidden Abelian Higgs Model]()

Considerati solo decadimenti leptonici

$\gamma_d \to \mu^+\mu^-$ e $\gamma_d \to e^+e^-$

I prodotti di decadimento sono estremamente collimati —> **Jet Leptonici (LJ)**

ΔR tra prodotti di decadimento

FRVZ

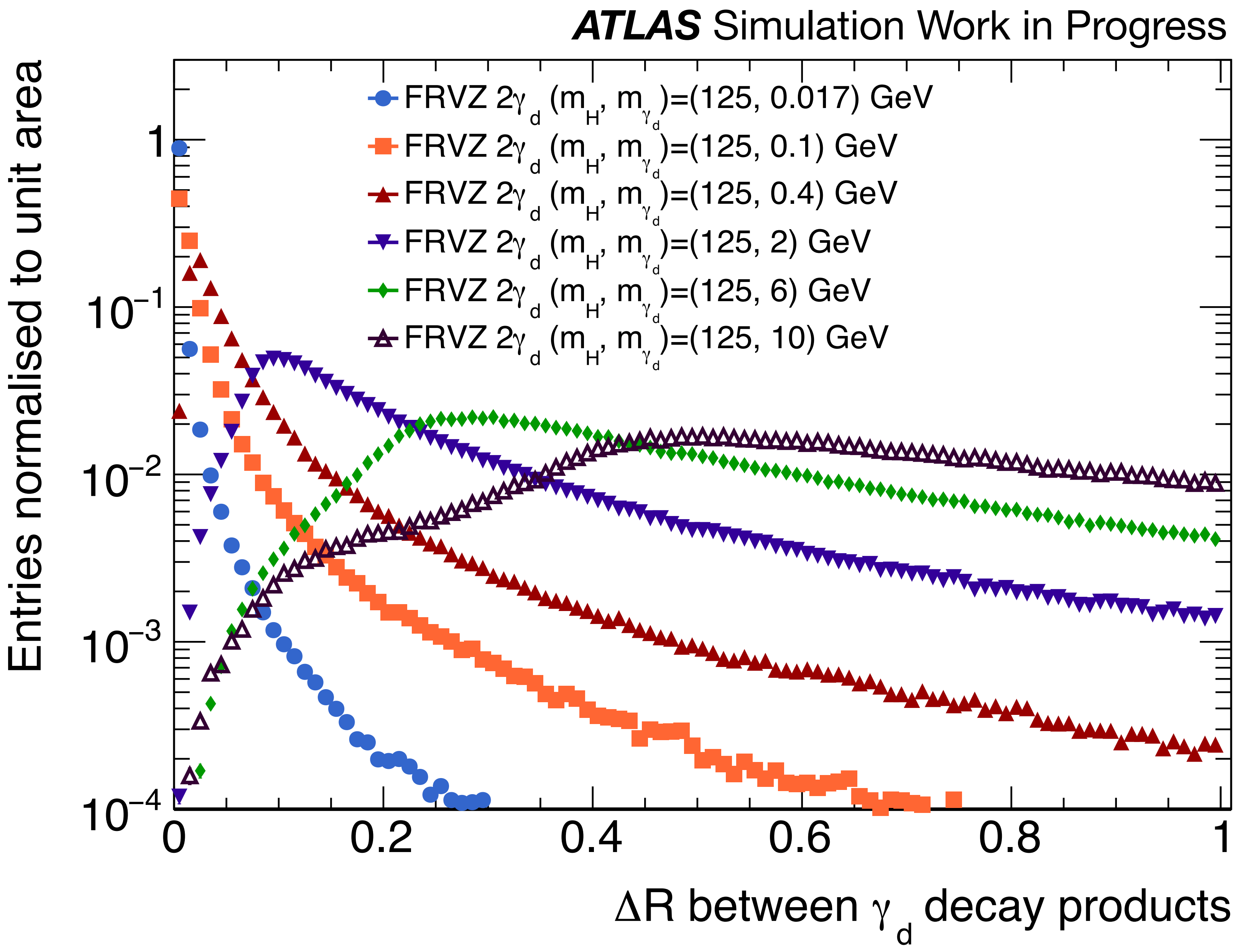

HAHM

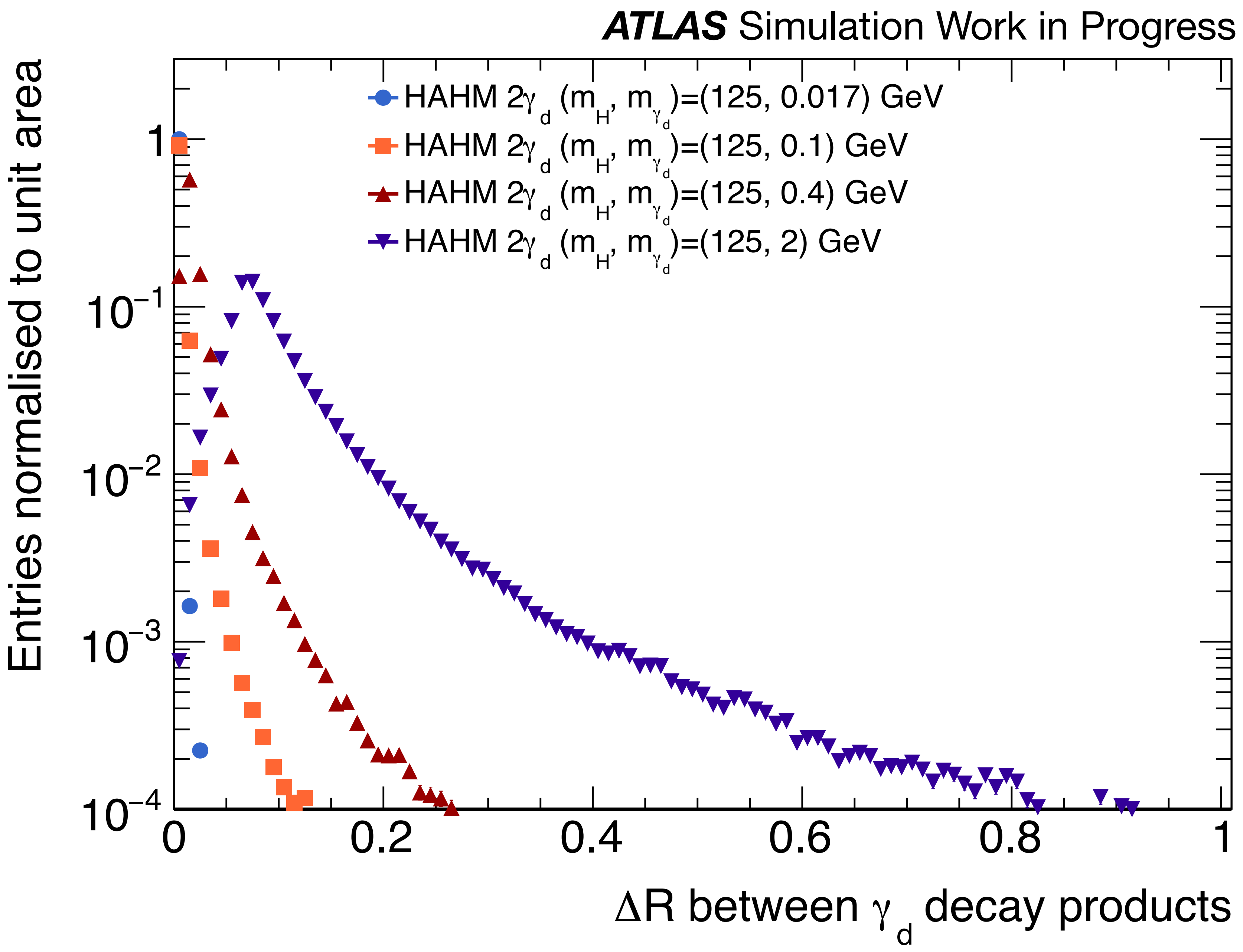

FRVZ

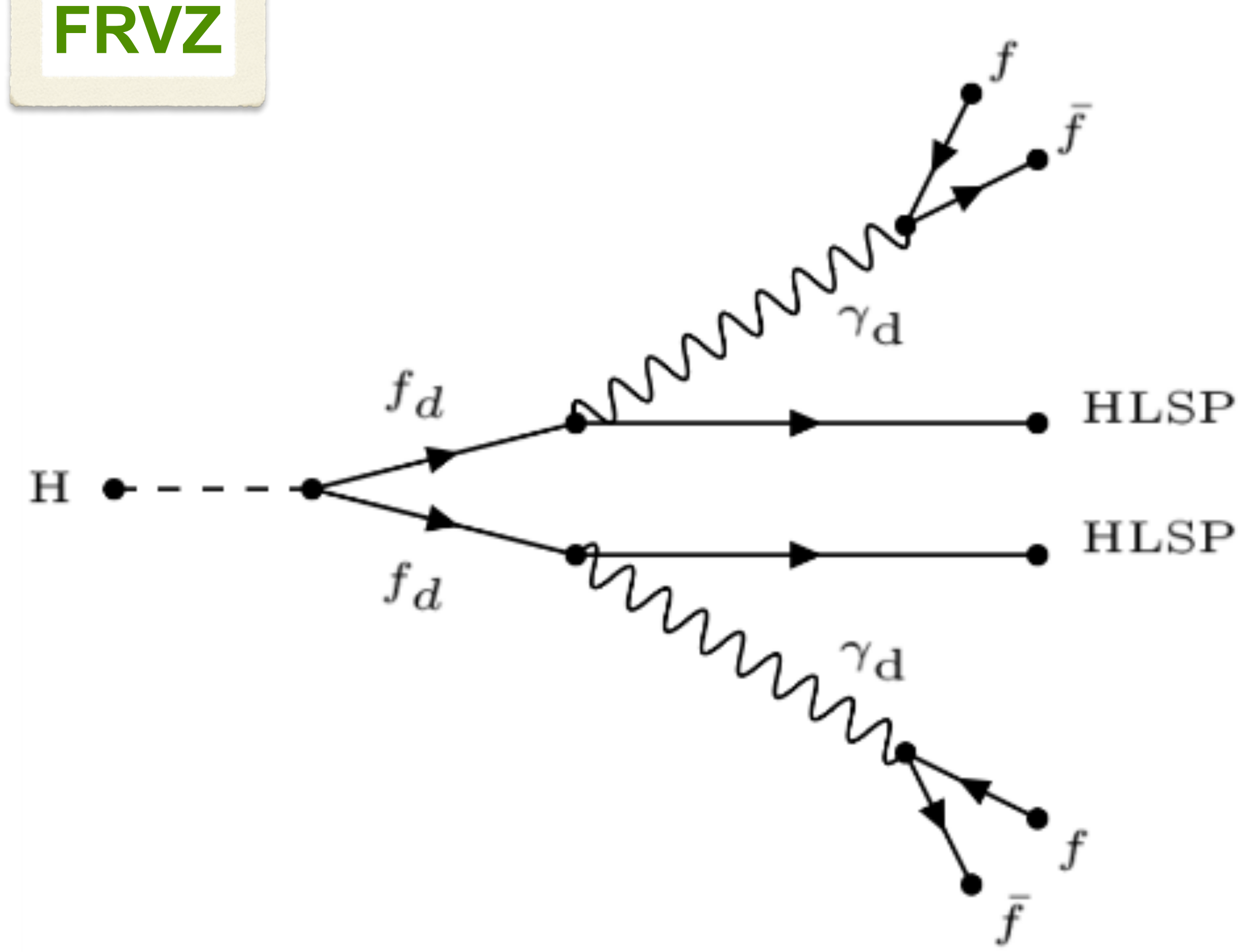

[Falkowsky-Ruderman-Volansky-Zupan]

HAHM

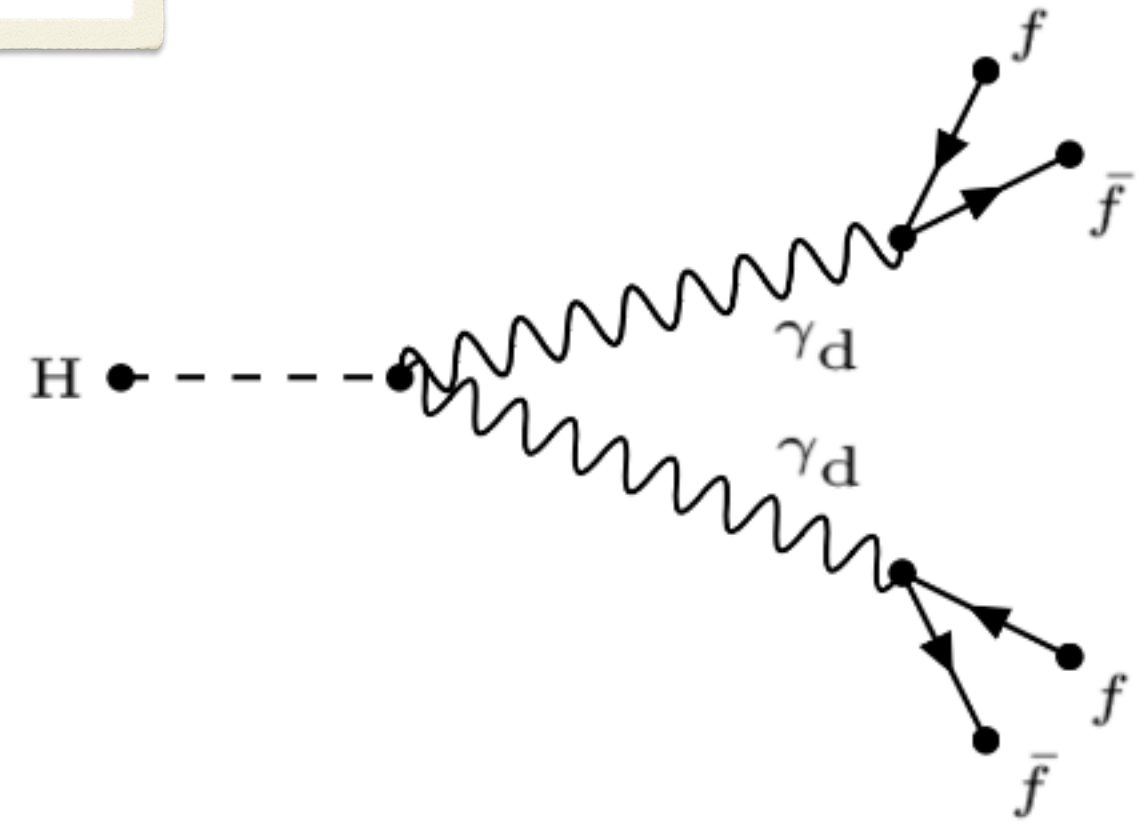

[Hidden Abelian Higgs Model]

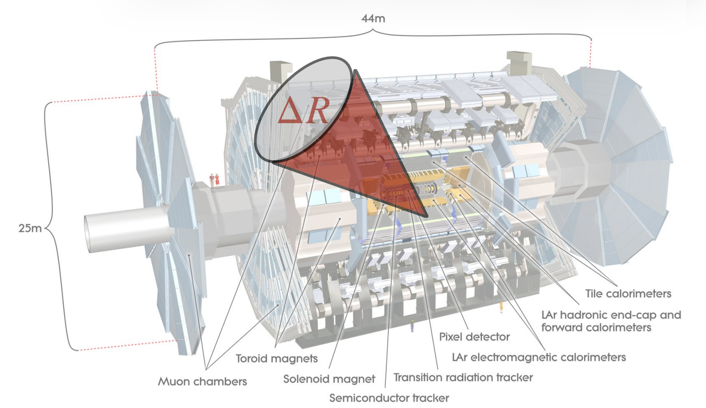

$$\Delta R = \sqrt{\Delta\eta^2 + \Delta\phi^2}$$

Nel modello HAHM i γ_d sono più *boosted* rispetto al modello FRVZ —> i prodotti di decadimento sono più collimati —> in HAHM più efficienza di segnale!

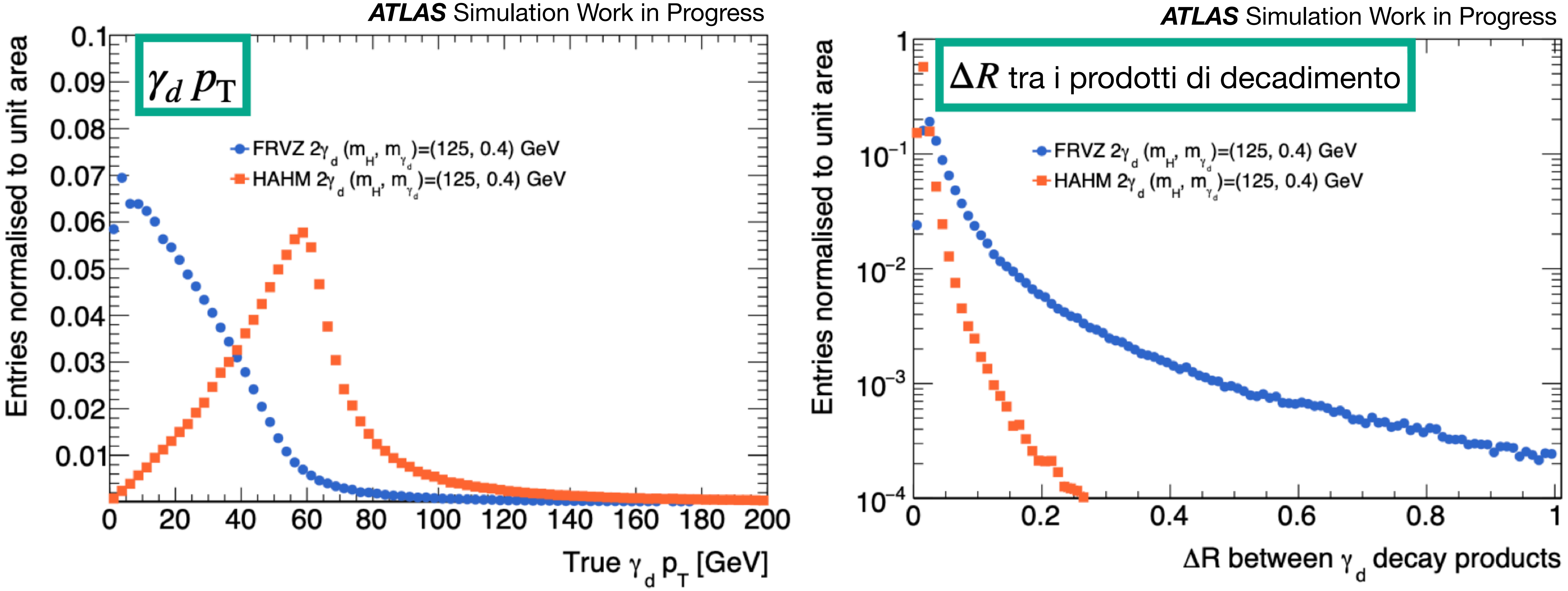

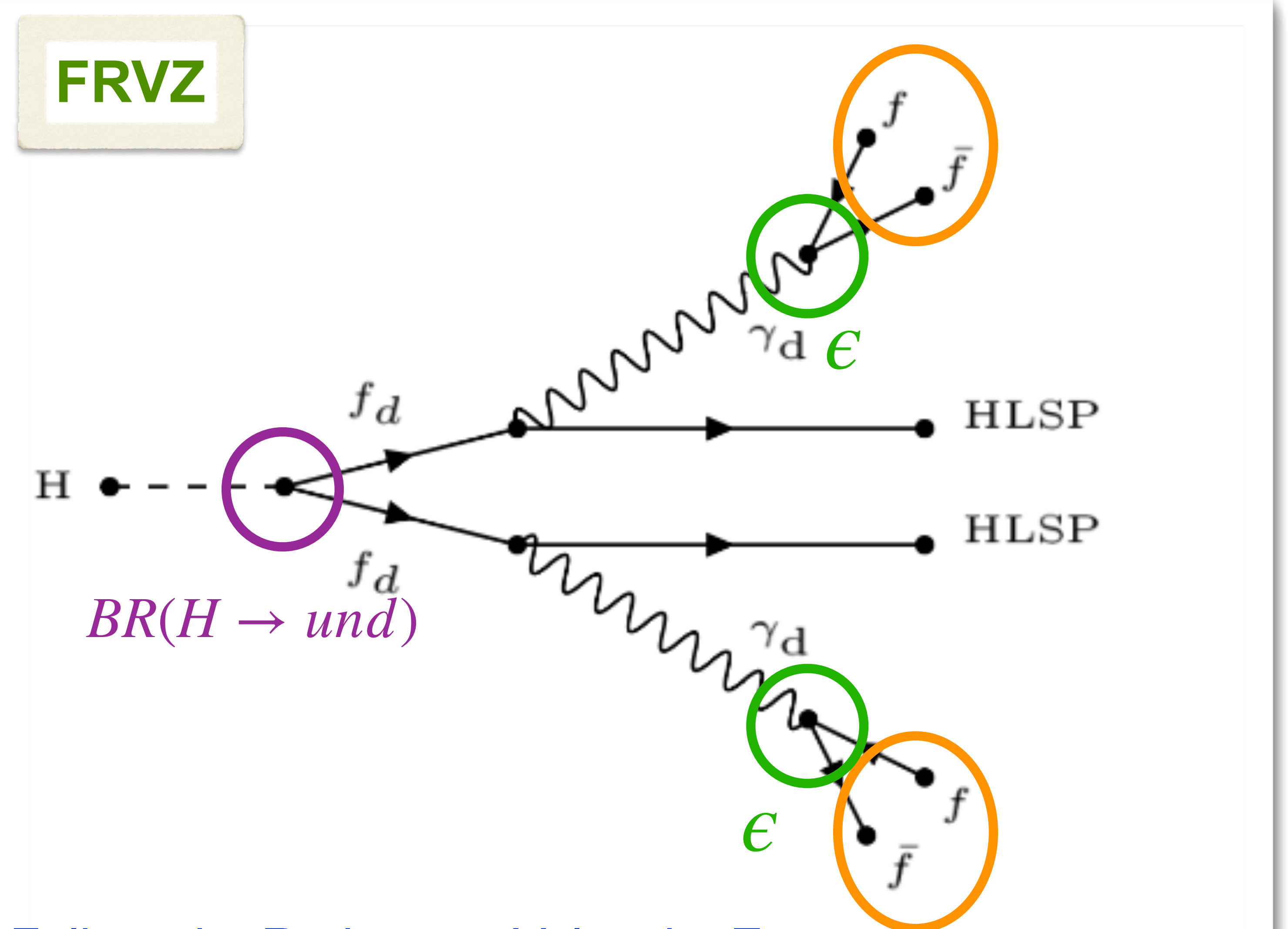

Falkowsky-Ruderman-Volansky-Zupan

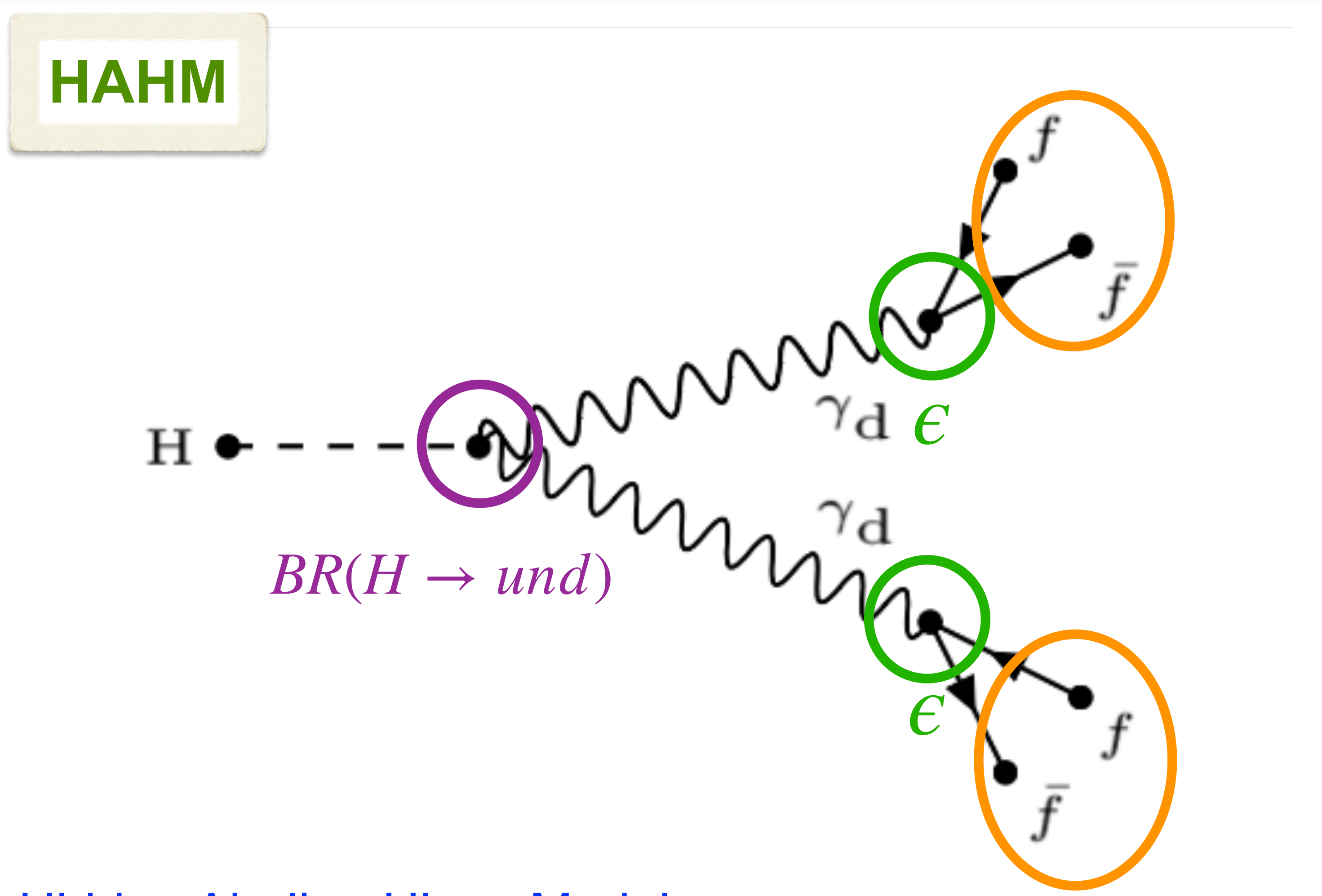

Hidden Abelian Higgs Model

Considerati solo decadimenti leptonici

$\gamma_d \to \mu^+\mu^-$ e $\gamma_d \to e^+e^-$

I prodotti di decadimento sono estremamente collimati —> **Jet Leptonici (LJ)**

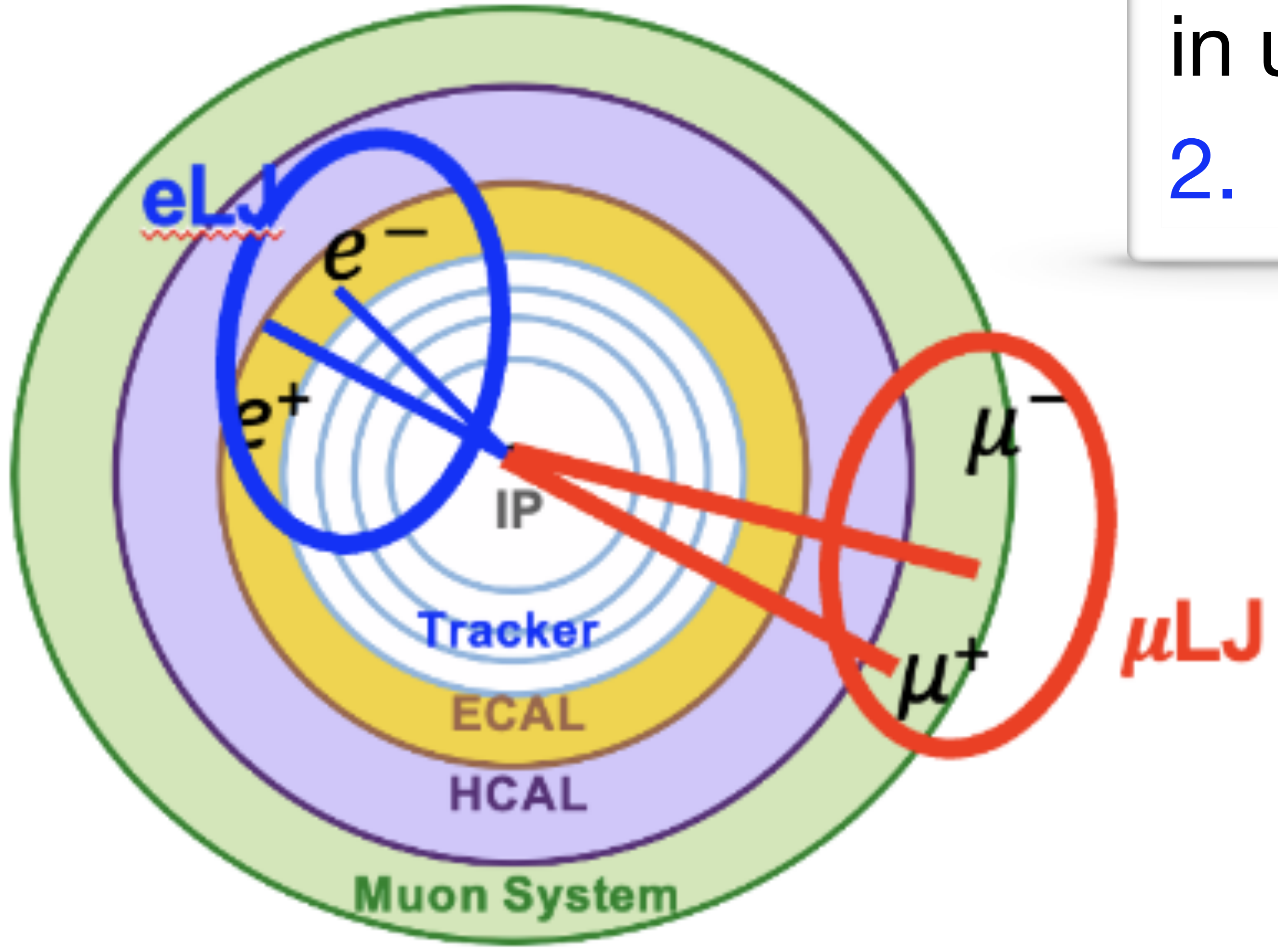

eLJ

1. ≥ 1 elettrone ricostruito con ≥ 2 tracce associate in un cono $\Delta R = 0.4$
2. ≥ 2 elettroni ricostruiti in un cono $\Delta R = 0.4$

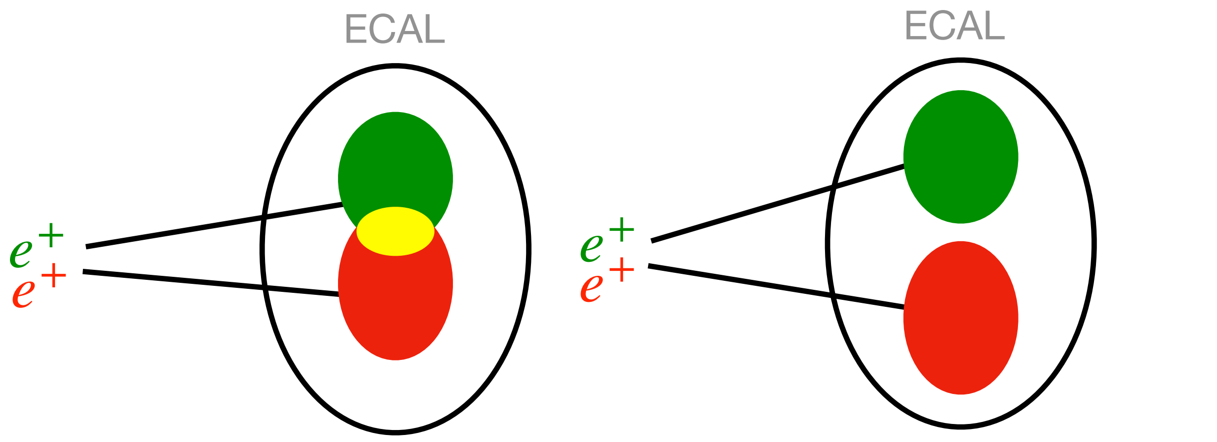

eLJ con 1 elettrone

eLJ con 2 elettroni

μLJ

≥ 2 muoni e nessun elettrone in un cono $\Delta R = 0.4$

Strategia di analisi

Analisi su dati di **Run-2** (2015-2018)

3 canali di studio —> 3 **regioni di segnale (SR)**
Valutazione dei fondi —> 3 **regioni di controllo (CR)** —> **DATA DRIVEN**

2LJ

Canale elettronico
2 eLJ

- V + jets —> e^+e^-
- processi SM —> e + traccia
- γ^* —> e^+e^-

ABCD

Canale muonico
2 μLJ

Risonanze —> $\mu^+\mu^-$

Bump-hunting

Canale misto
1 eLJ + 1 μLJ

- processi SM —> e + traccia
- γ^* —> e^+e^-
-Risonanze —> $\mu^+\mu^-$

Bump-hunting

Più dettagli in backup

Modelling canale misto

Regione di segnale	Regione di Controllo
1μLJ + 1eLJ	1μLJ + 0eLJ + 0μ + 2e
Simulazioni MC	**Data-driven**

Ottima risoluzione su $m_{\mu\mathrm{LJ}}$ —> bump-hunting su $m_{\mu\mathrm{LJ}}$

$f(m_{\mu\mu})$: modelling della forma del segnale (in SR dai MC)

$\int f(m_{\mu\mu})$: Acceptance X Efficiency (in SR dai MC)

$B(m_{\mu\mu})$: modelling della forma del fondo (in CR nei dati)

$\int B(m_{\mu\mu})$: estratta da SR nei dati

(dopo unblinding —> vedere dati veri in SR)

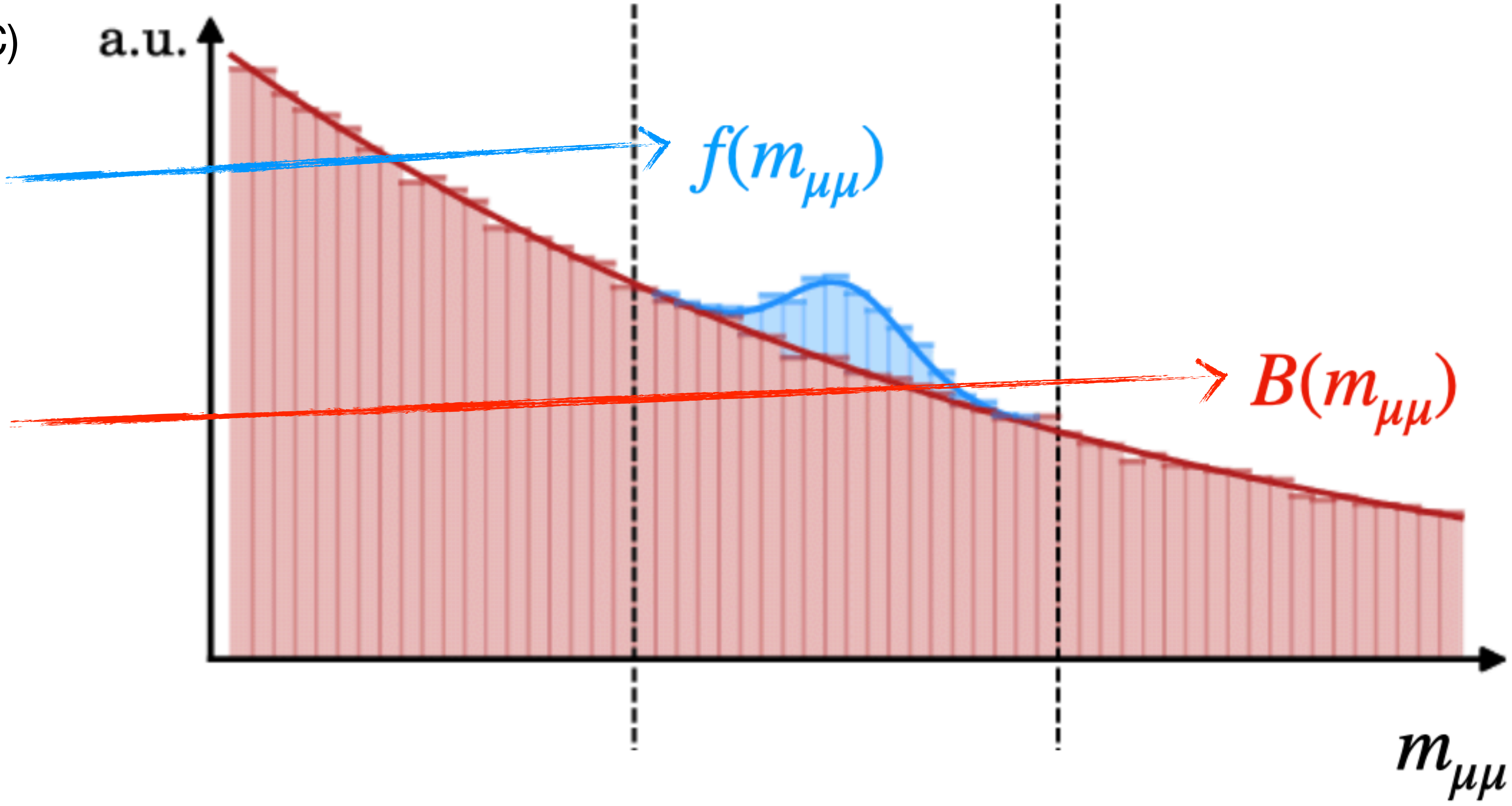

Più dettagli in backup

Limiti attesi: $BR(H \to 2\gamma_d + X)$

- Limite superiore atteso su $BR(H \to 2\gamma_d + X)$ al 95% CLs
- Risonanze verranno vetate
- Fit con 1000 eventi
- Eventi attesi: ~100 eventi (da estrapolazione dati di Run-1)
- Limiti Run-1[https://arxiv.org/abs/1511.05542]: fino a 2 GeV, solo per FRVZ

FRVZ

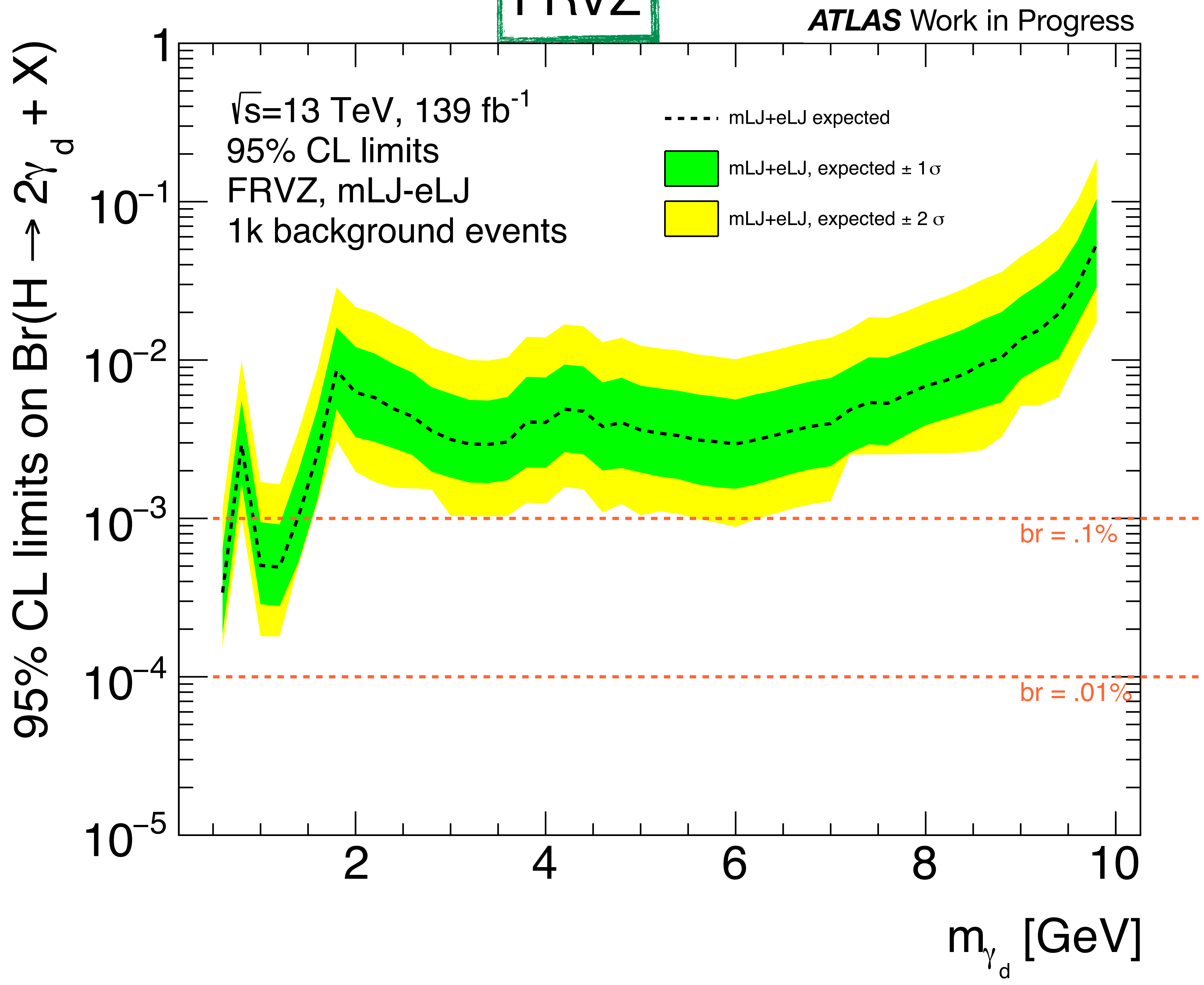

HAHM

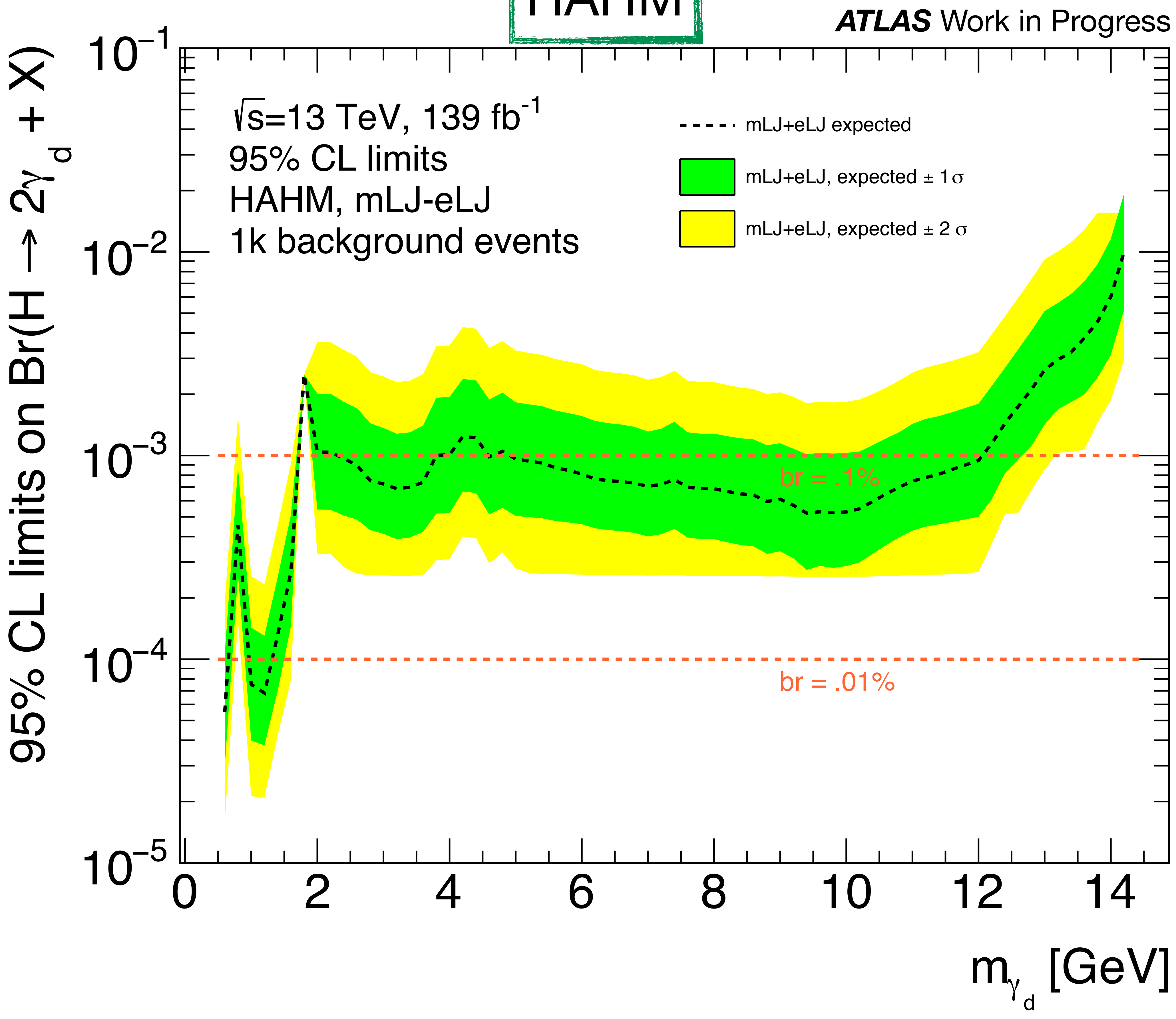

- Canale elettronico: $m_{\gamma_d} < 240$ MeV
- Canale muonico e misto: $m_{\gamma_d} > 240$ MeV

eLJ-eLJ

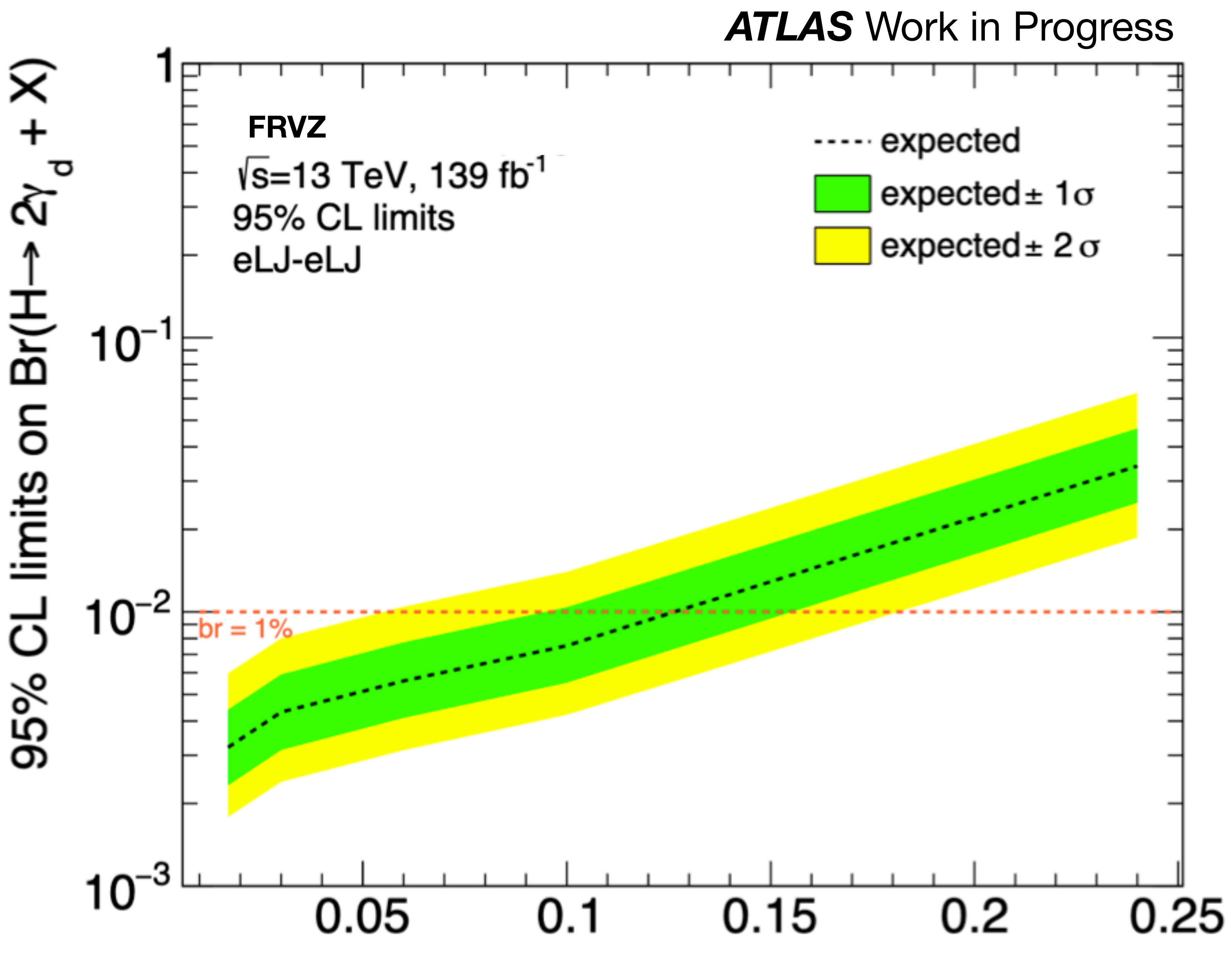

μLJ-μLJ

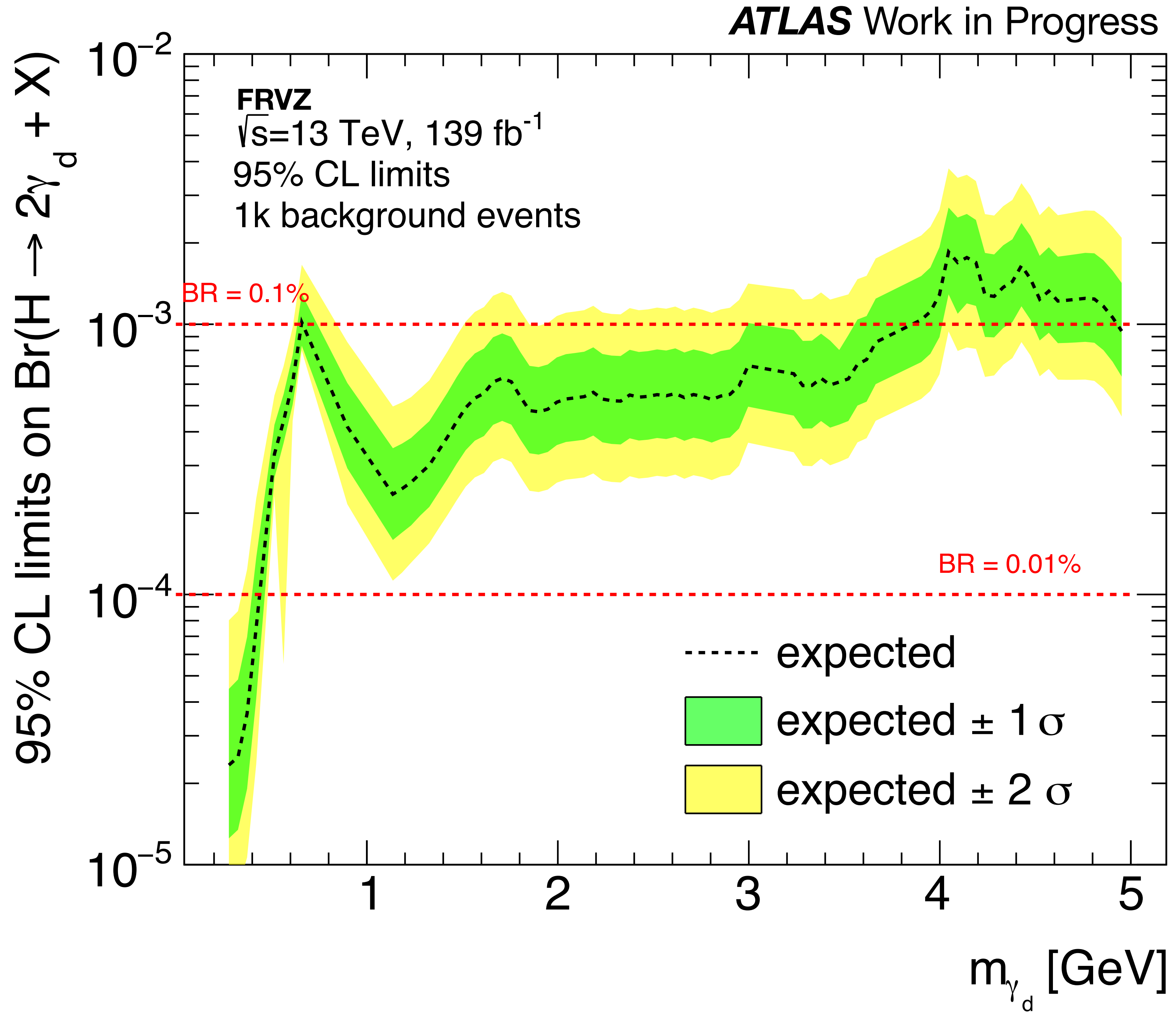

μLJ-eLJ

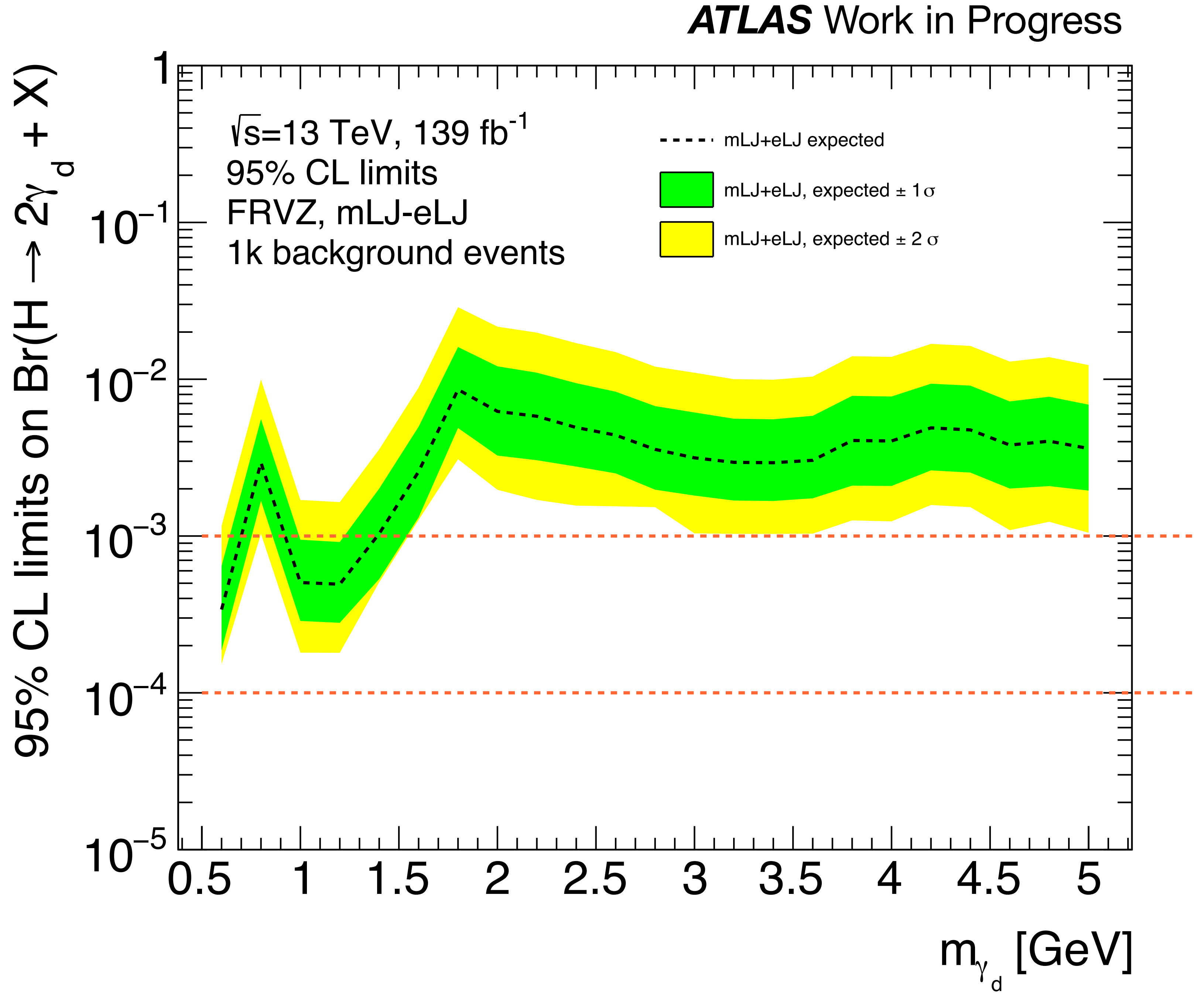

Conclusioni

- Estensione del limite sul $BR(H \rightarrow 2\gamma_d + X)$ per m_{γ_d} più alte rispetto a Run-1
- Run-1[https://arxiv.org/abs/1511.05542]: limiti fino ad un $BR(H \rightarrow 2\gamma_d + X) = 0.1$ %
- Prima analisi prompt per modello HAHM

Prossimi step dopo unblinding:

- Estrapolazione limiti veri $BR(H \rightarrow 2\gamma_d + X)$
- Life-time re-weighting
- Combinazione dei tre canali e interpretazione portale vettore

Bibliografia

- A.F. et al., **Hidden Higgs Decaying to Lepton Jets** [https://arxiv.org/abs/1002.2952]
- D.C. et al., **Dark Photons with High-Energy Colliders** [https://arxiv.org/abs/1412.0018]
- P.I. et al., **Serendipity in dark photon searches** [https://arxiv.org/abs/1801.04847]
- Atlas Collaboration, **A search for prompt lepton-jets in pp collisions at $\sqrt{s} = 8$ TeV with the ATLAS detector** [https://arxiv.org/abs/1511.05542]
- R.L. Workman et al., **Review of Particle Physics** [PTEP 2022 (2022) 083C01]
- Tech. rep. Geneva: CERN, **Search for light long-lived neutral particles from Higgs boson decays via vector-boson-fusion production from pp collisions at $\sqrt{s} = 13$ TeV with the ATLAS detector** [https://cds.cern.ch/record/2870215]

Backup

Simulazioni MC

FRVZ

m_H [GeV]	number of γ_D	m_{γ_D} [GeV]	m_{HLSP} [GeV]	m_{f_d} [GeV]
125	2	0.017	2	5
125	2	0.03	2	5
125	2	0.06	2	5
125	2	0.1	2	5
125	2	0.24	2	5
125	2	0.4	2	5
125	2	0.9	2	5
125	2	2	2	10
125	2	6	4	25
125	2	10	6	35
125	2	15	10	45
125	2	25	10	45
125	2	40	7	55

HAHM

m_H [GeV]	number of γ_D	m_{γ_D} [GeV]
125	2	0.017
125	2	0.01
125	2	0.4
125	2	2
125	2	10
125	2	15
125	2	25
125	2	40

Efficienza di ricostruzione μLJ

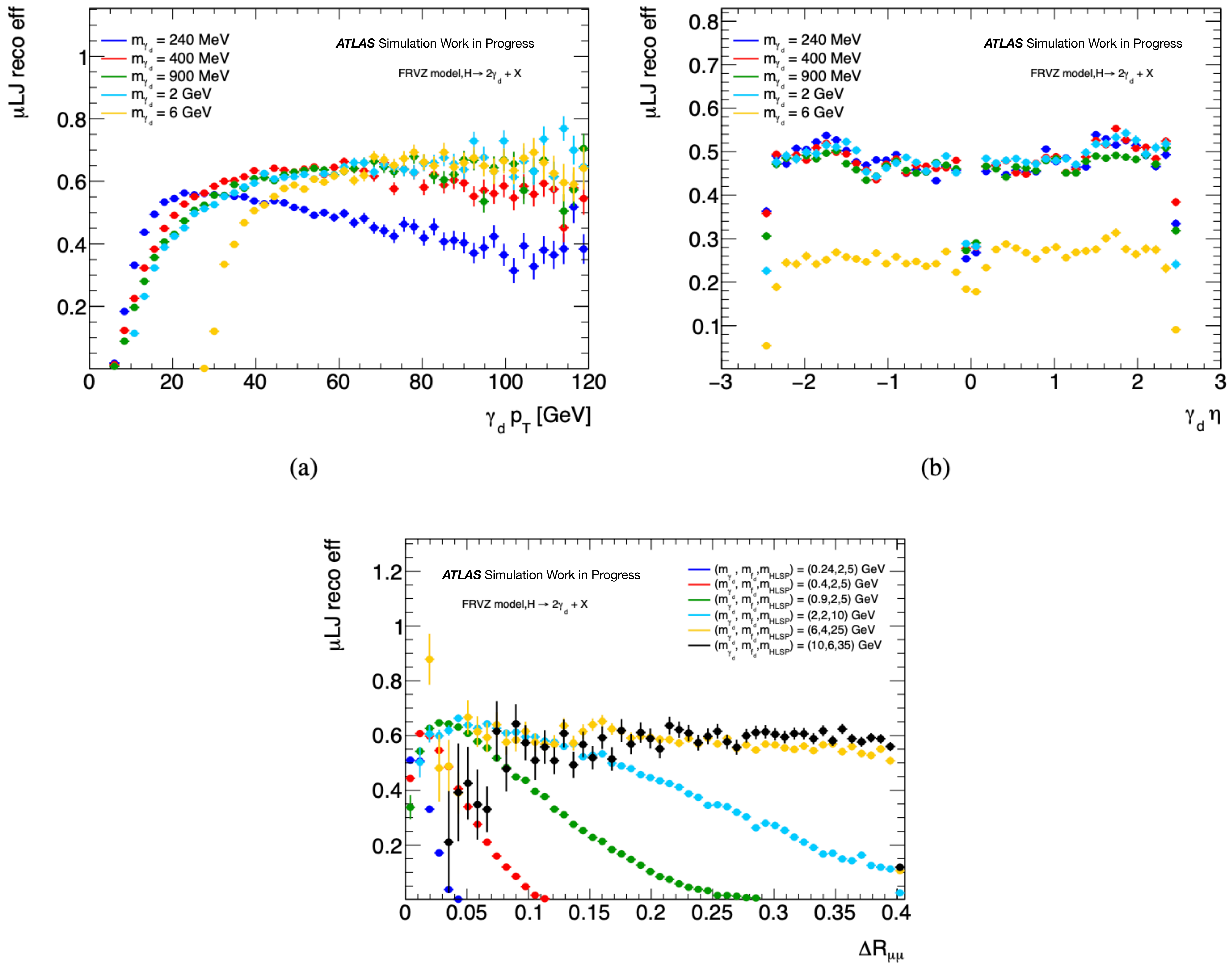

(c)

Figure 5.2: The reconstruction efficiency for μLJ produced by the decay of γ_d according to the FRVZ model. (a) shows the efficiency as a function of the transverse momentum of the γ_d. (b) shows the reconstruction efficiency as a function of the dark photon η, while (c) shows the reconstruction efficiency as a function of the opening angle ΔR between its decay products.

ATLAS EXPERIMENT

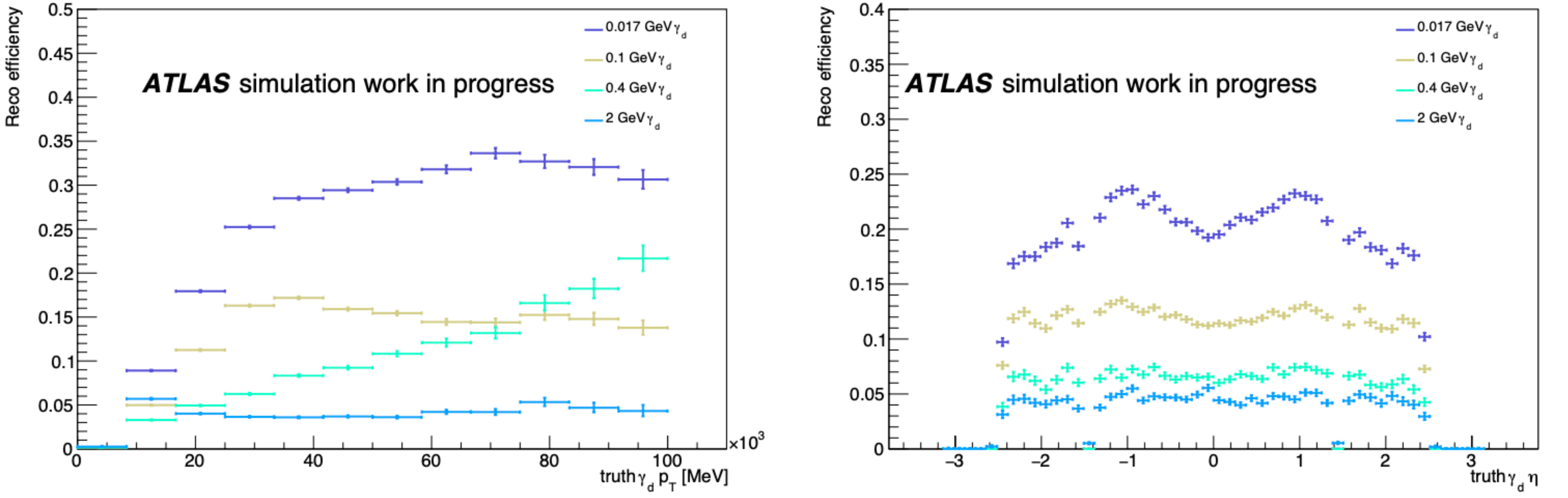

(a) (b)

Figure 5.5: The reconstruction efficiency for eLJs produced by the decay of γ_{d} into e^+e^-. Figure (a) shows the reconstruction efficiency for γ_{d} as a function of the transverse momentum, input to the MC generation and referred to as true γ_{d}. Figure (b) shows the reconstruction efficiency for γ_{d} as a function of the pseudorapidity.

Numero di elettroni nei eLJ

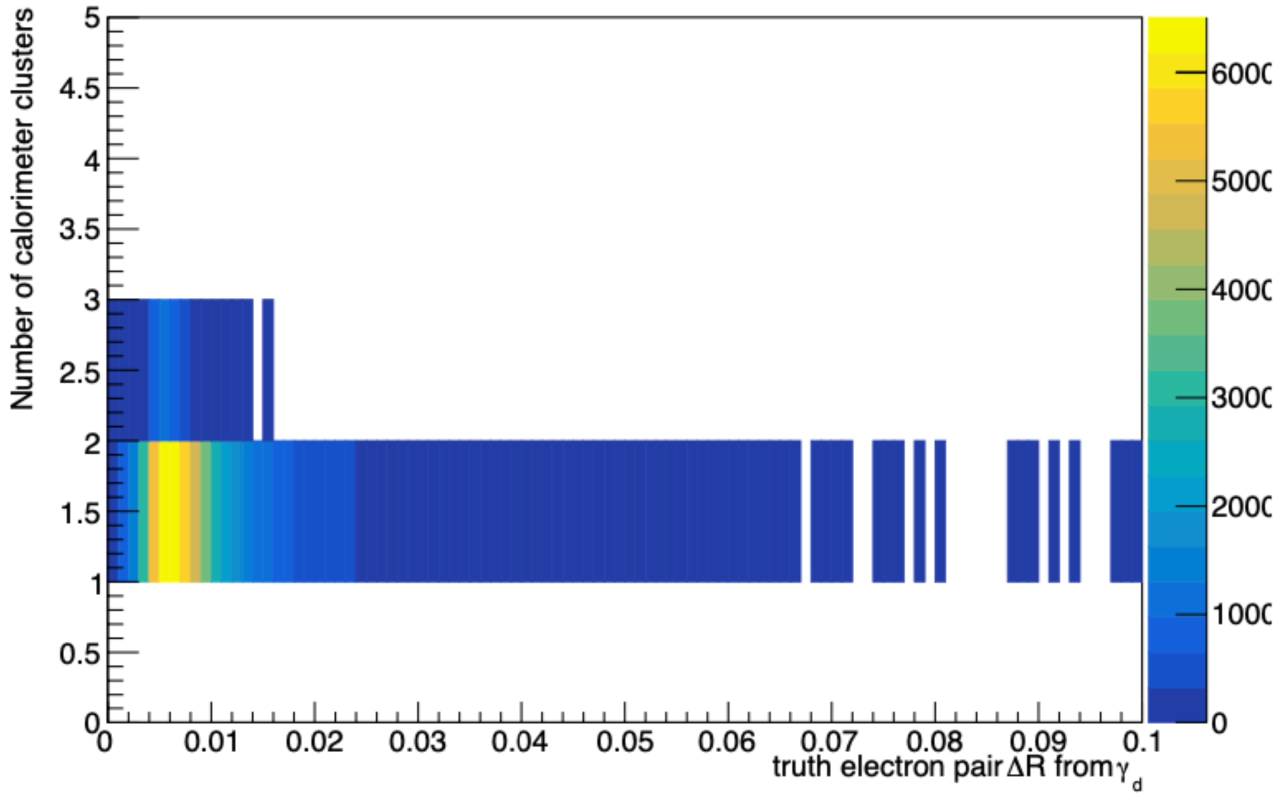

(a)

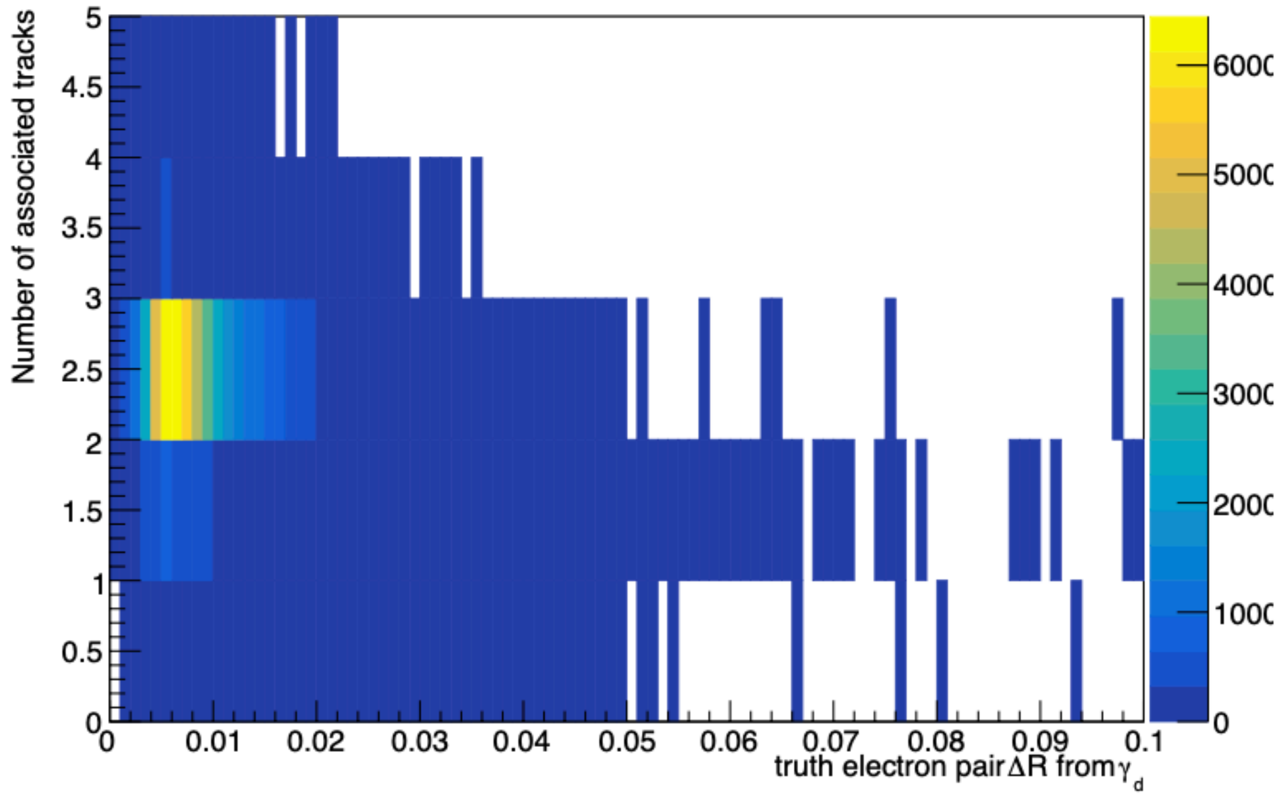

(b)

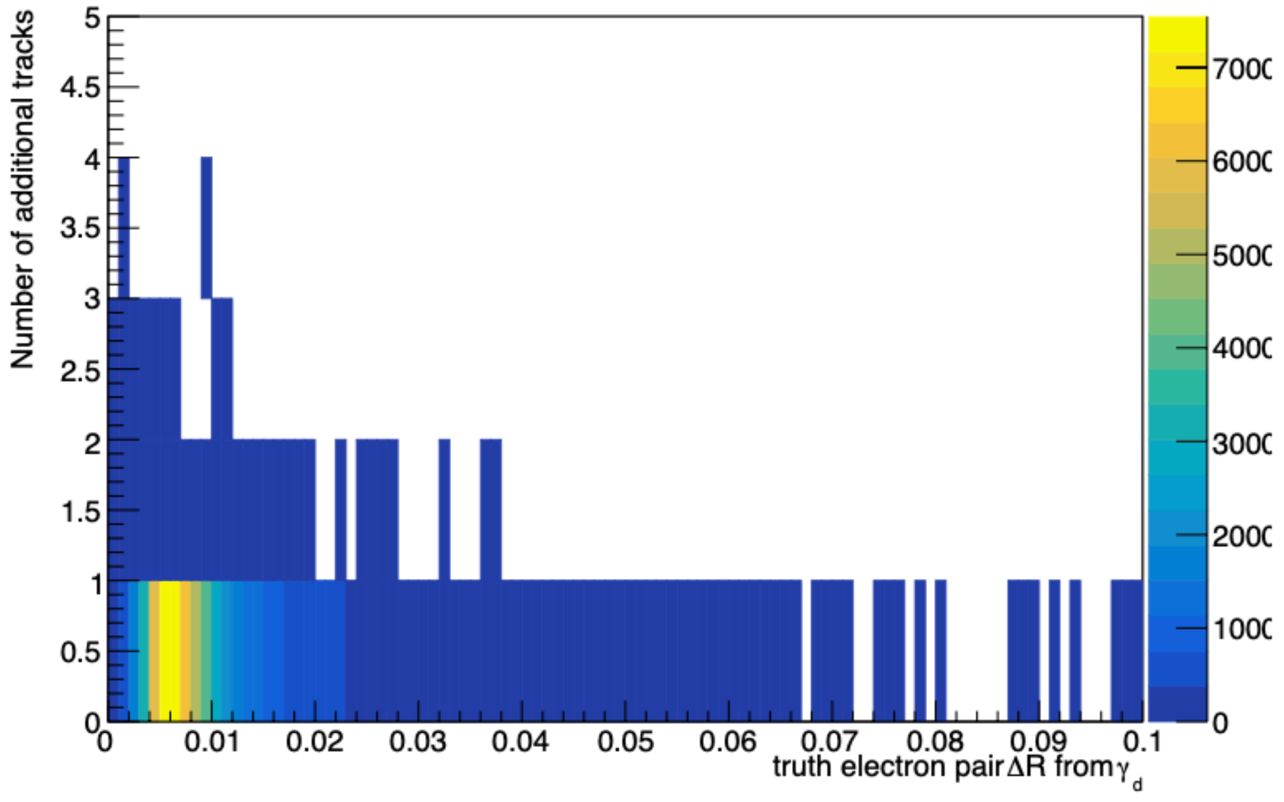

(c)

Figure 5.4: (a) Number of calorimeter clusters in eLJ as a function of ΔR between truth electrons. Number of (b) associated and (c) non-associated tracks in eLJ, as a function of ΔR between truth electrons. These plots are produced from a signal sample with a dark photon mass of 0.1 GeV.

Preselezione e strategia di trigger

- Preselezione degli eventi:
  - L'evento deve essere nella GRL + presenza di almeno un "good primary vertex"
  - Ricostruzione di almeno 2 LJ
  - Passare strategia di trigger
  - Trigger matching
- 1μLJ + 1eLJ —> OR logico di trigger di **singolo elettrone**, **di-muon** e **trigger misti** e-μ

Type	Data-taking periods	Trigger
Single-electron	2015	HLT_e24_lhmedium_L1EM20VH
		HLT_e60_lhmedium
		HLT_e120_lhloose
	2016 A-end	HLT_e26_lhtight_nod0_ivarloose
		HLT_e60_lhmedium_nod0
		HLT_e140_lhloose_nod0
Di-muon	2015	HLT_mu18_mu8noL1
	2015 - 2016 A	HLT_2mu10
	2016 A - E	HLT_mu20_mu8noL1
	2016 B - end - 2017 - 2018	HLT_2mu14
	2016 F - end - 2017 -2018	HLT_mu22_mu8noL1
Electron-muon	2015	HLT_e7_lhmedium_mu24
		HLT_e17_lhloose_mu14
	2016 - 2017 -2018	HLT_e17_lhloose_nod0_mu14
	2016 A	HLT_e24_lhmedium_nod0_L1EM20VHI_mu8noL1
	2016 B-E	HLT_e7_lhmedium_nod0_mu24
	2016 F-end	HLT_e26_lhmedium_nod0_L1EM22VHI_mu8noL1
	2017-2018	HLT_e26_lhmedium_nod0_mu8noL1

Massa invariante μLJ

- μLJ sempre con 2 muoni: massa invariate con i muoni ricostruiti
- Buona risoluzione della massa invariante (come nel canale muonico)

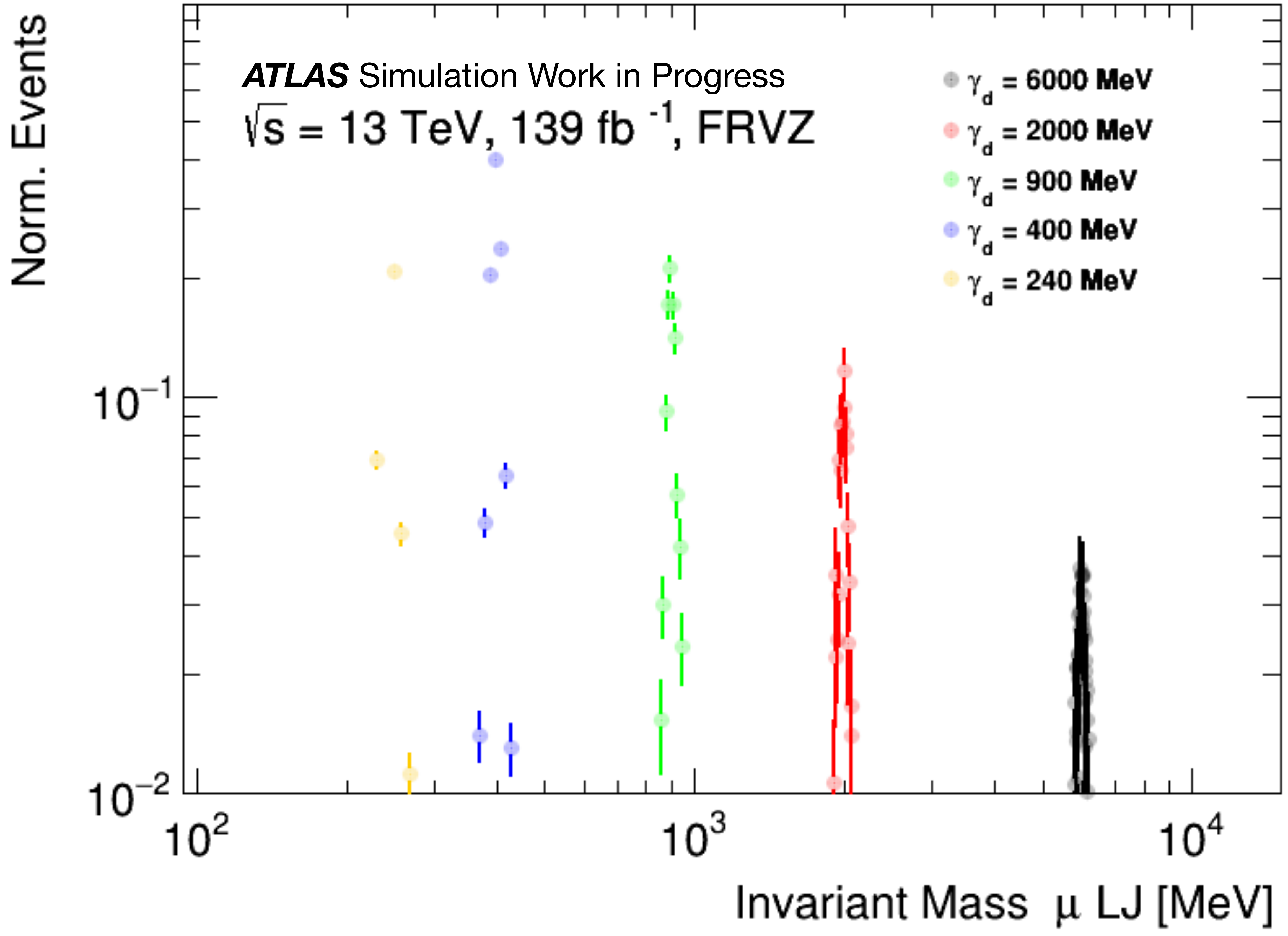

Massa invariante eLJ

- eLJ con 1 elettrone: massa invariate ricostruita dalle tracce:
  1. Traccia *best-matched* con stessa carica dell'elettrone
  2. Traccia con carica opposta con più alto p_T
- eLJ con 2 elettroni: massa invariate dagli elettroni ricostruiti

eLJ con 2 elettroni

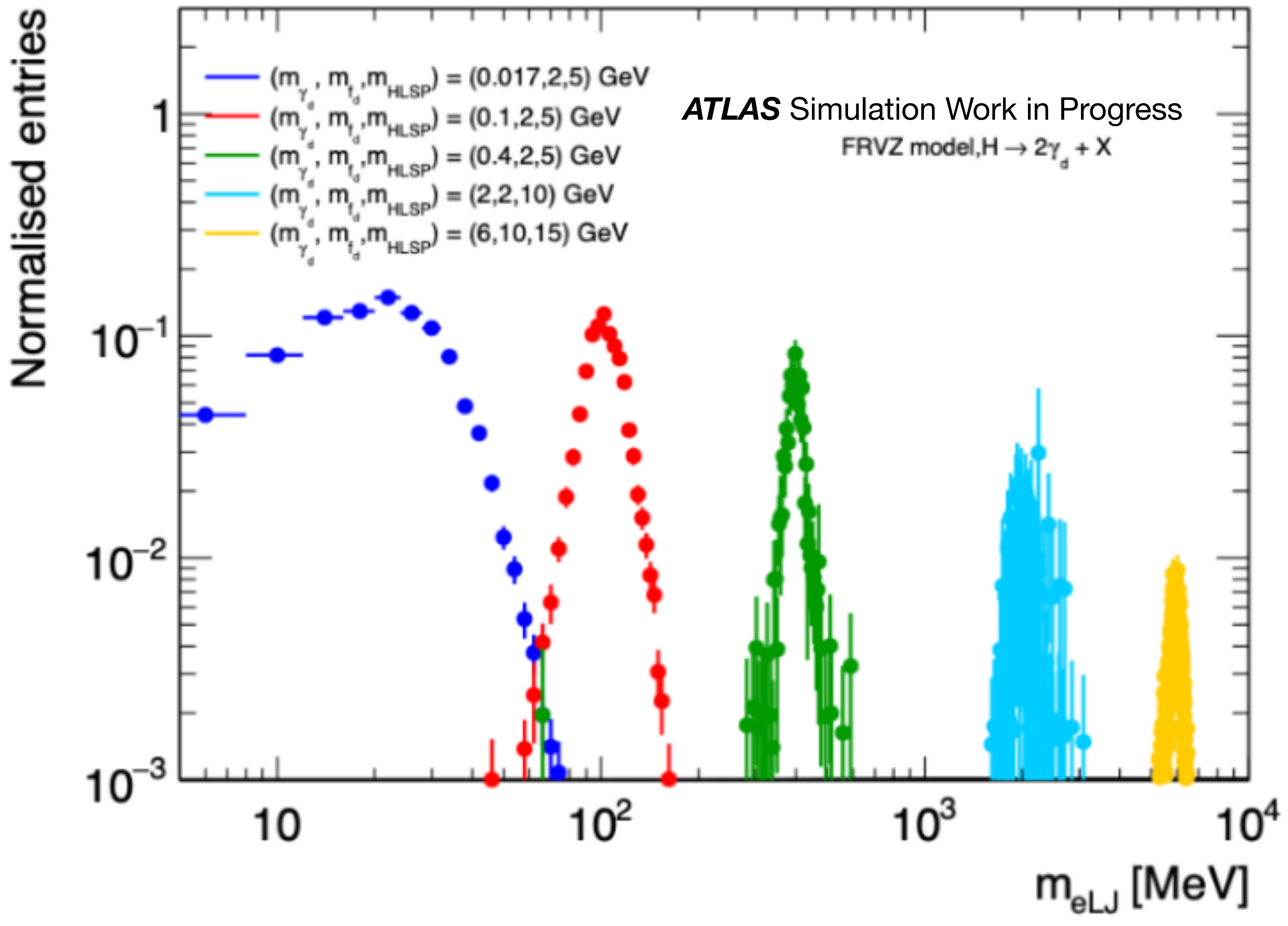

eLJ con 1 elettrone

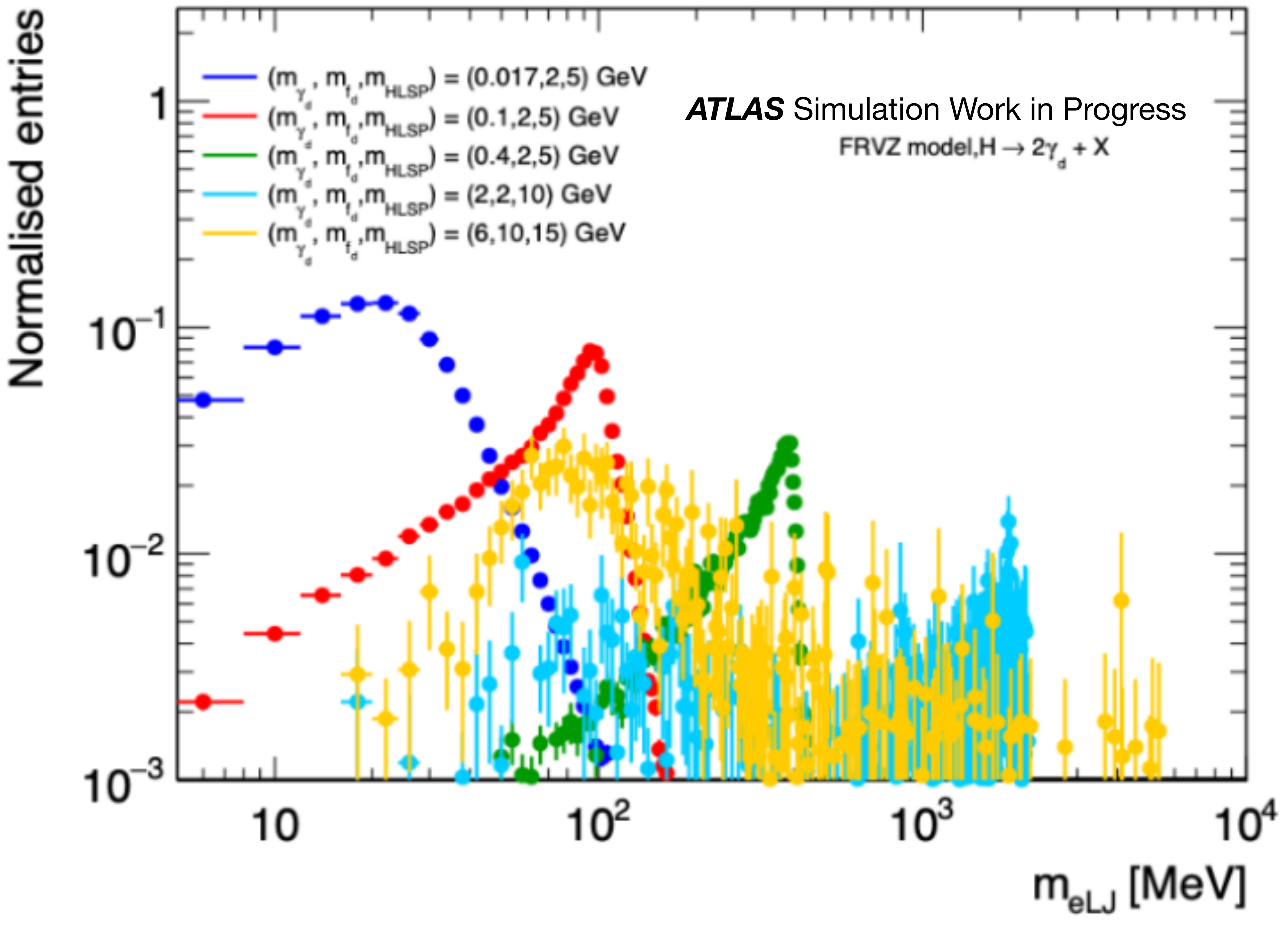

Massa invariante eLJ: 1 elettrone VS 2 elettroni

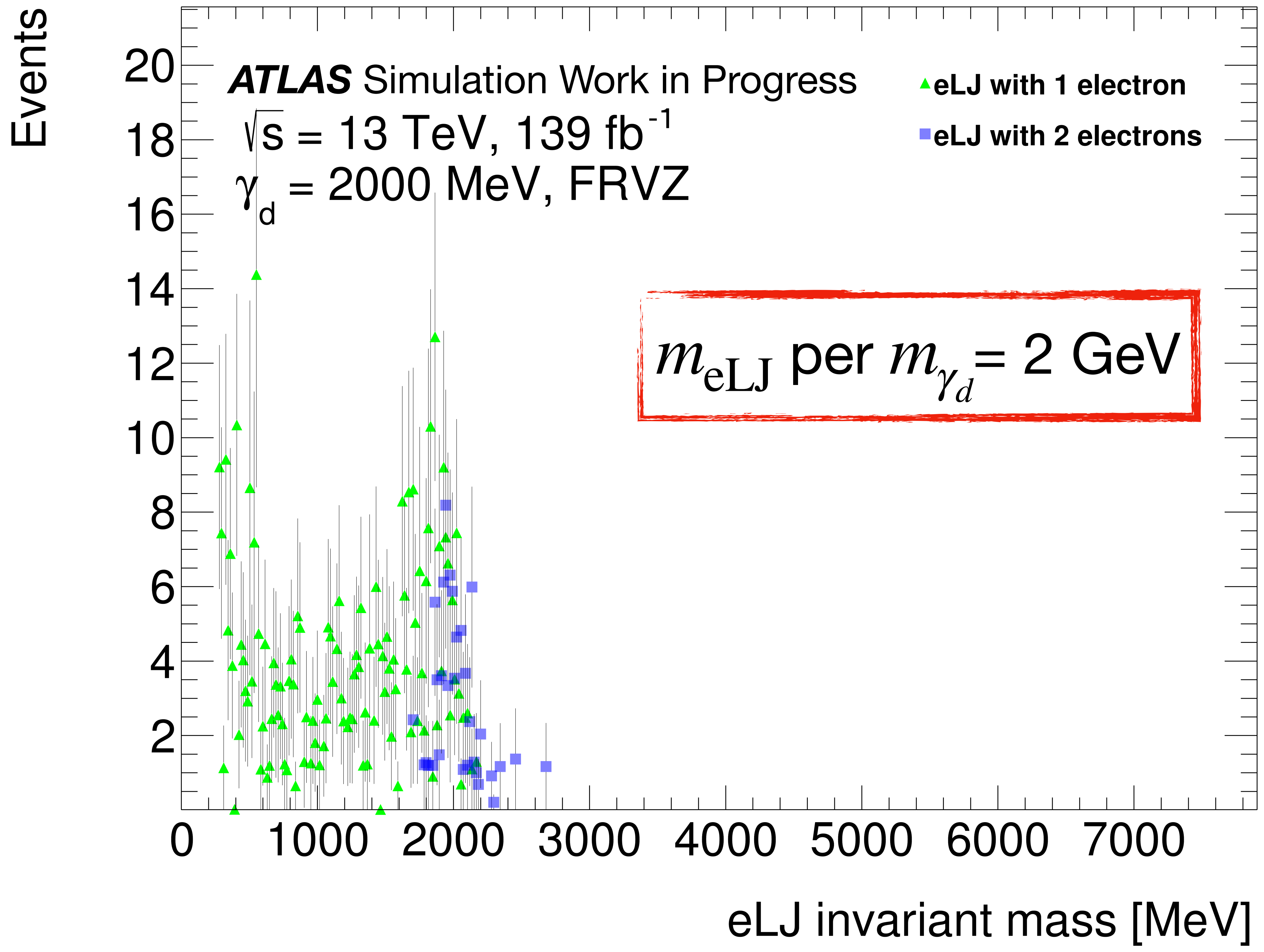

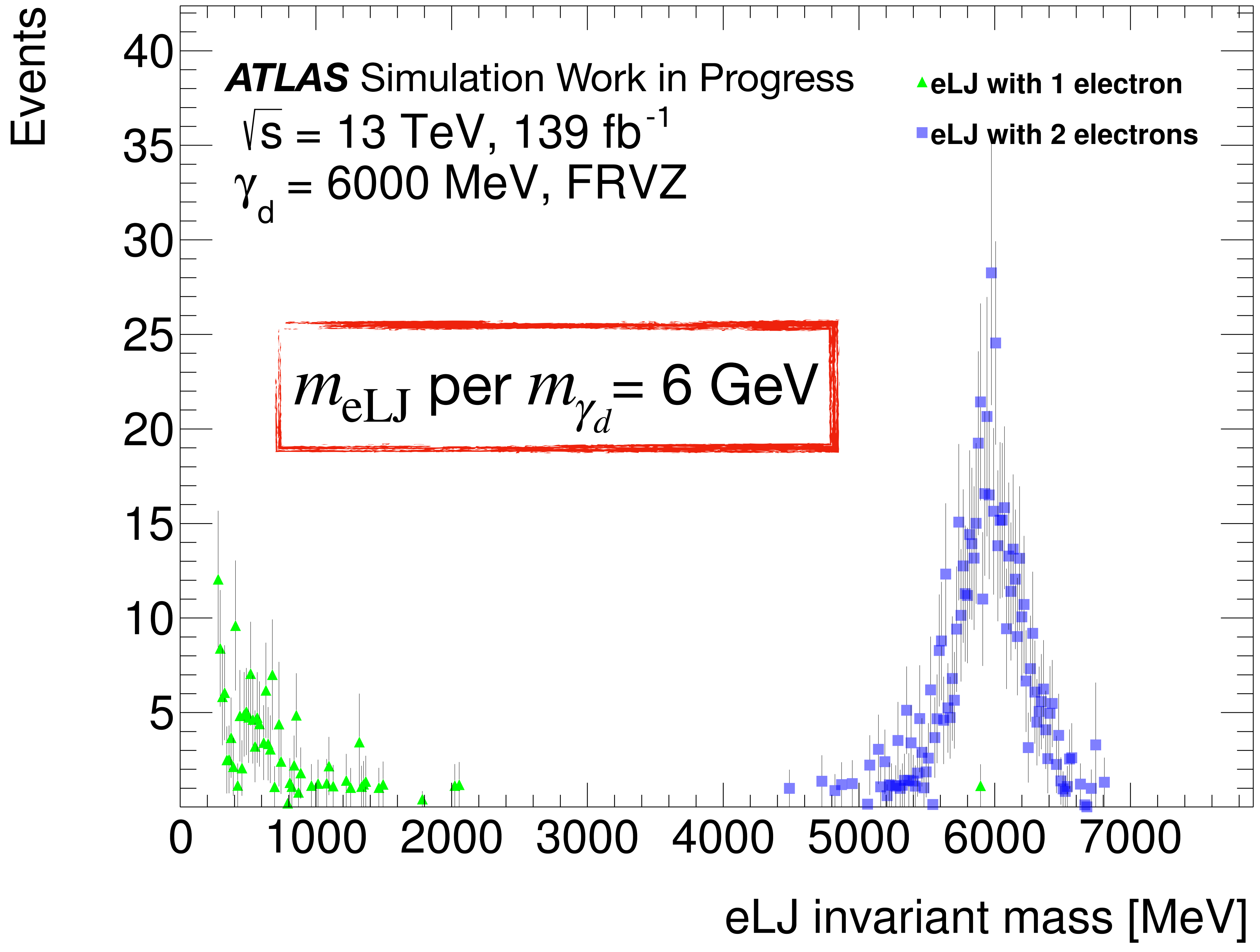

eLJ ricostruiti con 1 elettrone per alte m_{γ_d}:

- Due elettroni troppo lontani per ricostruire un eLJ
- Due elettroni sono abbastanza vicini, ma uno fallisce requirements del WP e ISO —> eLJ ricostruito da un elettrone + traccia random

Efficienze di trigger e Trigger matching

Type	Data-taking periods	Trigger
Single-electron	2015	HLT_e24_lhmedium_L1EM20VH
		HLT_e60_lhmedium
		HLT_e120_lhloose
	2016 A-end	HLT_e26_lhtight_nod0_ivarloose
		HLT_e60_lhmedium_nod0
		HLT_e140_lhloose_nod0
Di-muon	2015	HLT_mu18_mu8noL1
	2015 - 2016 A	HLT_2mu10
	2016 A - E	HLT_mu20_mu8noL1
	2016 B - end - 2017 - 2018	HLT_2mu14
	2016 F - end - 2017 -2018	HLT_mu22_mu8noL1
Electron-muon	2015	HLT_e7_lhmedium_mu24
		HLT_e17_lhloose_mu14
	2016 - 2017 -2018	HLT_e17_lhloose_nod0_mu14
	2016 A	HLT_e24_lhmedium_nod0_L1EM20VHI_mu8noL1
	2016 B-E	HLT_e7_lhmedium_nod0_mu24
	2016 F-end	HLT_e26_lhmedium_nod0_L1EM22VHI_mu8noL1
	2017-2018	HLT_e26_lhmedium_nod0_mu8noL1

FRVZ

	240 MeV	400 MeV	900 MeV	2 GeV	6 GeV
2015	0.64 ± 0.04	0.65 ± 0.06	0.83 ± 0.08	0.86 ± 0.13	0.94 ± 0.06
2016 A	0.70 ± 0.09	0.69 ± 0.19	$1.00^{+0.00}_{-0.35}$	0.67 ± 0.27	$1.00^{+0.00}_{-0.48}$
2016 B-E	0.505 ± 0.021	0.500 ± 0.029	0.63 ± 0.05	0.60 ± 0.08	0.926 ± 0.032
2016 F-end	0.497 ± 0.015	0.575 ± 0.020	0.681 ± 0.034	0.56 ± 0.06	0.830 ± 0.032
2017	0.600 ± 0.013	0.679 ± 0.016	0.733 ± 0.028	0.65 ± 0.05	0.863 ± 0.028
2018	0.615 ± 0.010	0.681 ± 0.013	0.741 ± 0.022	0.653 ± 0.034	0.907 ± 0.017

HAHM

	400 MeV	2 GeV	10 GeV
2015	0.939 ± 0.015	0.86 ± 0.07	0.987 ± 0.013
2016 A	0.90 ± 0.04	$1.00^{+0.00}_{-0.34}$	$1.00^{0.00}_{-0.14}$
2016 B-E	0.824 ± 0.012	0.79 ± 0.04	0.934 ± 0.015
2016 F-end	0.863 ± 0.008	0.832 ± 0.023	0.988 ± 0.004
2017	0.926 ± 0.005	0.917 ± 0.014	0.9939 ± 0.0025
2018	0.911 ± 0.004	0.869 ± 0.014	0.9882 ± 0.0030

Trigger matching:

- Se trigger di singolo elettrone: trigger matching con almeno un elettrone nel eLJ
- Se di-muon trigger: trigger matching con entrambi i muoni nel μLJ
- Se e-μ trigger: trigger matching sia l'elettrone che con il muone

ATLAS EXPERIMENT

Fondo

eLJ
- elettroni ricostruiti attraversati da tracce
- elettroni provenienti da fotoni virtuali γ^*

μLJ: Risonanze che decadono in coppie di muoni

Regione di segnale

1μLJ + 1eLJ

$|\eta|$eLJ < 1.37

$|\Delta\phi|(\mu\mathrm{LJ}, e\mathrm{LJ}) > 2$

$q_{\mathrm{eLJ}}, q_{\mu\mathrm{LJ}} = 0$

$p_{\mathrm{T}}^{\mathrm{imb}}(\mu\mathrm{LJ}, e\mathrm{LJ}) < 0.8$

Simulazioni MC

Regione di Controllo

1μLJ + 0eLJ + 0μ + 2e

$|\eta|ee < 1.37$

$|\Delta\phi|(\mu\mathrm{LJ}, ee) > 2$

$q_{\mu\mathrm{LJ}} = 0$

$m^{\mathrm{imb}}(\mu\mathrm{LJ}, ee) > 0.6$

Data-driven

Più dettagli in backup

Regione di Segnale e di Controllo

	SR	CR
Triggers	single-e/di-μ/$e-\mu$	single-e/di-μ/$e-\mu$
Segnatura	1μLJ + $1e$LJ	1μLJ + $0e$LJ + 0μ + $2e$
traccia p_{T} eLJ	> 5 GeV	> 5 GeV
eLJ $\|\eta\|$	< 1.37	/
$\|\Delta\phi\|(\mu\mathrm{LJ},e\mathrm{LJ})$	> 2	> 2
q_{eLJ}	$= 0$	/
$q_{\mu\mathrm{LJ}}$	$= 0$	$= 0$
$\|p_{\mathrm{T}}^{imb}\|$ $(\mu\mathrm{LJ},e\mathrm{LJ})$	< 0.8	/
$m_{imb}(\mu\mathrm{LJ},e\mathrm{LJ})$	/	> 0.6

In CR: coppia di elettroni usata come un "*finto*" eLJ

Ortogonalità con canale muonico ed elettronico

V + *jets* in regione ad alto η

γ_d prodotti "*back-to-back*"

Neutralità dei LJ

Distribuzione del p_{T} dei LJ non sbilanciata

Rimuove segnale per alti m_{γ_d}

Regione di Segnale

ATLAS EXPERIMENT

FRVZ

m_{γ_d}	240 MeV	400 MeV	900 MeV	2 GeV	6 GeV
Triggers	44210 ± 240	41150 ± 230	35090 ± 210	45380 ± 240	49680 ± 250
1 μLJ, 1 eLJ	3880 ± 70	2470 ± 50	834 ± 32	331 ± 20	711 ± 29
Trigger matching	3650 ± 70	2370 ± 50	802 ± 31	324 ± 20	698 ± 29
eLJ p_{T} track > 5 GeV	3630 ± 70	2340 ± 50	795 ± 31	315 ± 20	689 ± 28
eLJ $\lvert\eta\rvert < 1.37$	2500 ± 60	1670 ± 50	613 ± 27	203 ± 16	501 ± 24
$\lvert\Delta\phi\rvert(\mu\mathrm{LJ},e\mathrm{LJ}) > 2$	1750 ± 50	1080 ± 40	354 ± 21	100 ± 11	361 ± 21
$q_{eLJ} = 0$	1700 ± 50	1070 ± 40	341 ± 21	88 ± 10	341 ± 20
$q_{\mu\mathrm{LJ}} = 0$	1700 ± 50	1070 ± 40	341 ± 21	88 ± 10	341 ± 20
$\lvert p_{\mathrm{T}}^{imb}\rvert < 0.8$	1320 ± 40	793 ± 31	275 ± 19	54 ± 8	323 ± 19

HAHM

m_{γ_d}	400 MeV	2 GeV	10 GeV
Triggers	126600 ± 400	98570 ± 350	150100 ± 400
1 μLJ, 1 eLJ	12400 ± 120	1500 ± 40	3710 ± 70
Trigger matching	12310 ± 120	1480 ± 40	3700 ± 70
eLJ p_{T} track > 5 GeV	12270 ± 120	1470 ± 40	3670 ± 70
eLJ $\lvert\eta\rvert < 1.37$	8840 ± 110	1080 ± 40	2610 ± 60
$\lvert\Delta\phi\rvert(\mu\mathrm{LJ},e\mathrm{LJ}) > 2$	6810 ± 90	625 ± 27	2260 ± 50
$q_{eLJ} = 0$	6630 ± 90	581 ± 26	2190 ± 50
$q_{\mu\mathrm{LJ}} = 0$	6630 ± 90	581 ± 26	2190 ± 50
$\lvert p_{\mathrm{T}}^{imb}\rvert < 0.8$	5470 ± 80	425 ± 22	2130 ± 50

$\sigma_{\mathrm{ggF}} = 48.51$ pb, L = 139 fb^{-1}, BR$(H \to 2\gamma_d + X) = 5\,\%$

Regione di Controllo

ATLAS EXPERIMENT

FRVZ

Selection cuts	240 MeV	400 MeV	900 MeV	2 GeV	6 GeV
Triggers	44210 ± 240	41150 ± 230	35090 ± 210	45380 ± 240	49680 ± 250
1 μLJ, 0 eLJ, 0 μ, $e \geq 2$	9.5 ± 3.4	5.5 ± 2.5	12 ± 4	21 ± 5	650 ± 28
Trigger matching	6.1 ± 2.7	3.4 ± 2.0	7.0 ± 2.9	17 ± 4	579 ± 26
ee p_T track > 5 GeV	6.1 ± 2.7	3.4 ± 2.0	7.0 ± 2.9	15 ± 4	579 ± 26
$\lvert\Delta\phi\rvert(\mu\mathrm{LJ}, ee) > 2$	2.4 ± 1.7	2.2 ± 1.6	2.4 ± 1.7	11.2 ± 3.5	433 ± 22
$q_{\mu\mathrm{LJ}} = 0$	2.4 ± 1.7	2.2 ± 1.6	2.4 ± 1.7	11.2 ± 3.5	433 ± 22
$m_{imb} > 0.6$	2.4 ± 1.7	2.2 ± 1.6	2.4 ± 1.7	6.4 ± 2.6	1.3 ± 0.9

HAHM

Selection cuts	400 MeV	2 GeV	10 GeV
Triggers	126600 ± 400	98570 ± 350	150100 ± 400
1 μLJ, 0 eLJ, 0 μ, $e \geq 2$	23 ± 5	14 ± 4	3320 ± 60
Trigger matching	22 ± 5	10.2 ± 3.4	3250 ± 60
ee p_T track > 5 GeV	22 ± 5	10.2 ± 3.4	3250 ± 60
$\lvert\Delta\phi\rvert(\mu\mathrm{LJ}, ee) > 2$	18 ± 5	4.4 ± 2.2	2730 ± 60
$q_{\mu\mathrm{LJ}} = 0$	18 ± 5	4.4 ± 2.2	2730 ± 60
$m_{imb} > 0.6$	12 ± 4	4.4 ± 2.2	3.9 ± 2.1

$\sigma_{\mathrm{ggF}} = 48.51$ pb, L = 139 fb^{-1}, BR$(H \rightarrow 2\gamma_d + X) = 5\,\%$

Modelling della forma del segnale

Double-Sided Crystal Ball

$$N \cdot \begin{cases} e^{-t^2/2} & \text{if } -\alpha_{\text{low}} \leq t \leq \alpha_{\text{high}} \\ \dfrac{e^{-0.5\alpha_{\text{low}}^2}}{\left[\frac{\alpha_{\text{low}}}{n_{\text{low}}}\left(\frac{n_{\text{low}}}{\alpha_{\text{low}}}-\alpha_{\text{low}}-t\right)\right]^{n_{\text{low}}}} & \text{if } t < -\alpha_{\text{low}} \\ \dfrac{e^{-0.5\alpha_{\text{high}}^2}}{\left[\frac{\alpha_{\text{high}}}{n_{\text{high}}}\left(\frac{n_{\text{high}}}{\alpha_{\text{high}}}-\alpha_{\text{high}}+t\right)\right]^{n_{\text{high}}}} & \text{if } t > \alpha_{\text{high}}, \end{cases}$$

$$t = (m_{\mu\mu} - \mu_{\text{CB}})/\sigma_{\text{CB}}$$

n_h = const = 6
n_l = const = 3

Parametrizzazione del canale muonico buona anche per il canale misto

Poca statistica per m_{γ_d} = 2 GeV —> escluso dall'estrapolazione dei parametri

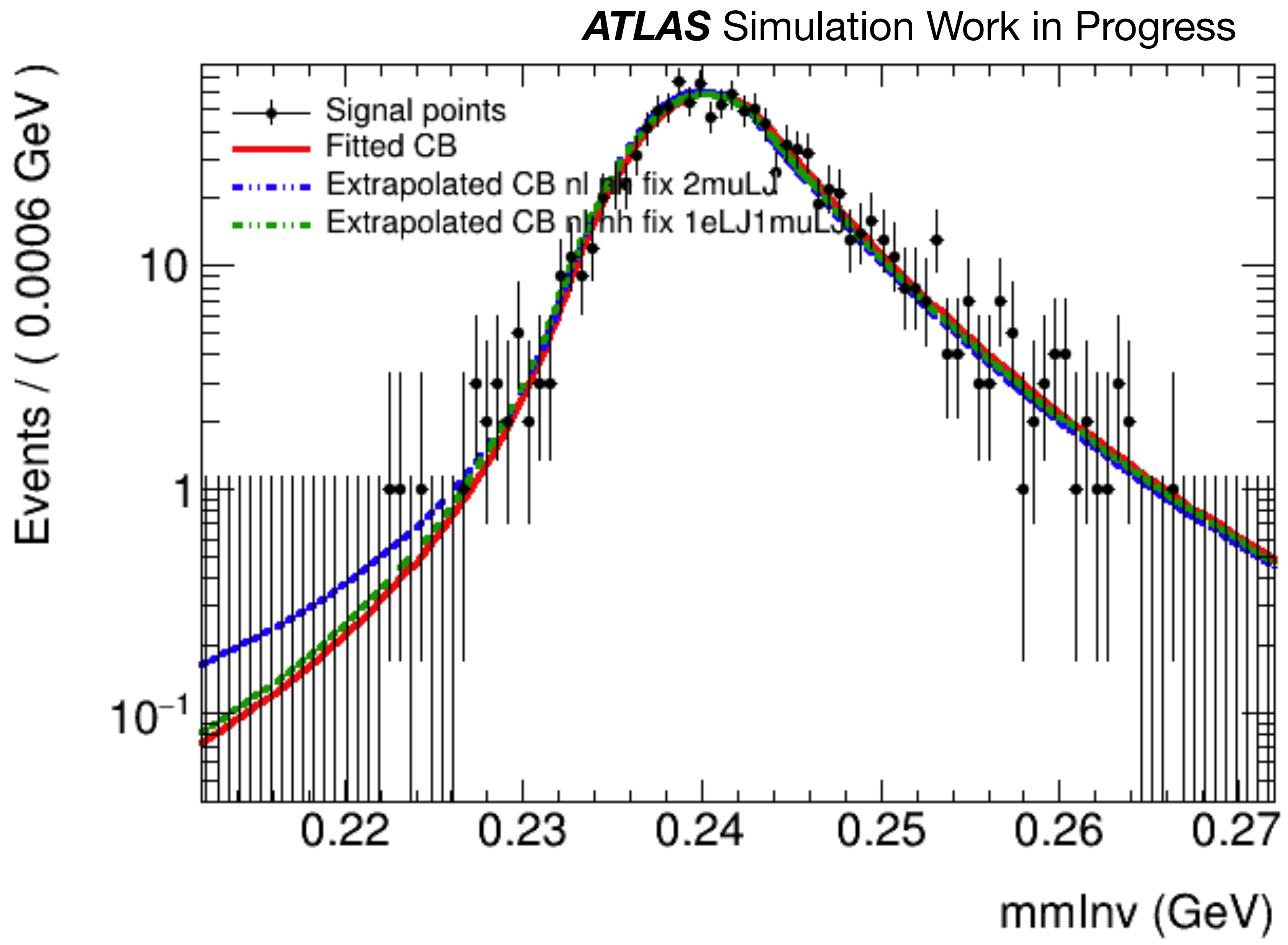

Modelling della forma del segnale: FRVZ

240 MeV

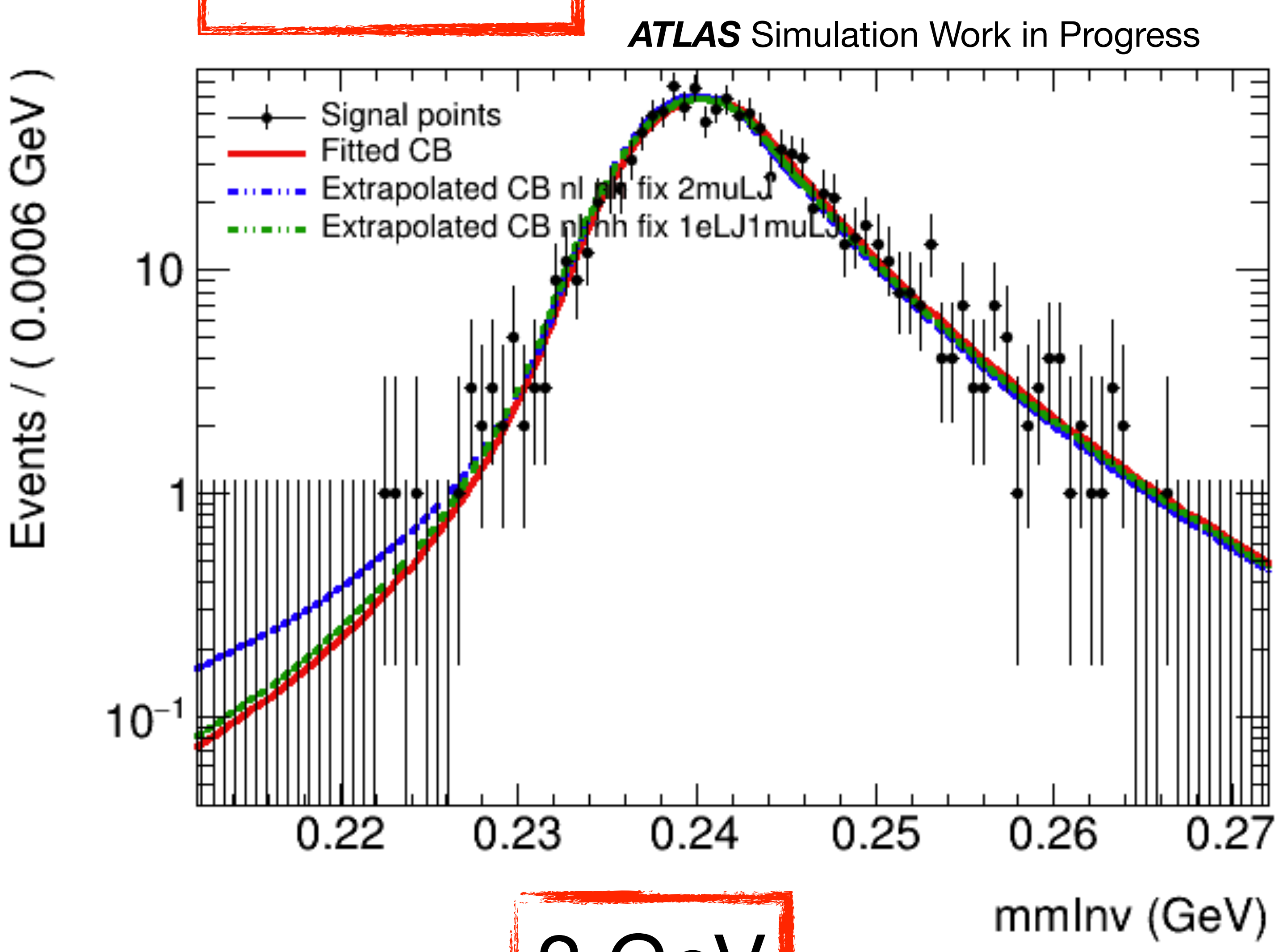

400 MeV

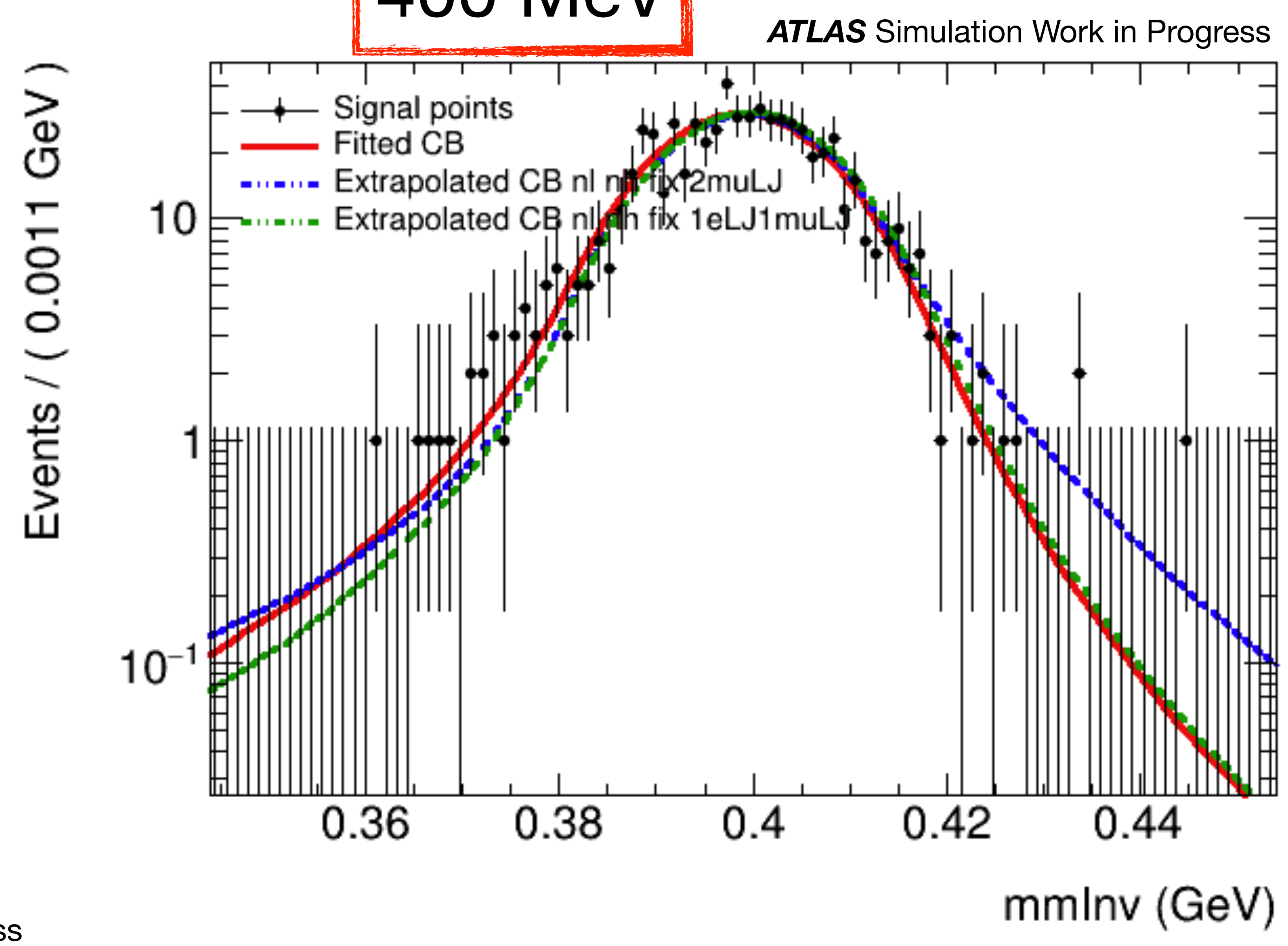

900 MeV

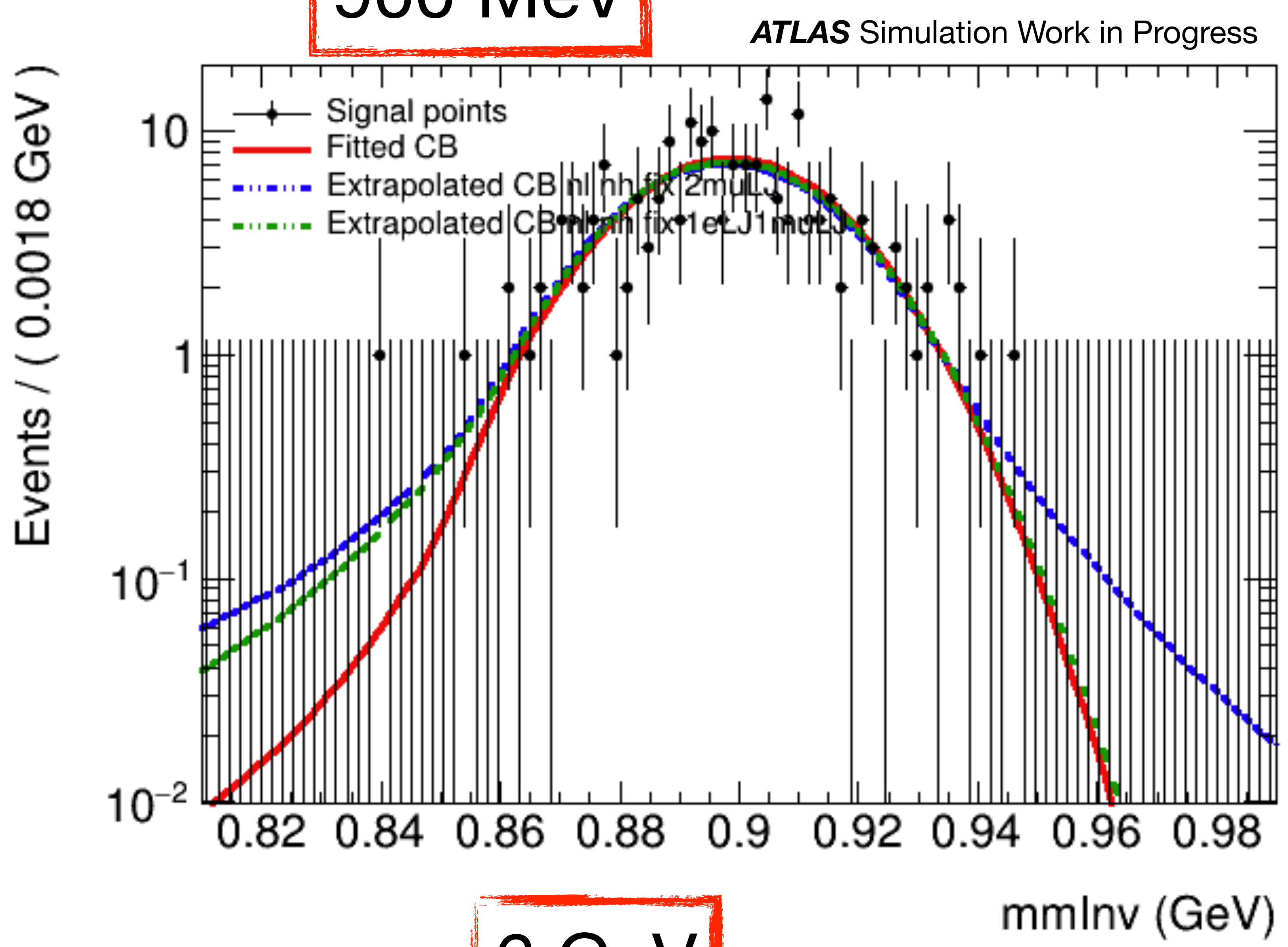

2 GeV

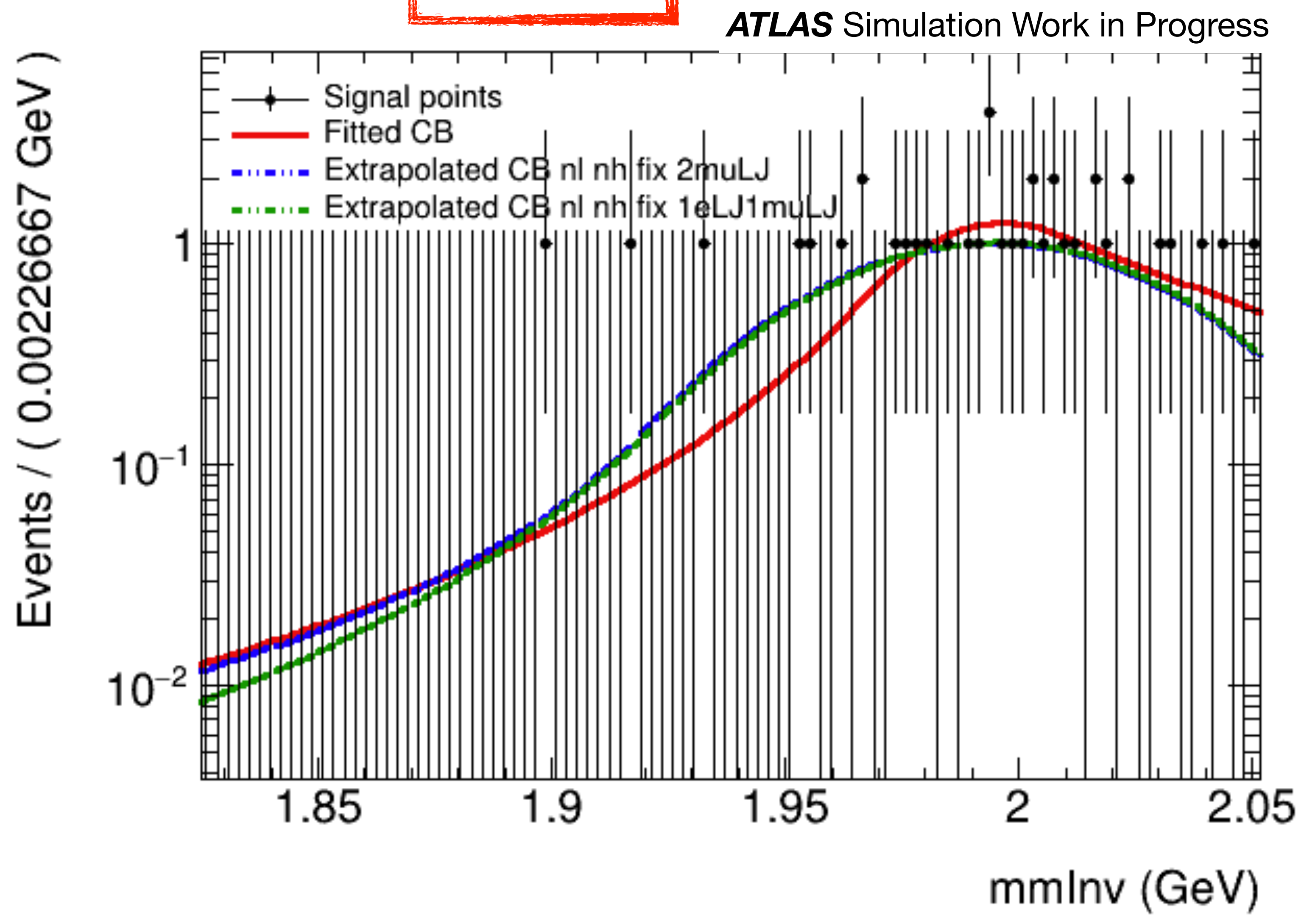

Fit DSCB

DSCB estrapolata 2μLJ

DSCB estrapolata μLJ-eLJ

6 GeV

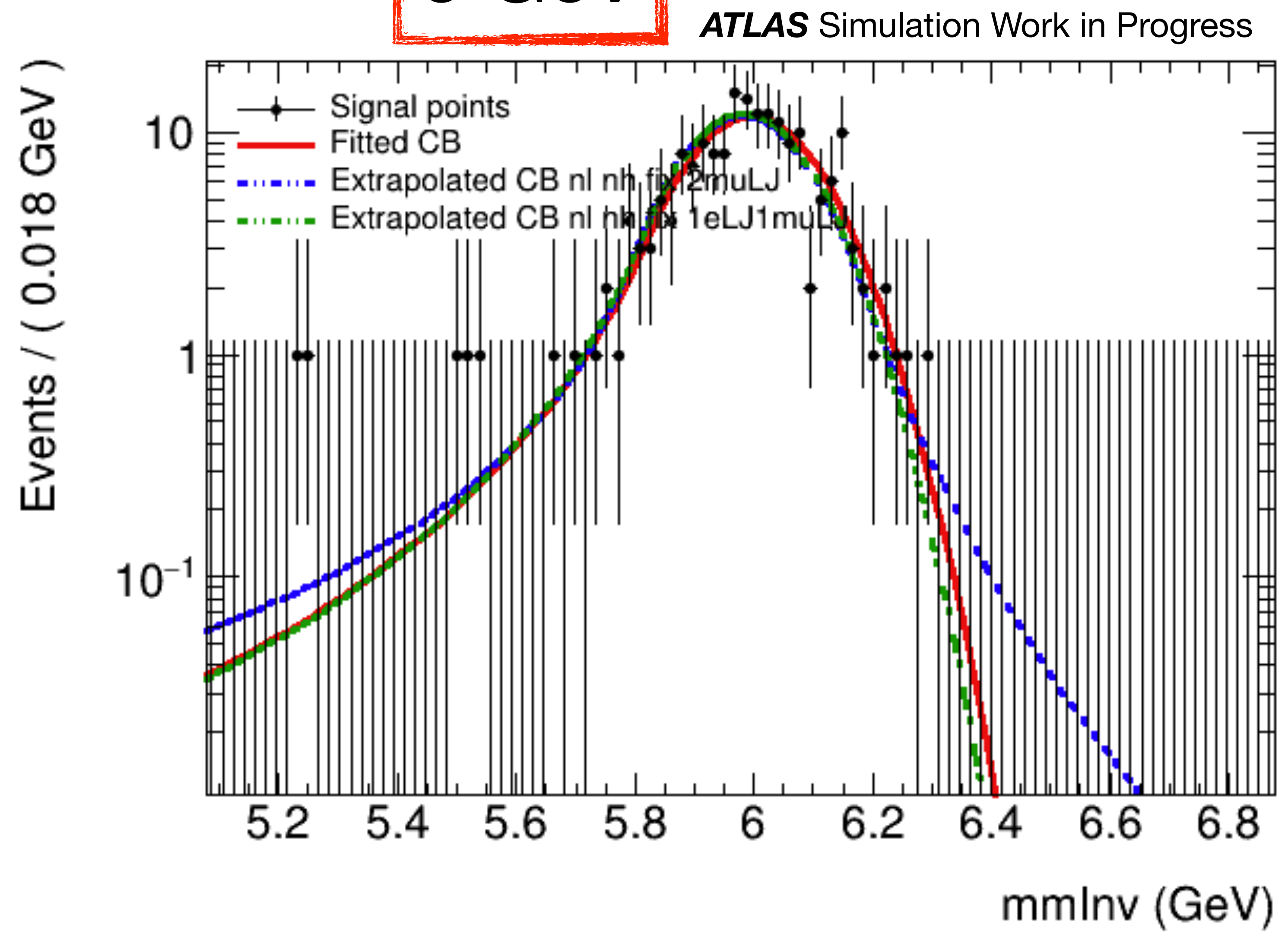

Estrapolazione dei parametri: FRVZ

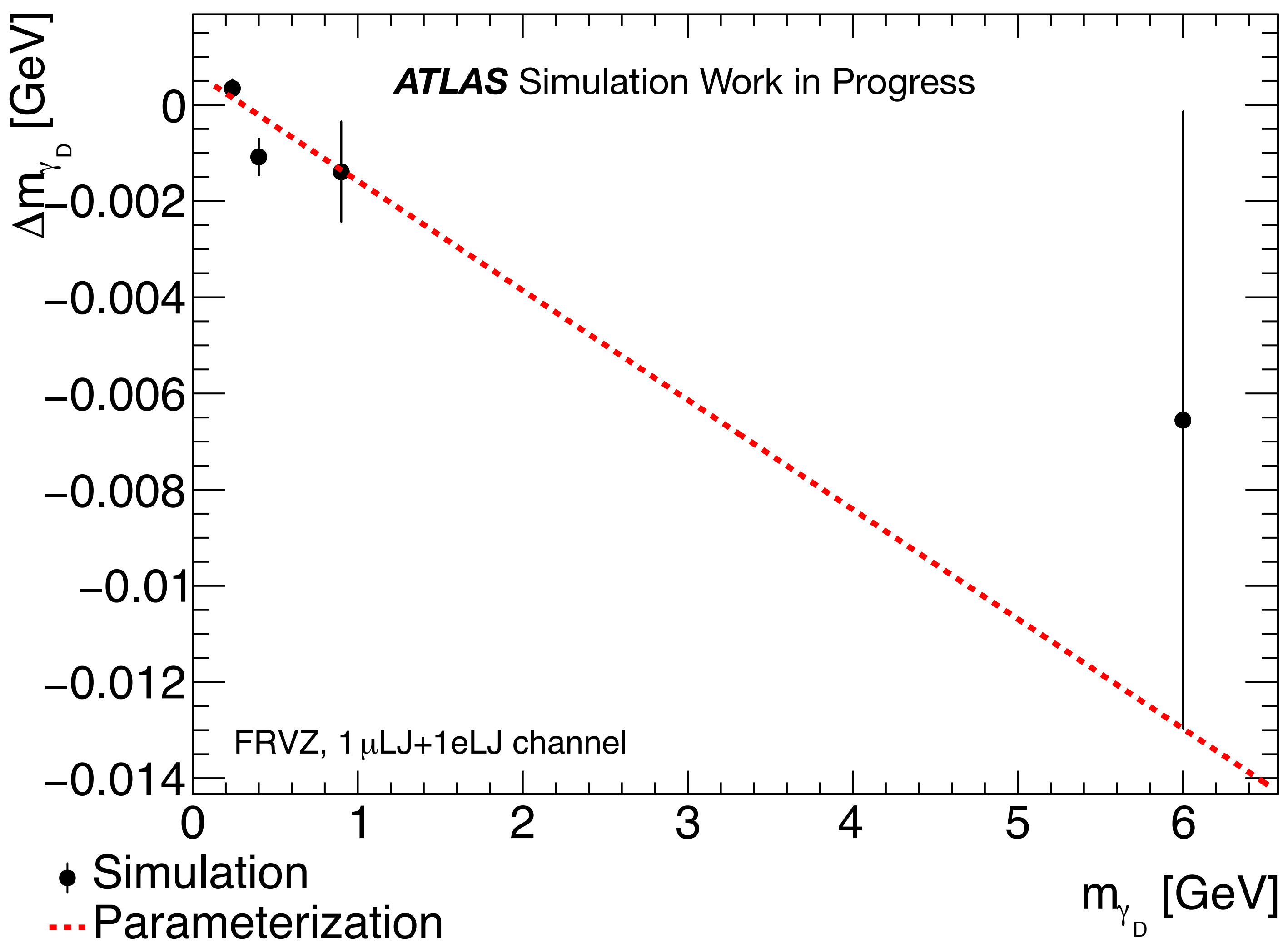

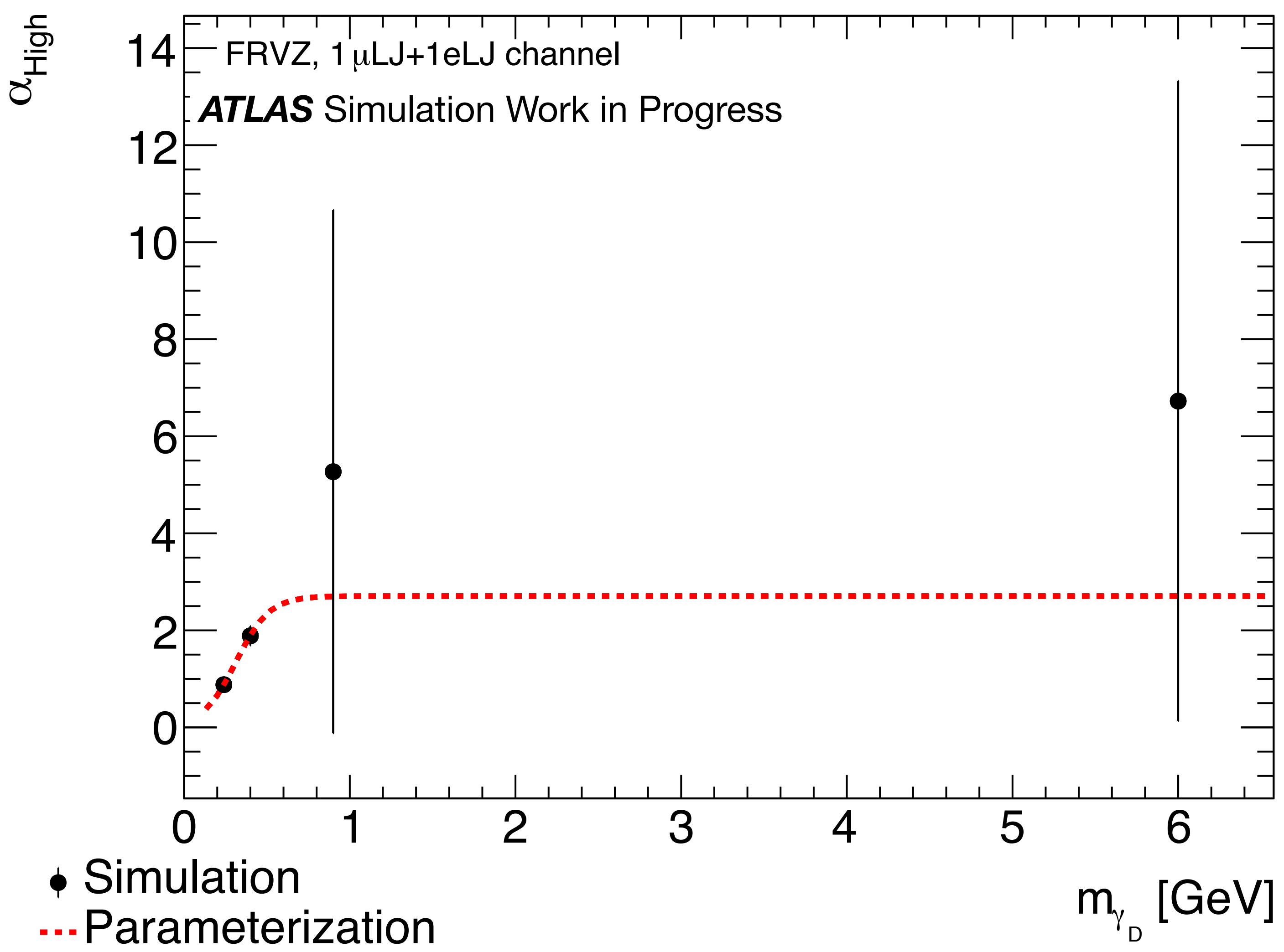

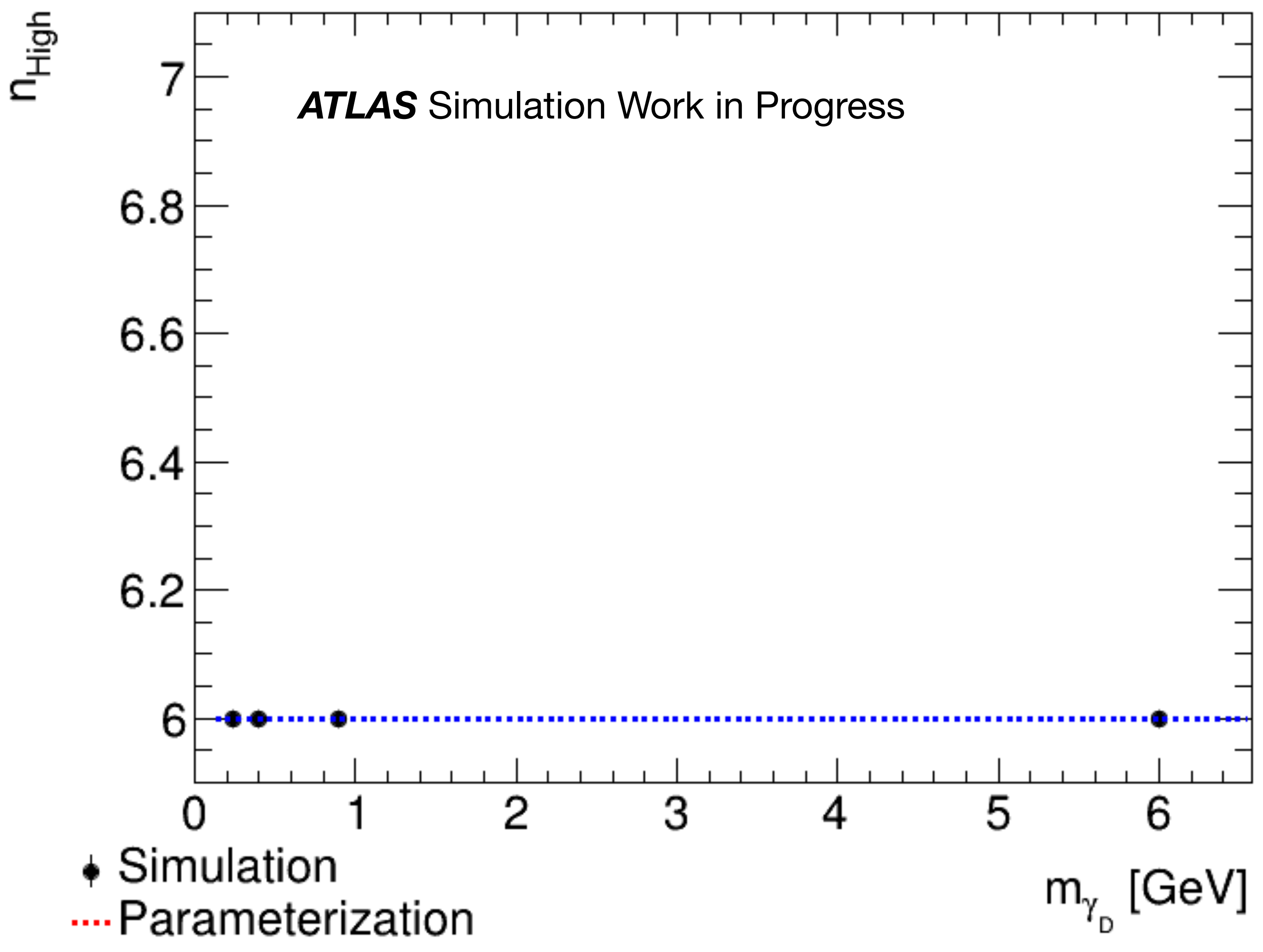

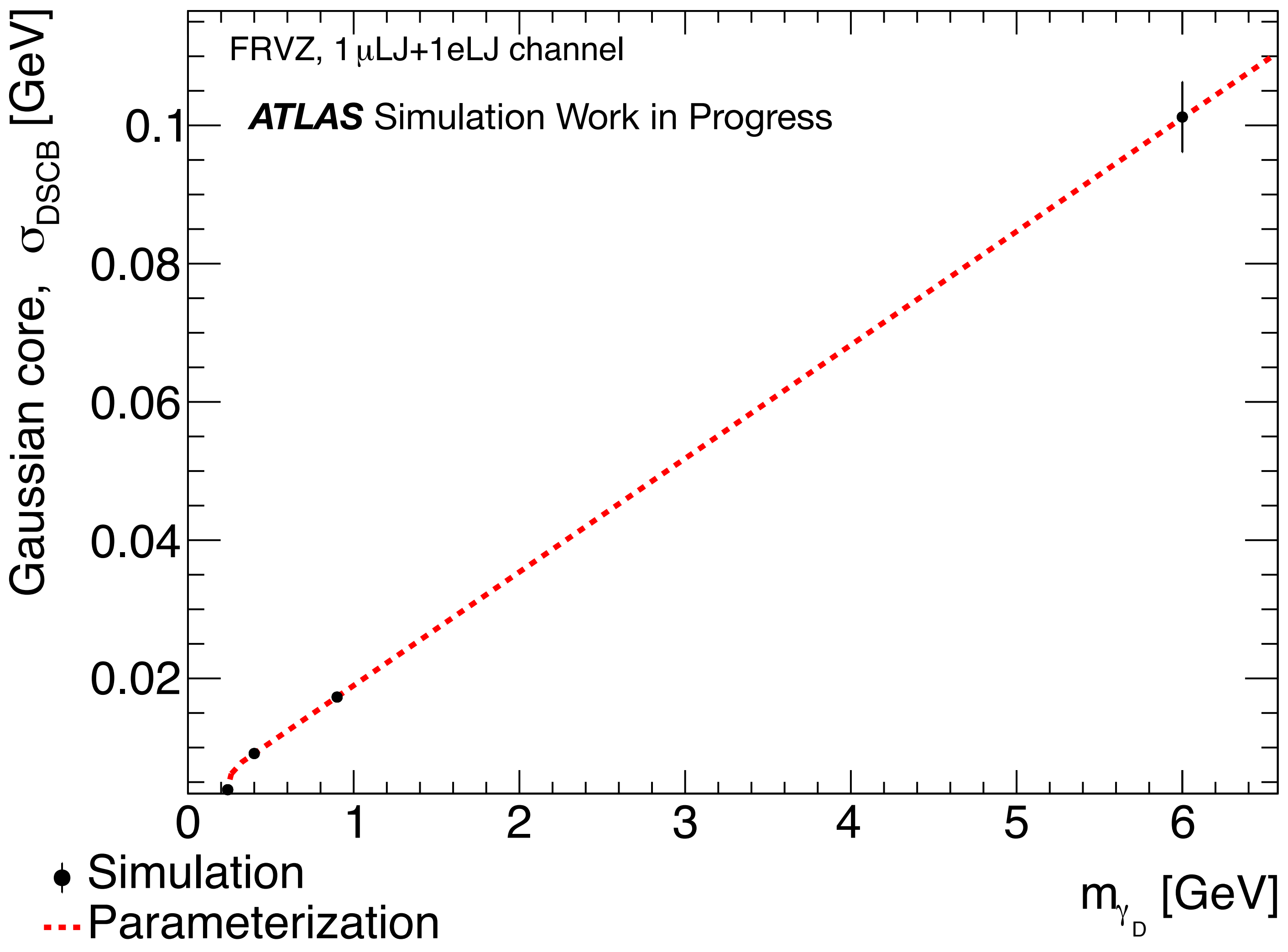

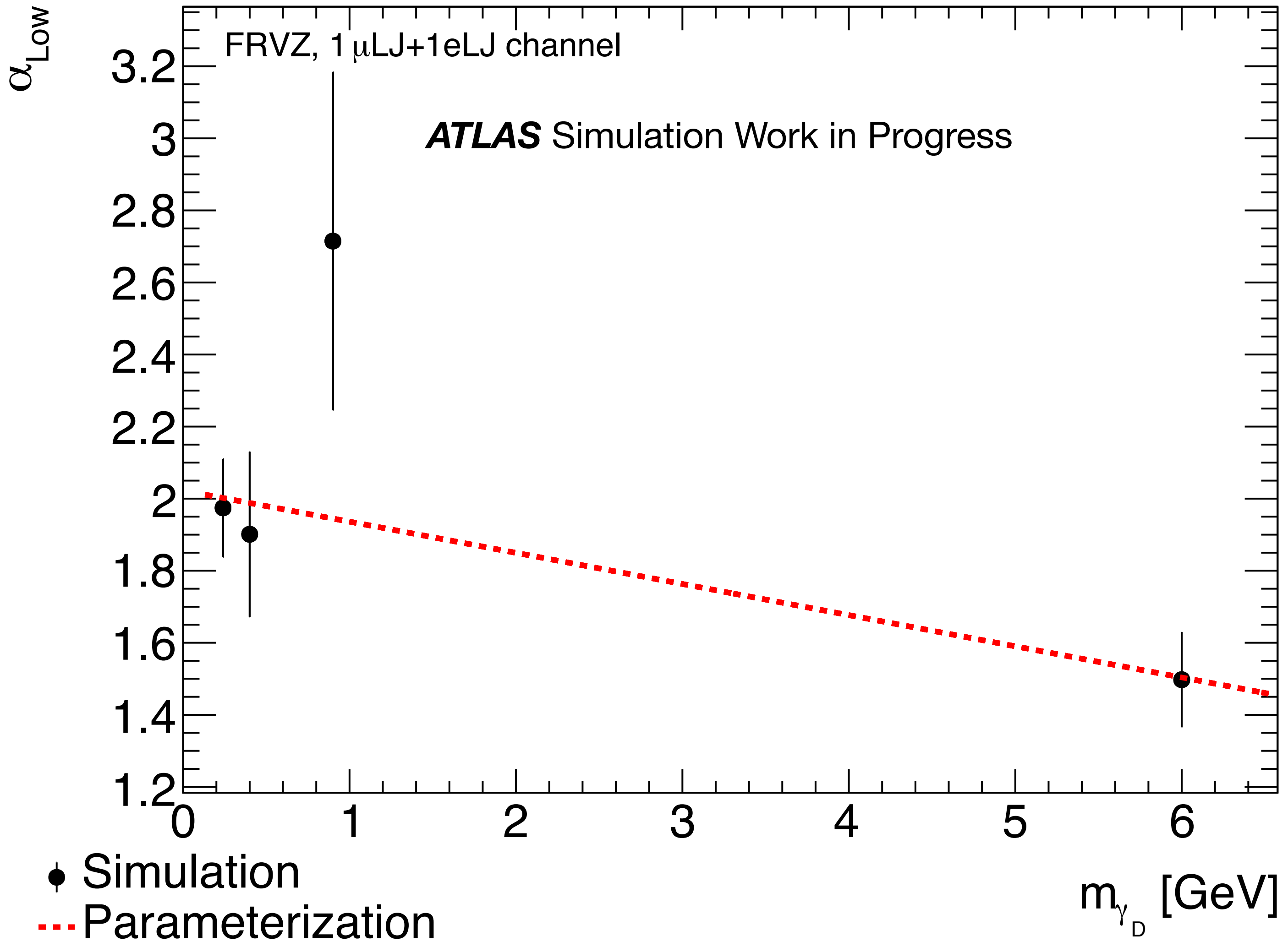

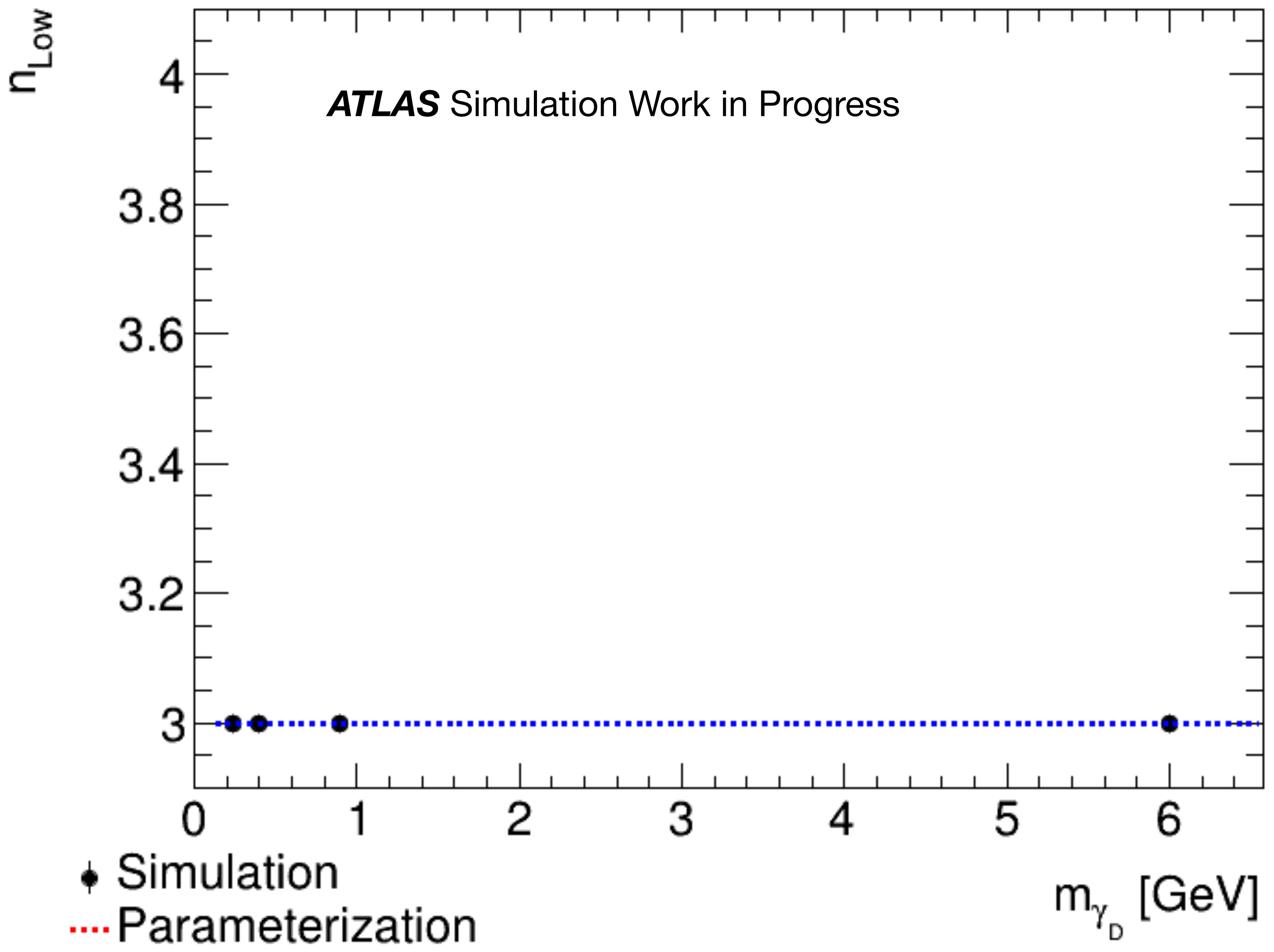

Modelling della forma del segnale: HAHM

400 MeV

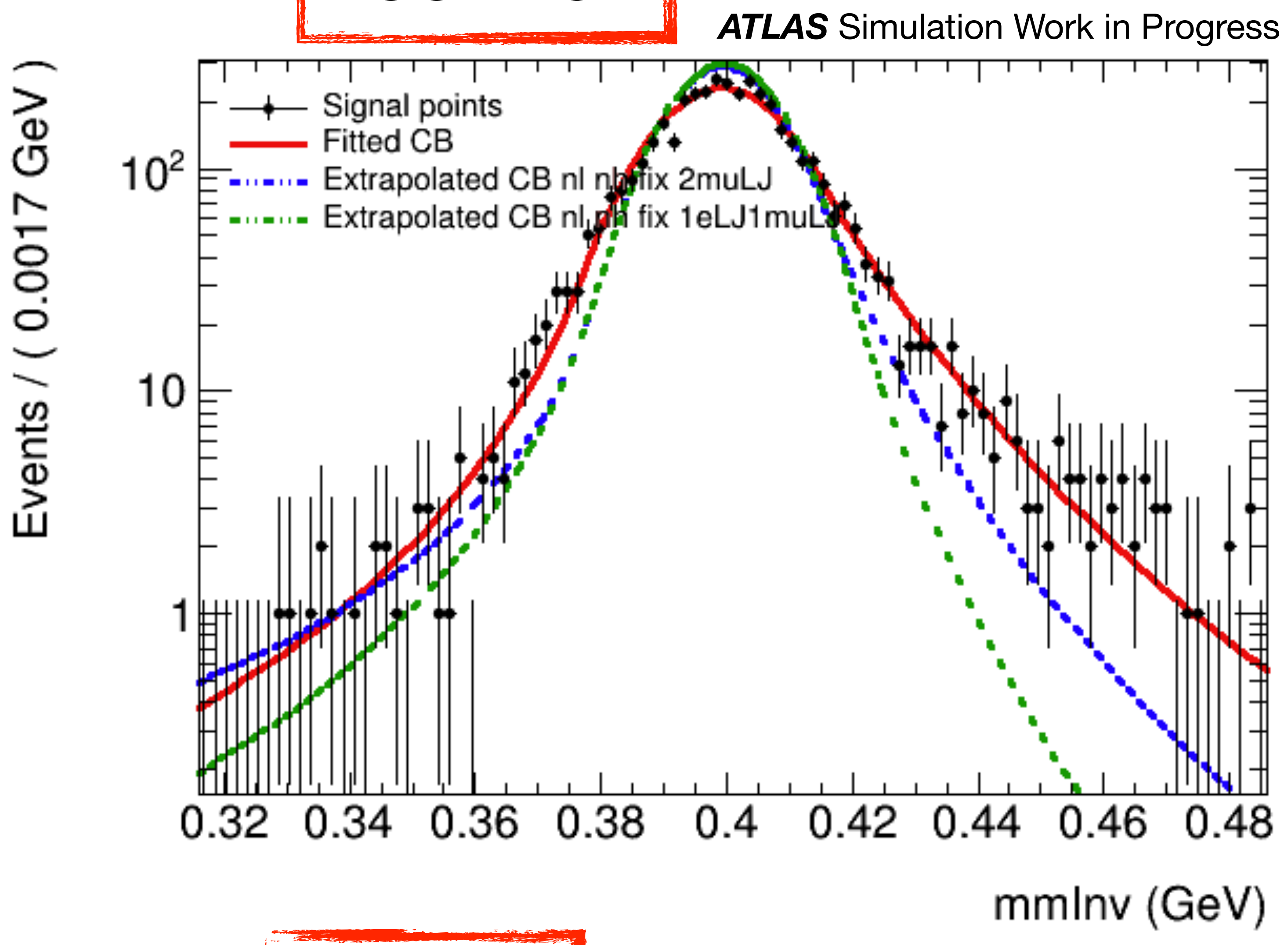

2 GeV

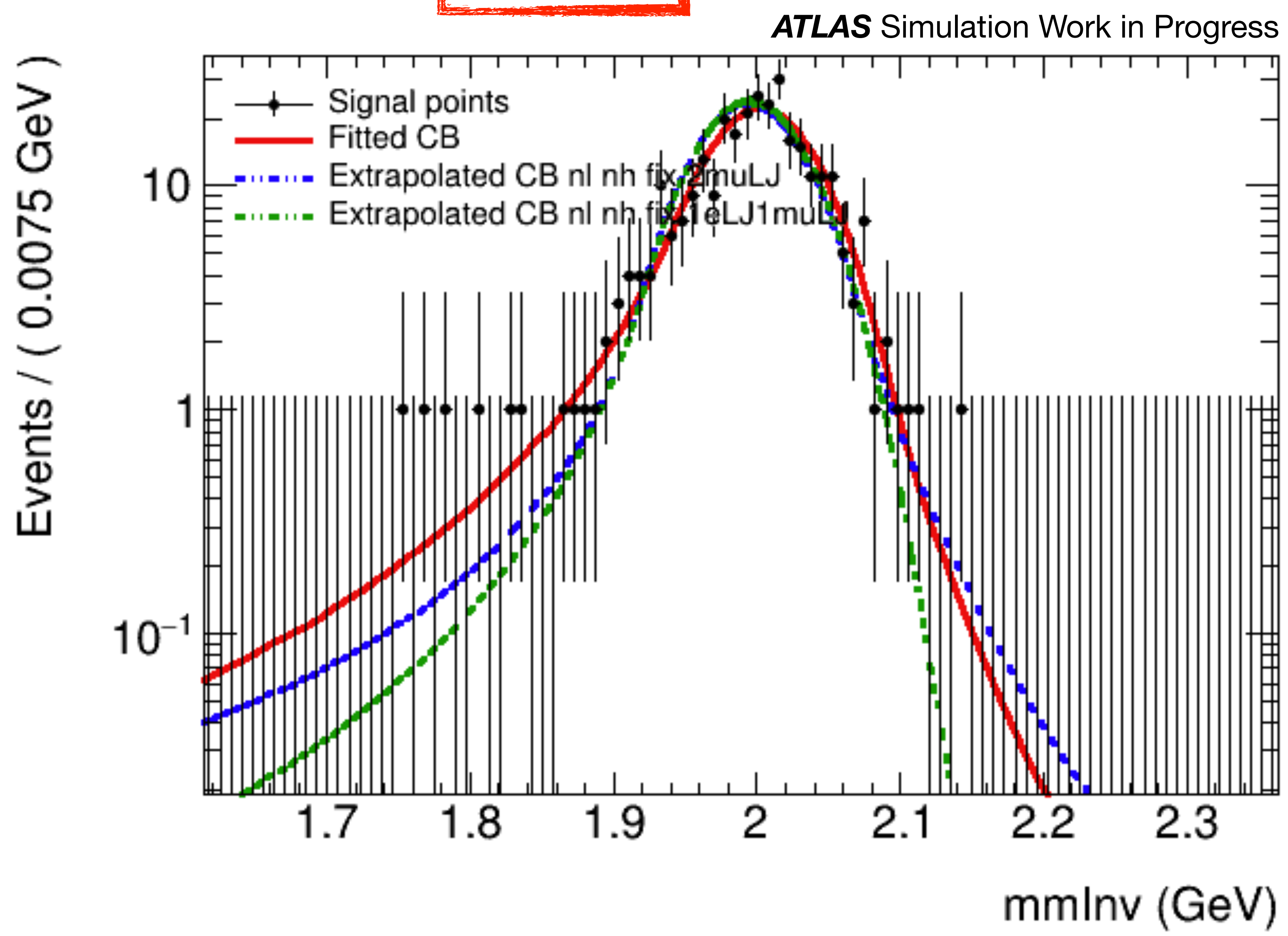

10 GeV

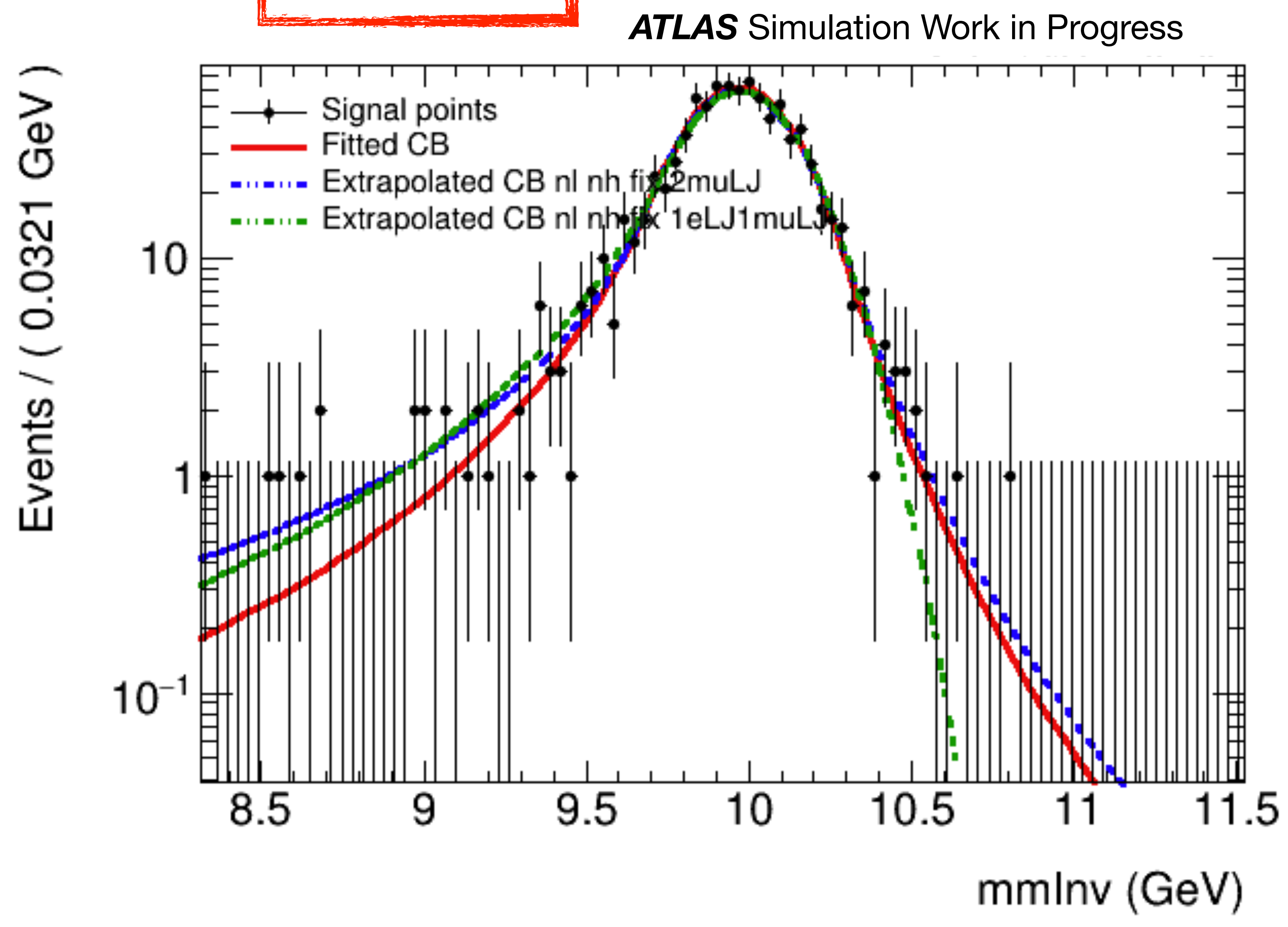

Fit DSCB

DSCB estrapolata 2μLJ

DSCB estrapolata μLJ-eLJ

Estrapolazione dei parametri: HAHM

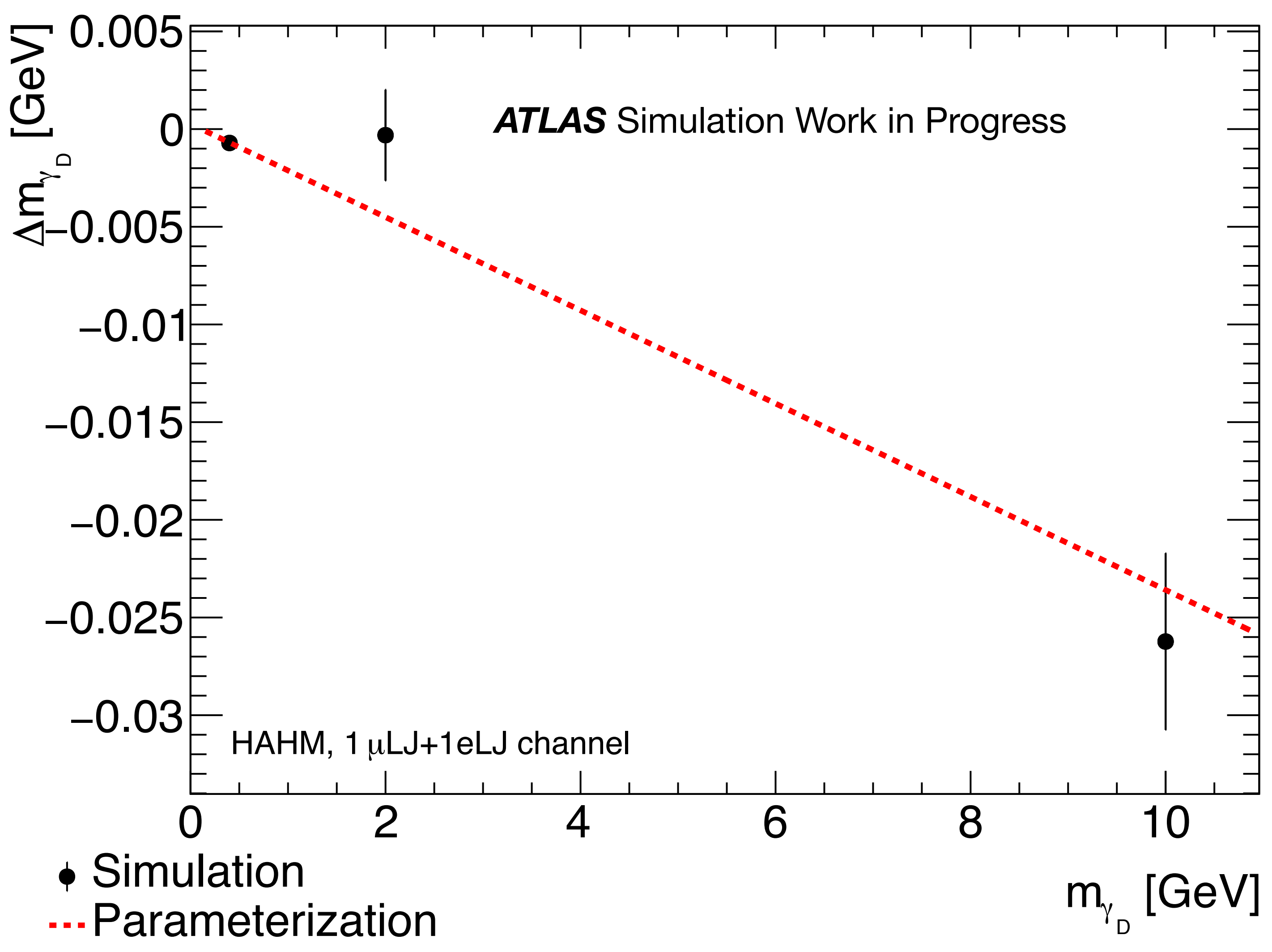

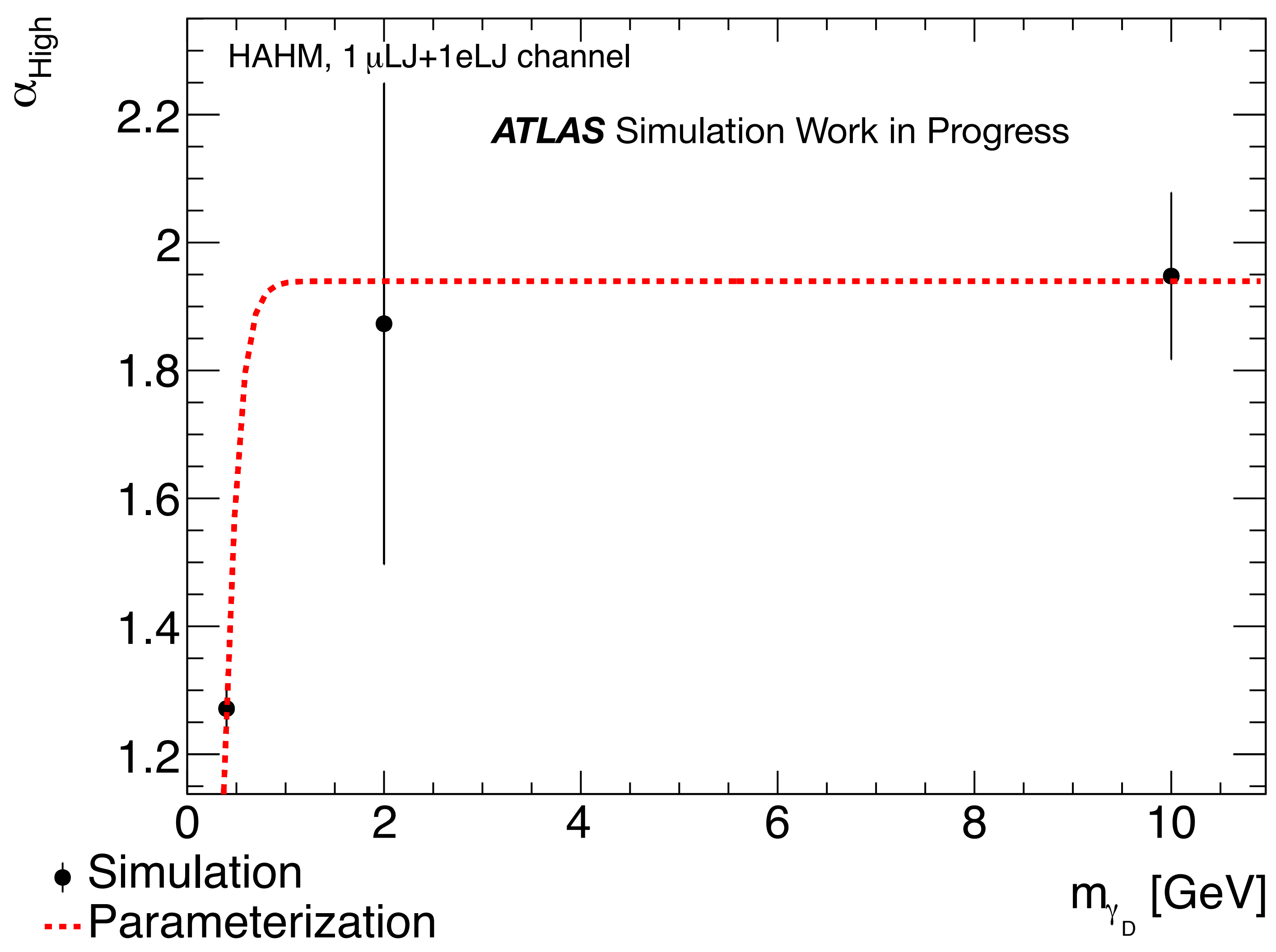

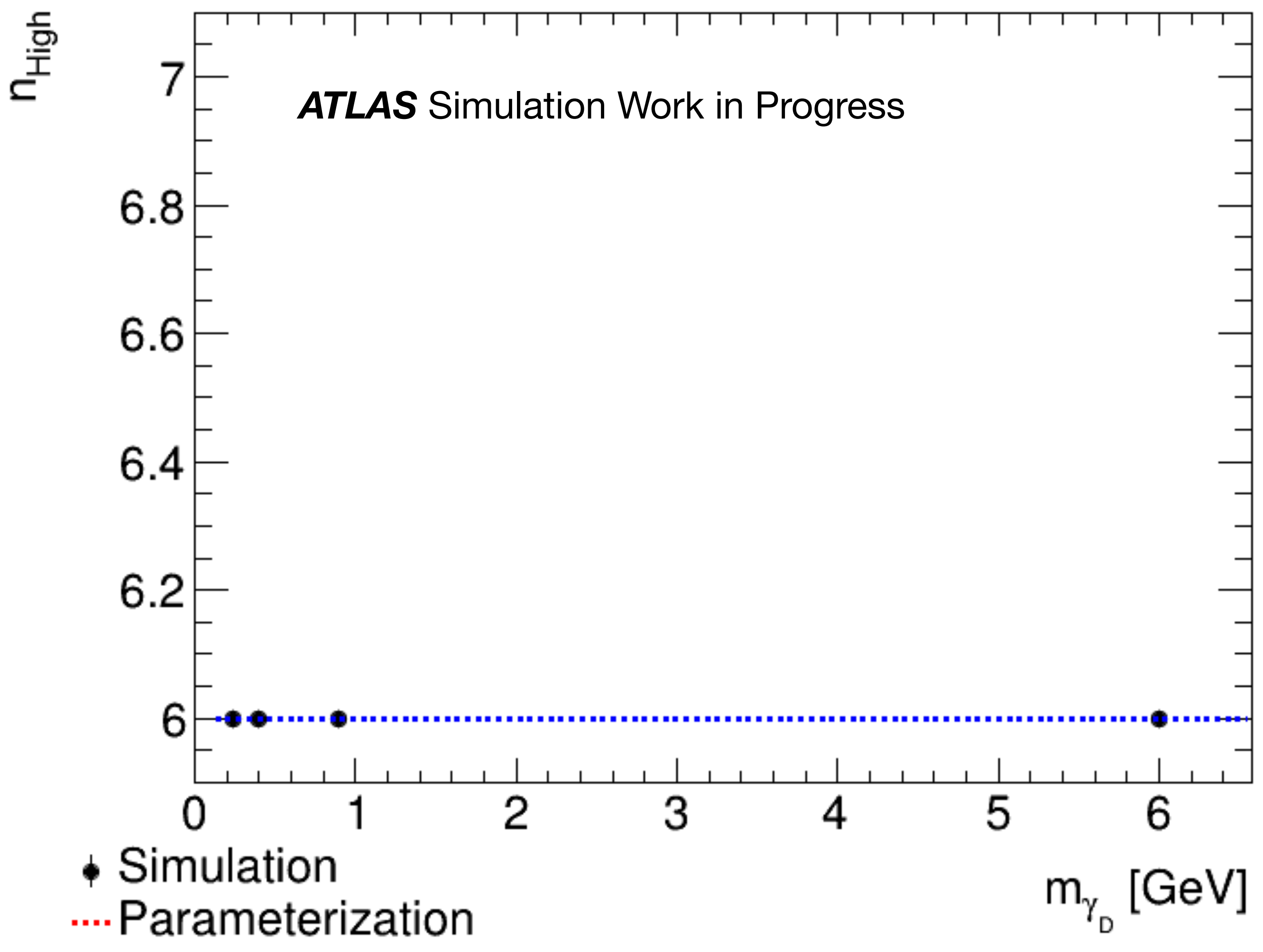

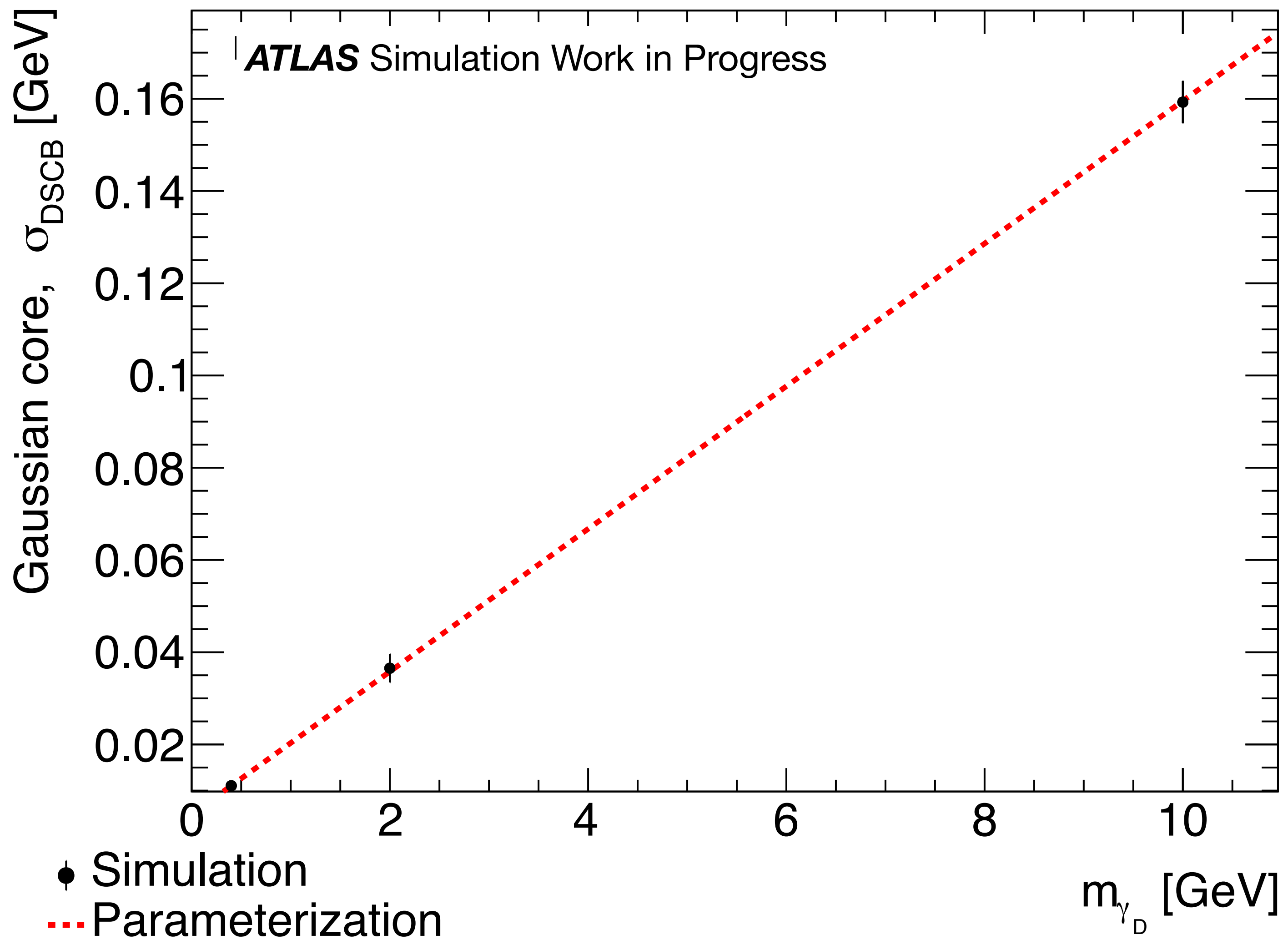

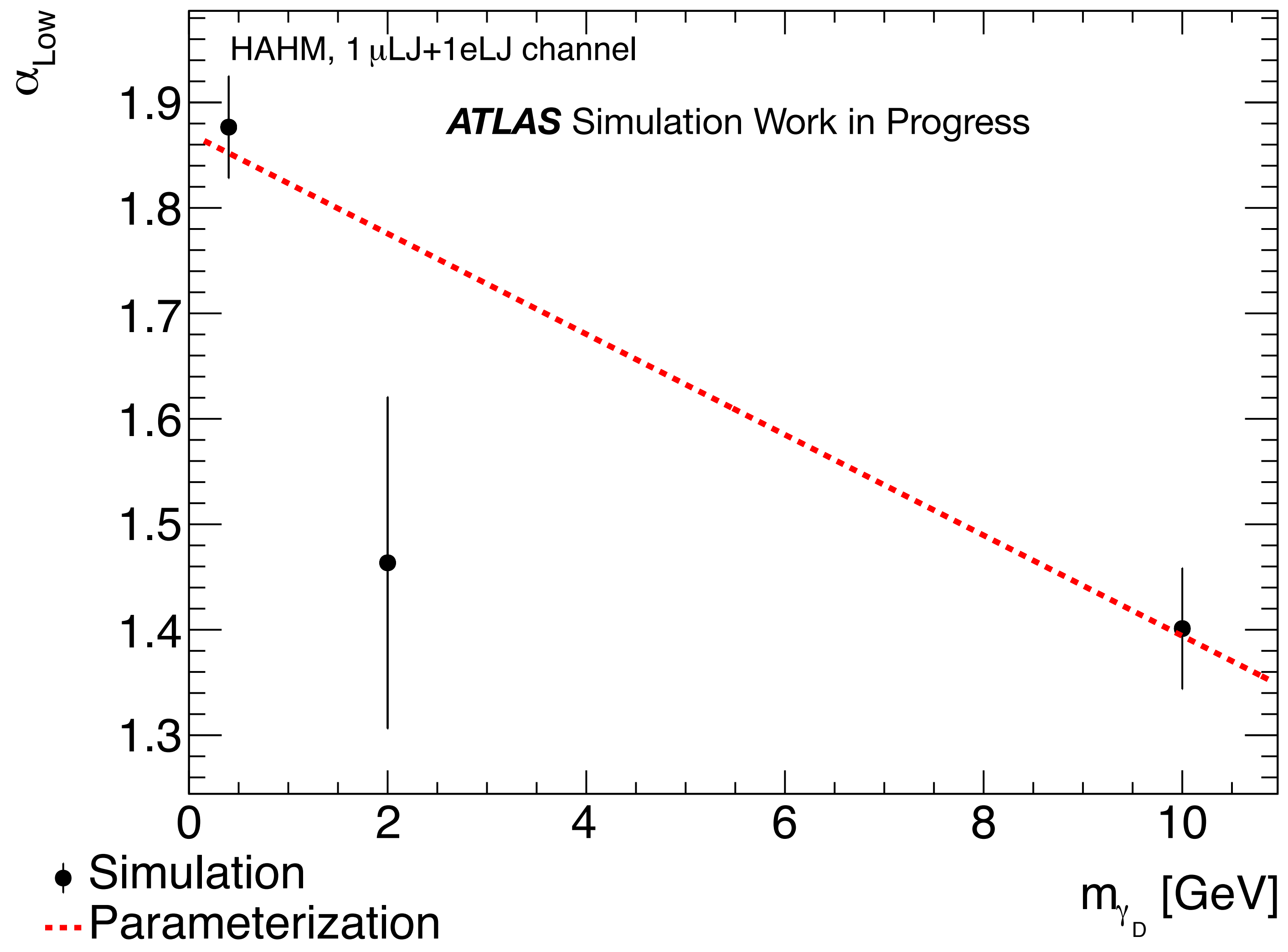

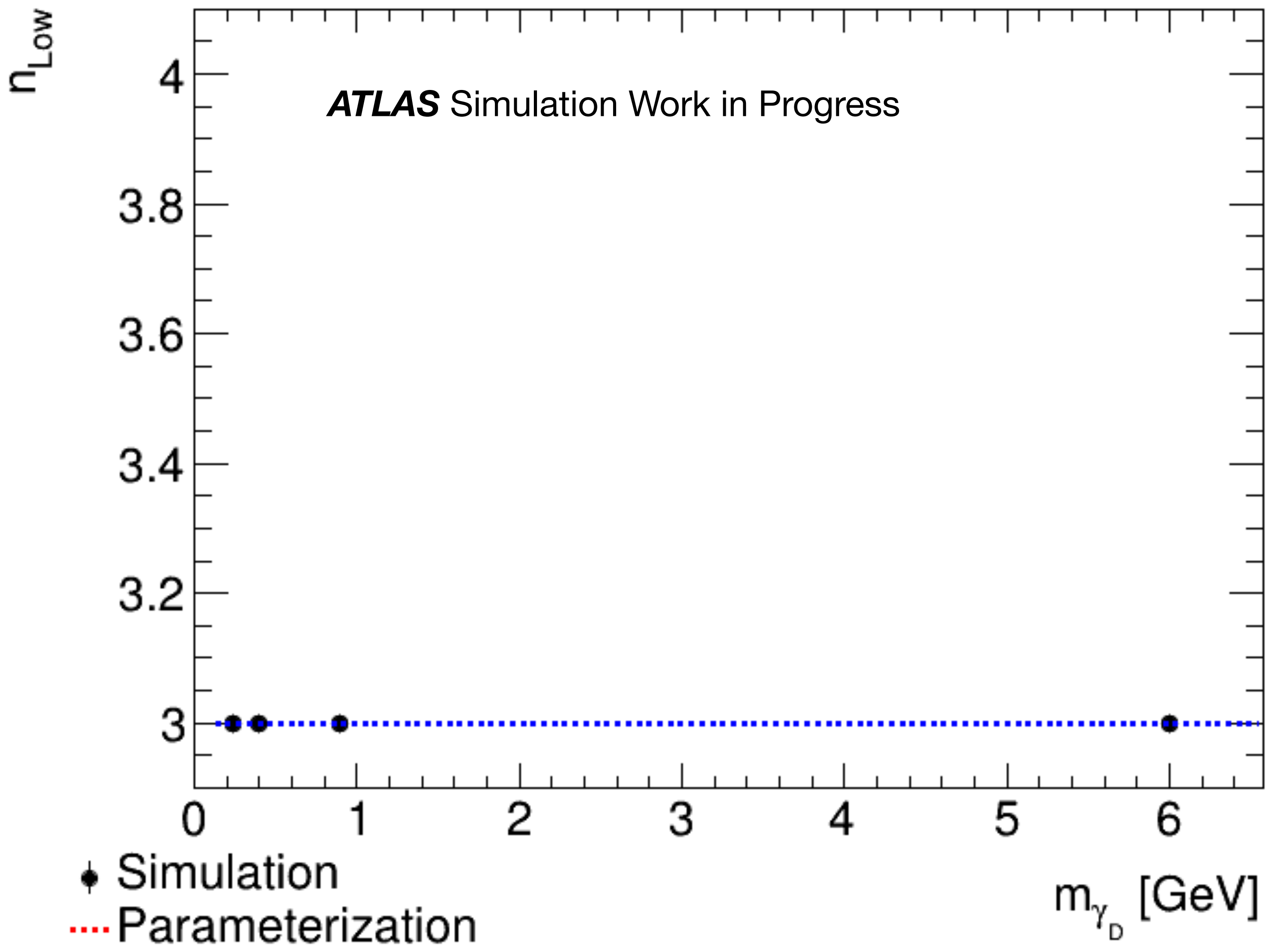

Injection test

Controllare se la resa del segnale *"iniettato"* è d'accordo con quello fittato

Leggera dipendenza del fit dal modelling (Usando la parametrizzazione del canale muonico)

Mismodelling coperto da incertezza del 5%

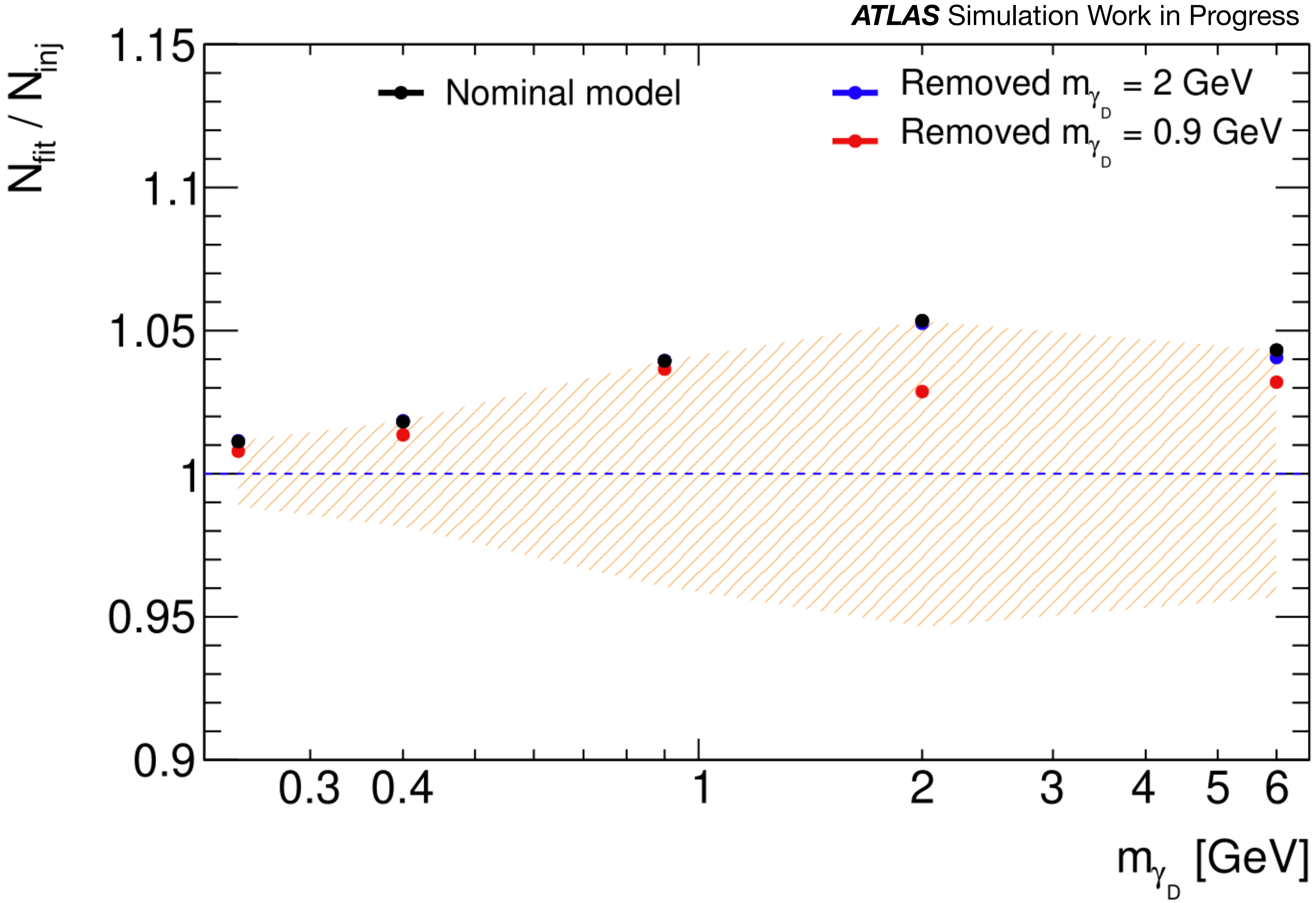

Acceptance X Efficiency

$$\mathcal{A} \times \epsilon|_{\mu\text{LJ}-e\text{LJchannel}} = \mathcal{A} \times \epsilon|_{\gamma_d \to 2\mu, \gamma_d \to 2e} BR(\gamma_d \to 2\mu) BR(\gamma_d \to 2e) \times 2$$

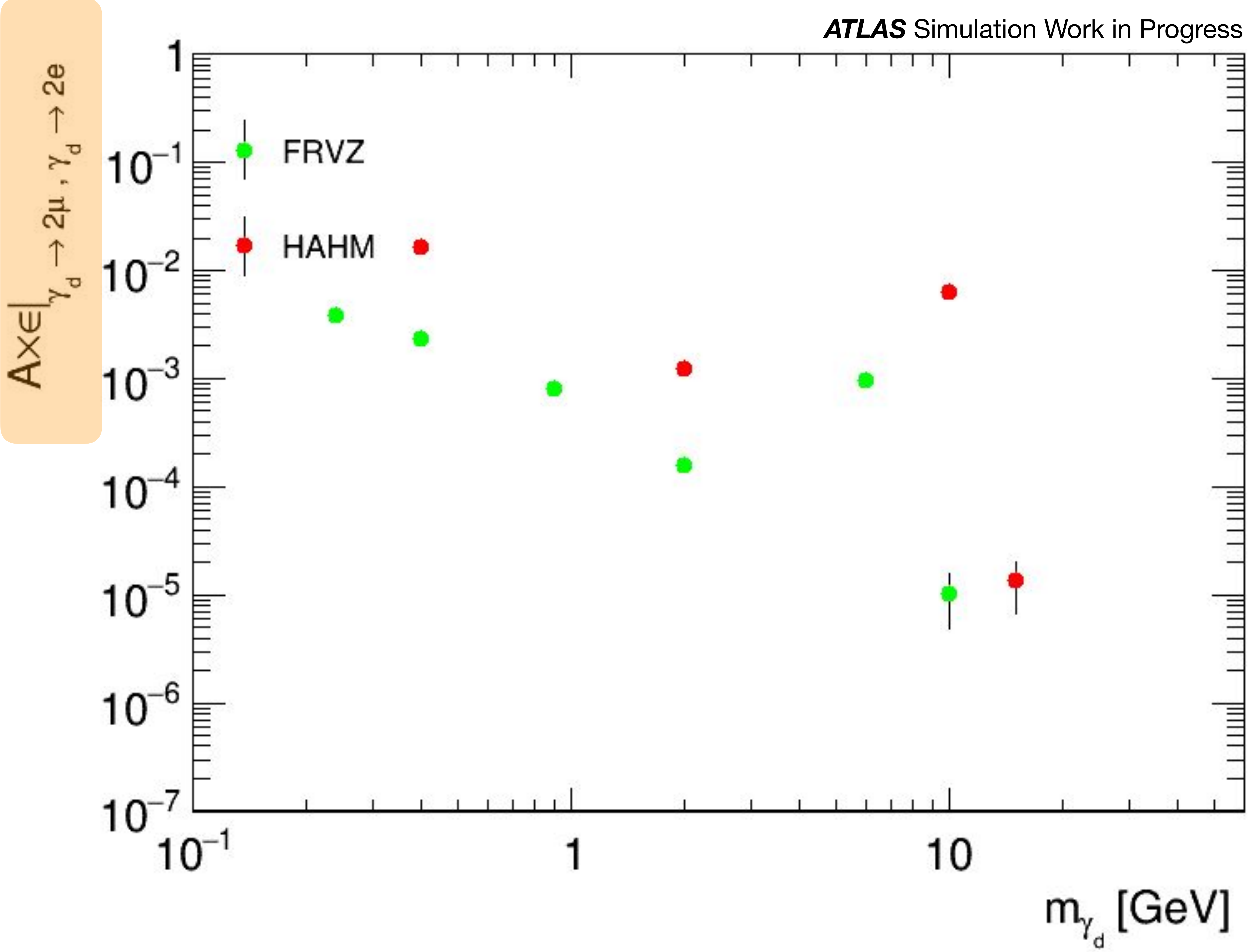

$A \times \epsilon$ può cambiare a causa di:

- $BR(\gamma_d \to 2\mu), BR(\gamma_d \to 2e)$
- ΔR dei prodotti di decadimento —> Efficienza di ricostruzione dei LJ
- p_T dei leptoni —> accettanza dei triggers

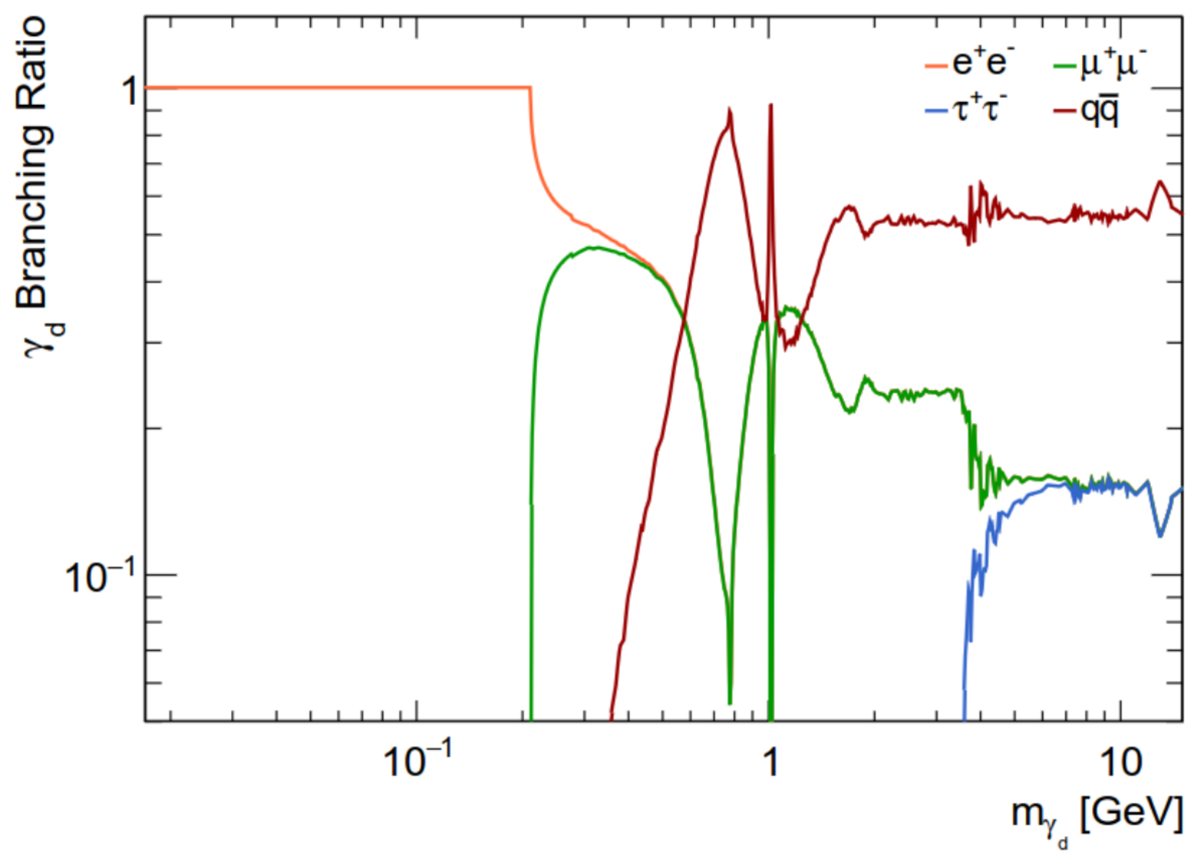

Acceptance X Efficiency: 1 elettrone in eLJ

$$\mathcal{A} \times \epsilon|_{\mu\text{LJ}-e\text{LJchannel}} = \mathcal{A} \times \epsilon|_{\gamma_d \to 2\mu, \gamma_d \to 2e} BR(\gamma_d \to 2\mu) BR(\gamma_d \to 2e) \times 2$$

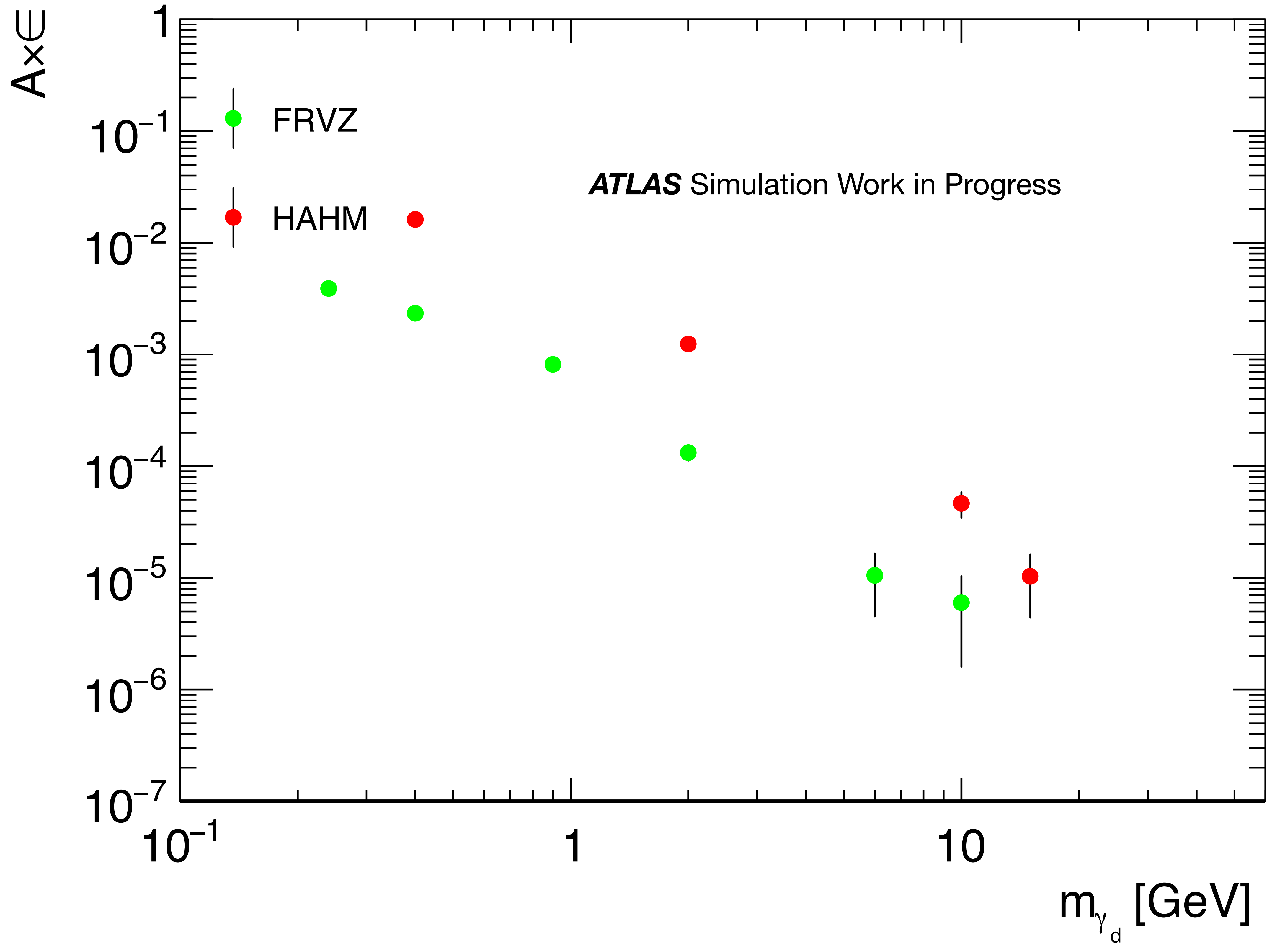

$A \times \epsilon$ può cambiare a causa di:

- $BR(\gamma_d \to 2\mu), BR(\gamma_d \to 2e)$
- ΔR dei prodotti di decadimento —> Efficienza di ricostruzione dei LJ
- p_{T} dei leptoni —> accettanza dei triggers

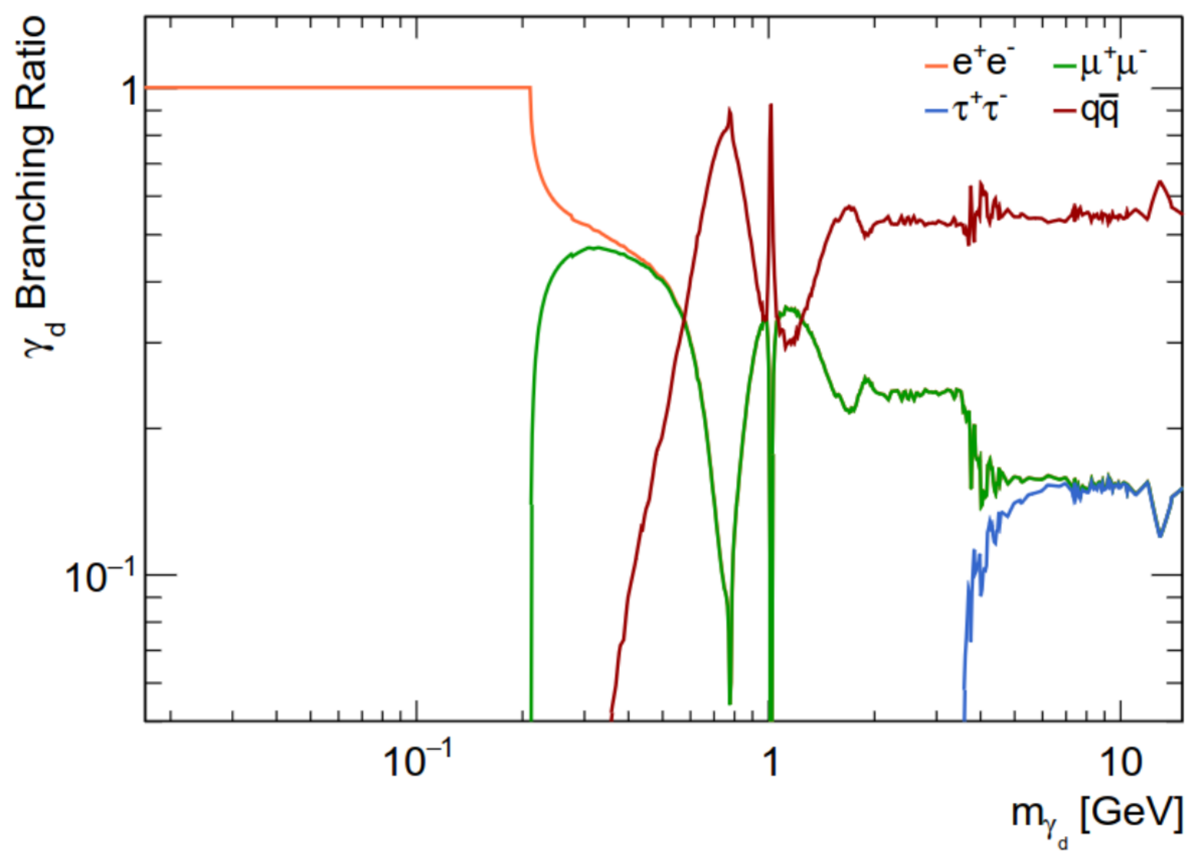

Acceptance X Efficiency: 2 elettroni in eLJ

$$\mathcal{A} \times \epsilon|_{\mu\mathrm{LJ}-e\mathrm{LJchannel}} = \mathcal{A} \times \epsilon|_{\gamma_d \to 2\mu, \gamma_d \to 2e} BR(\gamma_d \to 2\mu) BR(\gamma_d \to 2e) \times 2$$

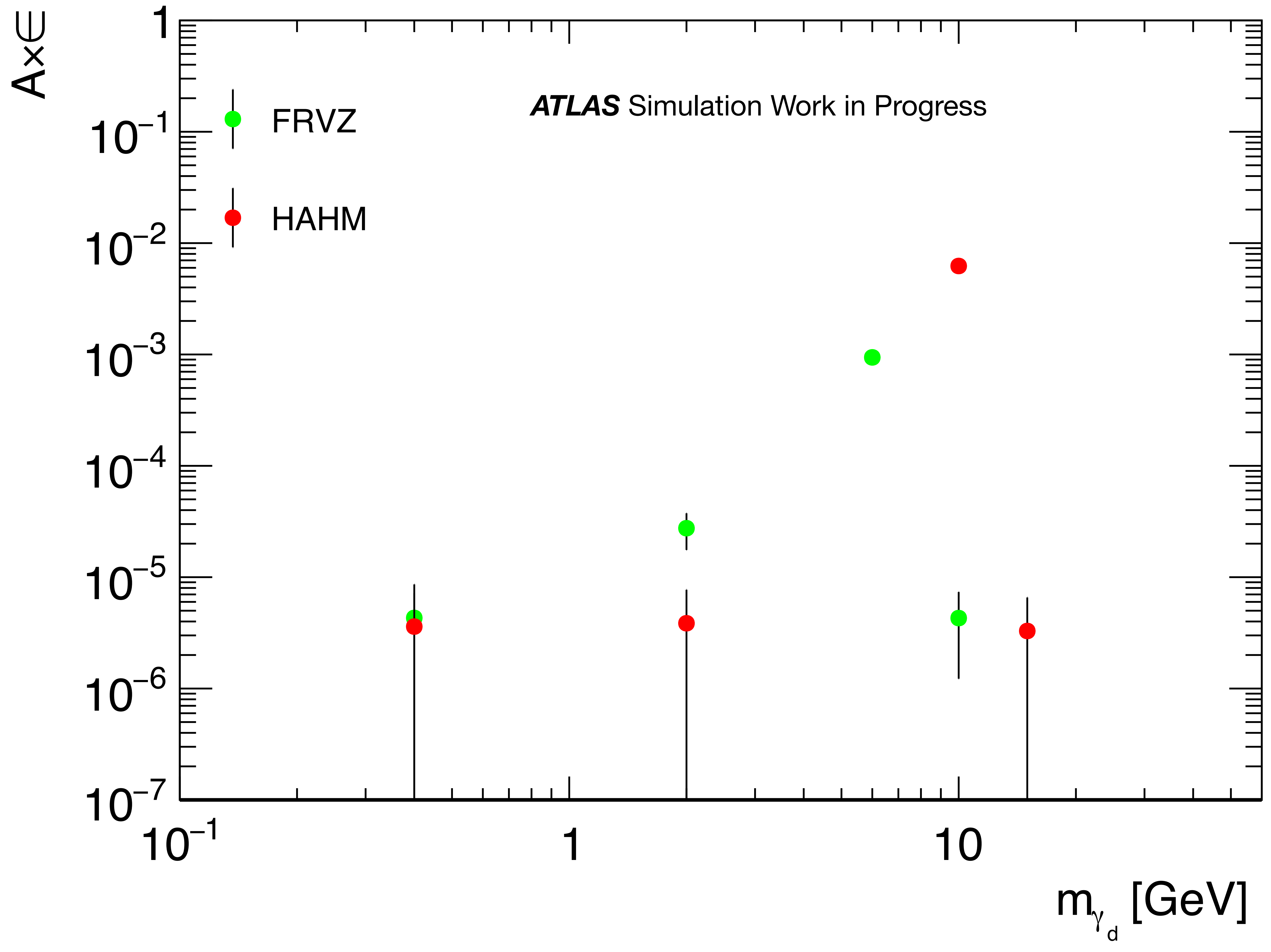

$A \times \epsilon$ può cambiare a causa di:

- $BR(\gamma_d \to 2\mu), BR(\gamma_d \to 2e)$
- ΔR dei prodotti di decadimento —> Efficienza di ricostruzione dei LJ
- p_T dei leptoni —> accettanza dei triggers

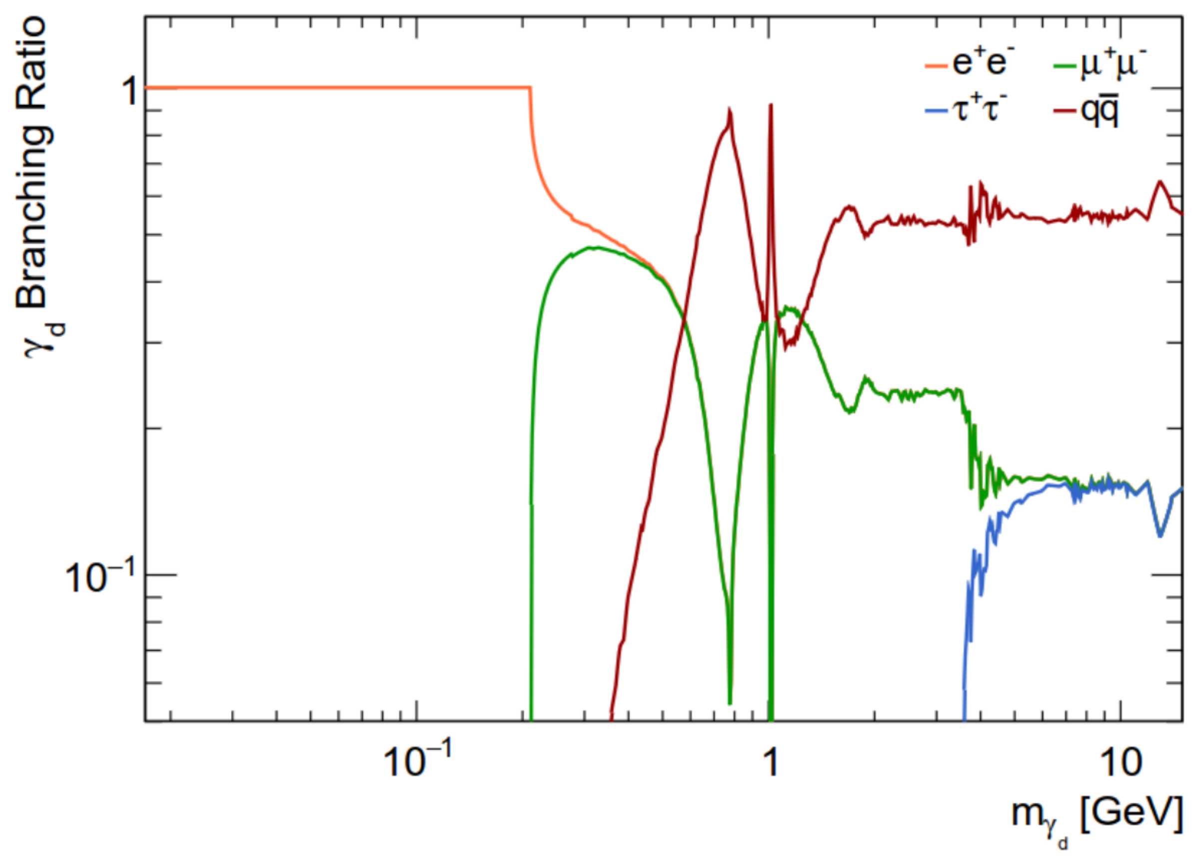

Modelling della forma del fondo

$$B(m_{\mu\mu}) = \left(1 - f_{\exp} - f_{J/\psi} - f_{\phi(1020)} - f_{\psi(2S)}\right) e^{-m_{\mu\mu}/\tau_2} + f_{\exp} e^{-m_{\mu\mu}/\tau} + f_{J/\psi} e^{-\left(\frac{m_{\mu\mu}-\mu_{J/\psi}}{\sigma_{J/\psi}}\right)^2} + f_{\psi(2S)} e^{-\left(\frac{m_{\mu\mu}-\mu_{\psi(2S)}}{\sigma_{\psi(2S)}}\right)^2} + f_{\phi(1020)} e^{-\left(\frac{m_{\mu\mu}-\mu_{\phi(1020)}}{\sigma_{\phi(1020)}}\right)^2}$$

Fondo estrapolato dai **dati veri** in CR

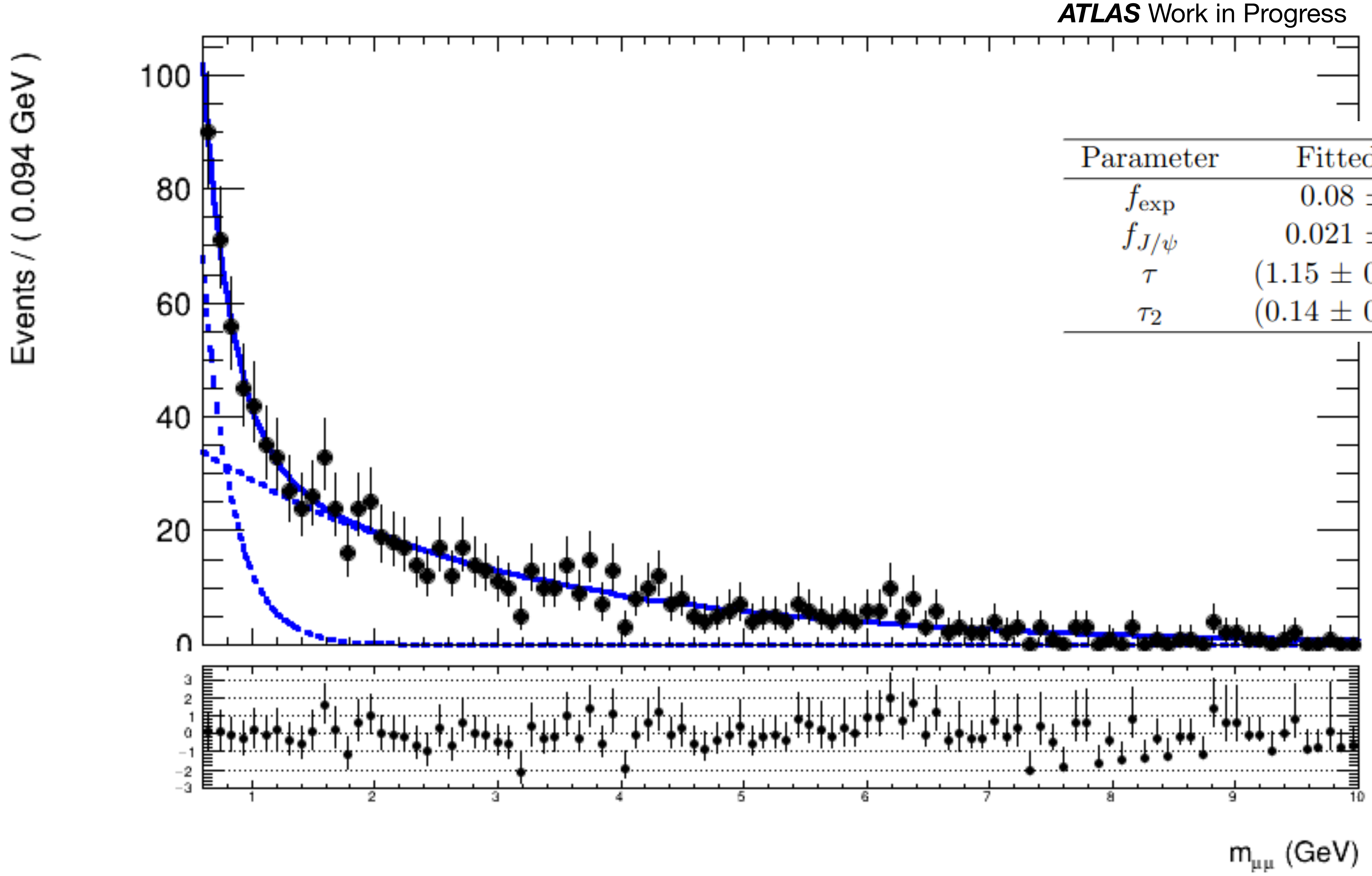

Parameter	Fitted value
$f_{\exp}$	0.08 ± 0.05
$f_{J/\psi}$	0.021 ± 0.008
τ	(1.15 ± 0.08) GeV
τ_2	(0.14 ± 0.04) GeV

- Somma di due esponenziali per background non risonante
- Risonanze parametrizzate come gaussiane

Incertezze sul modelling del fondo (Spurious Signal)

ATLAS EXPERIMENT

Scarso fondo —> rischio di segnale indotto (Spurious Signal)

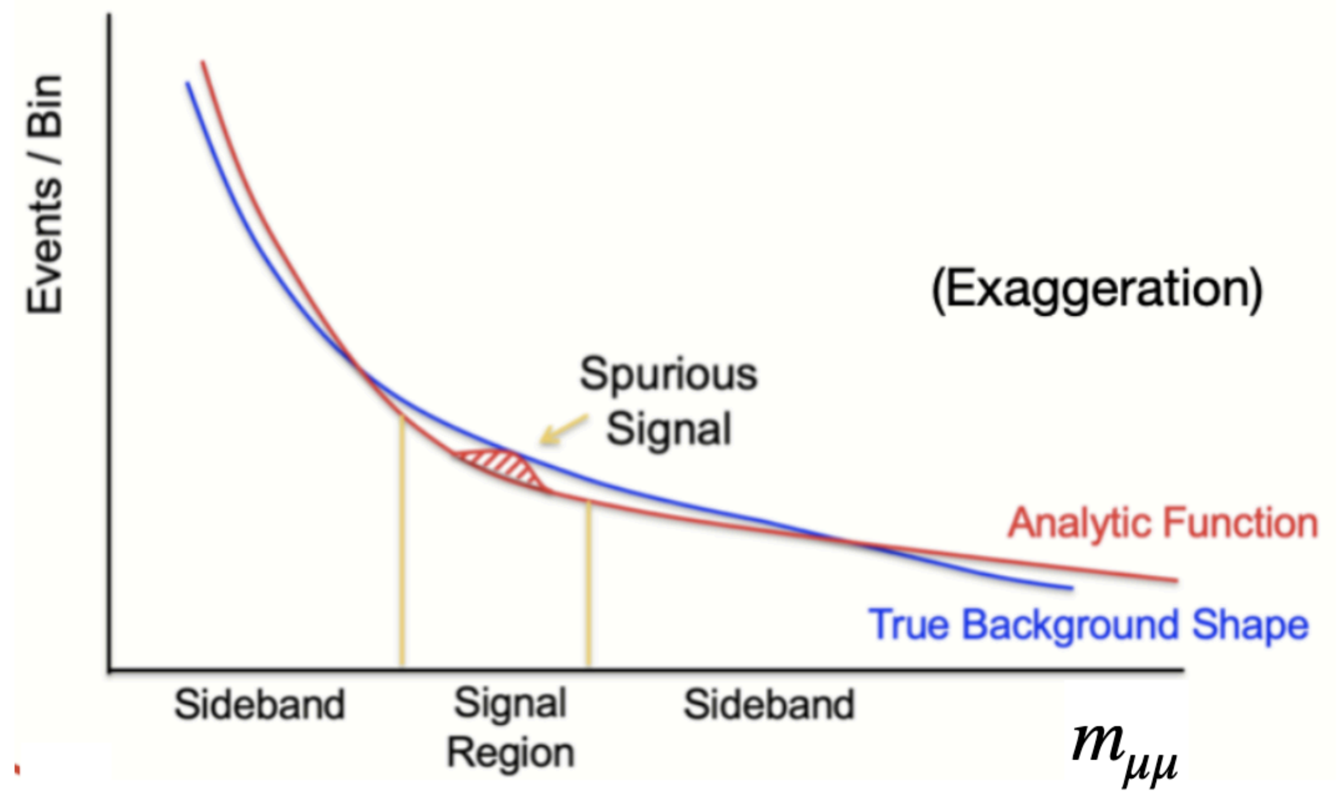

Smoothed template

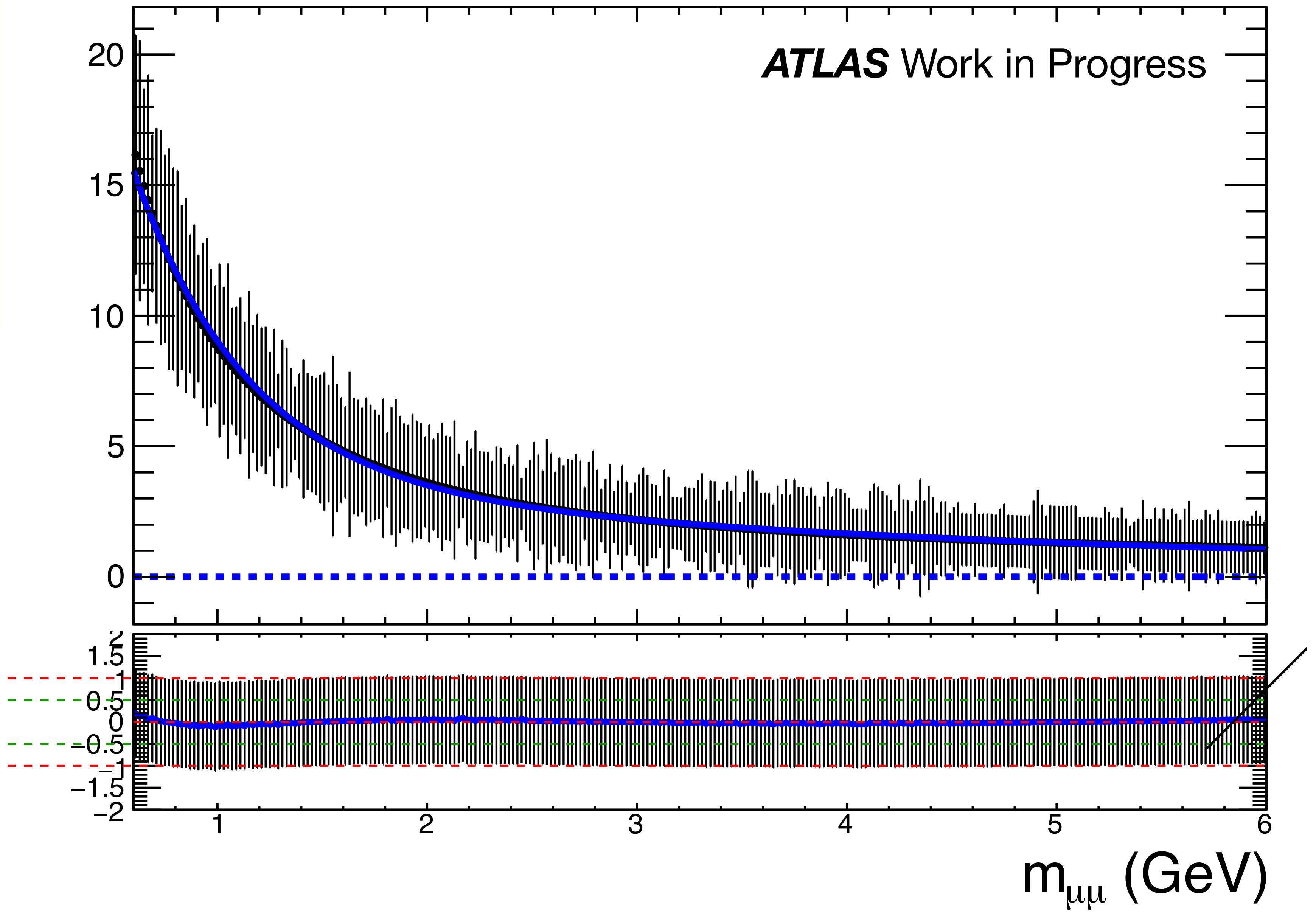

SS **prima** e **dopo smoothing**

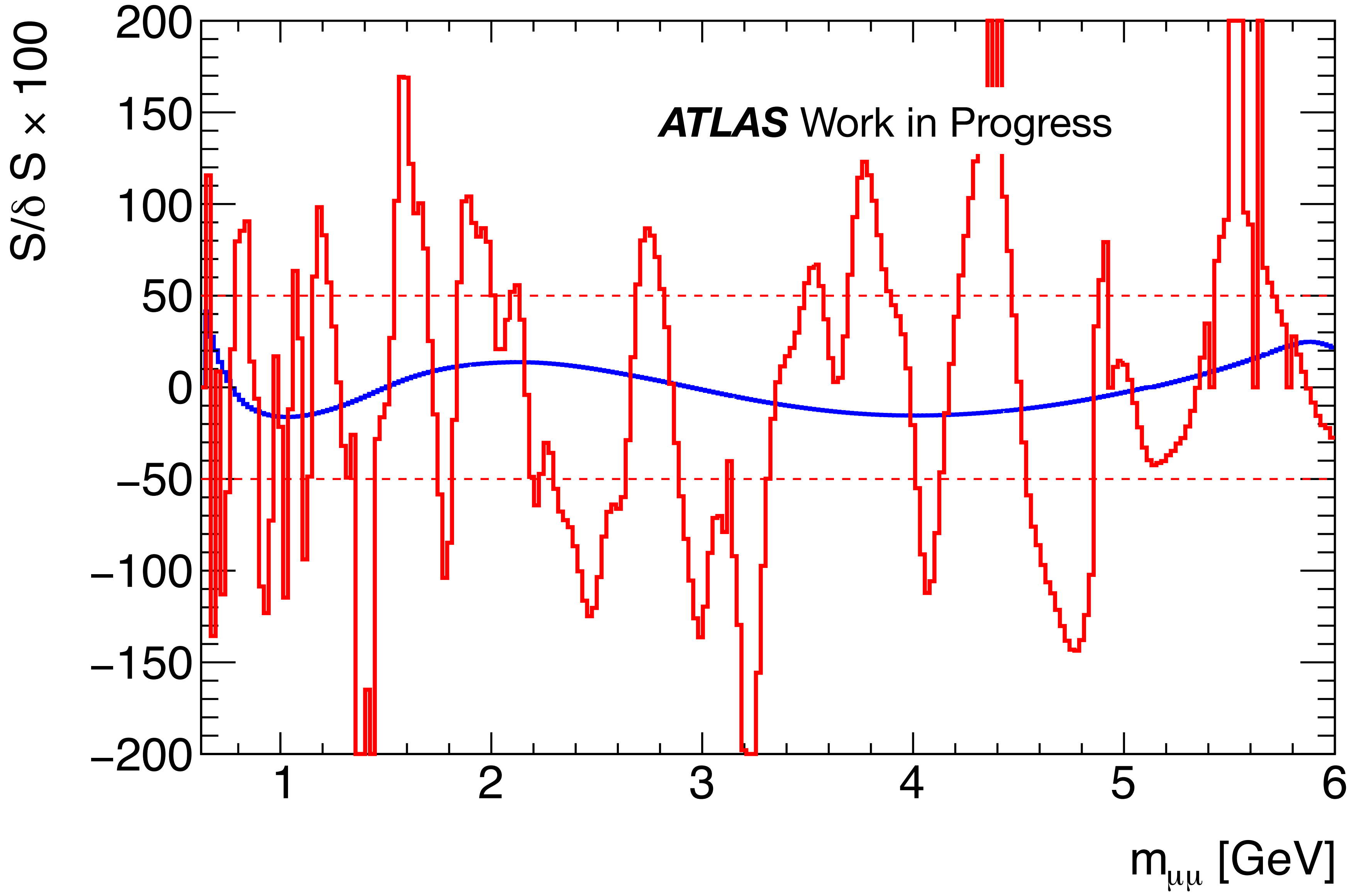

Sistematiche devono essere entro $0.5\sigma_{stat}$

Sistematiche dello Spurious Signal
calcolate via fit S+B
su template di solo fondo

→ Molto sensibile a fluttuazioni statistiche

▶ **Smoothed template**

Sistematiche

- Sistematiche su Scale Factors
- Sistematiche su variabili cinematiche

m_{γ_d} (GeV)	triggers (%)	μLJ reconstruction (%)	μLJ isolation (%)	μLJ TTVA (%)	eLJ reconstruction (%)	eLJ ID (%)	eLJ isolation (%)	PRW (%)	egamma resolution (%)	egamma scale (%)	muon ID (%)	muon MS (%)	muon scale (%)	Total (%)
0.24	0.77	0.06	1.10	0.04	0.38	0.53	0.07	2.17	0.23	0.29	0.12	0.22	0.12	2.68
0.40	0.49	0.04	1.16	0.04	0.36	0.48	0.06	1.33	0.15	0.01	0.18	0.06	0.35	1.98
0.90	0.63	0.08	1.14	0.07	0.25	0.26	0.03	6.56	0.56	0.58	0.52	0.03	0.04	6.77
2	0.65	0.01	1.00	0.19	0.69	1.33	0.91	7.59	4.75	4.71	0.04	0.03	0.03	10.34
6	1.84	0.10	0.55	0.03	1.37	3.98	2.66	2.66	0.06	0.32	0.32	0.69	0.66	6.06

Table 8.5: Summary table of the systematic uncertainties on FRVZ signal MC events in the μLJ- eLJ channel.

m_{γ_d} (GeV)	triggers (%)	μLJ reconstruction (%)	μLJ isolation (%)	μLJ TTVA (%)	eLJ reconstruction (%)	eLJ ID (%)	eLJ isolation (%)	PRW (%)	egamma resolution (%)	egamma scale (%)	muon ID (%)	muon MS (%)	muon scale (%)	Total (%)
0.40	0.28	0.10	0.53	0.04	0.36	0.25	0.02	0.01	0.04	0.07	0.06	0.06	0.17	0.78
2	0.15	0.12	0.56	0.01	0.37	0.26	0.04	3.9	0.02	0.48	0.01	0.00	0.00	4.00
10	0.35	0.16	0.28	0.01	1.14	0.42	0.06	0.43	0.04	0.11	0.04	0.00	0.00	1.38

Table 8.6: Summary table of the systematic uncertainties on HAHM signal MC events in the μLJ- eLJ channel.

Estrapolazione eventi Run-1 Run-2

Run-1: 7 eventi nei dati

Run-2: $\times 7\mathscr{L} \times 2\sigma_{pp}$ —> ~ 100 eventi attesi

Channel	Background (ABCD-likelihood method)	Background (total)	Observed events in data
eLJ–eLJ	2.9 ± 0.9	4.4 ± 1.3	6
muLJ–muLJ	2.9 ± 0.6	4.4 ± 1.1	4
eLJ–muLJ	6.7 ± 1.4	7.1 ± 1.4	2
eLJ–emuLJ	7.8 ± 2.0	7.8 ± 2.0	5
muLJ–emuLJ	20.2 ± 4.5	20.3 ± 4.5	14
emuLJ–emuLJ	1.3 ± 0.8	1.9 ± 0.9	0

Isolamento per coppie di muoni boosted

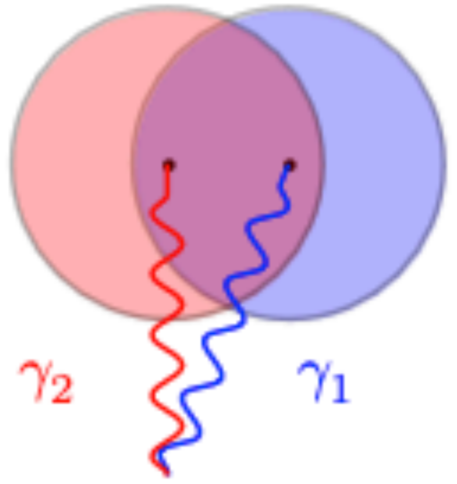

Recommended isoWP: PflowLoose VarRad: $\texttt{ptvarcone30} + 0.4 * \texttt{neflowisol20} < 0.16 p_T^{\mu}$,

μ in μLJ fails standard iso WP (ptvarcone30) → corrected isolation developed

Corrected isolation: as ptvarcone30, removing track belonging to close-by muon (isoCloseByTool)

ptvarcone30 for μ in μLJ: **old** vs **new**

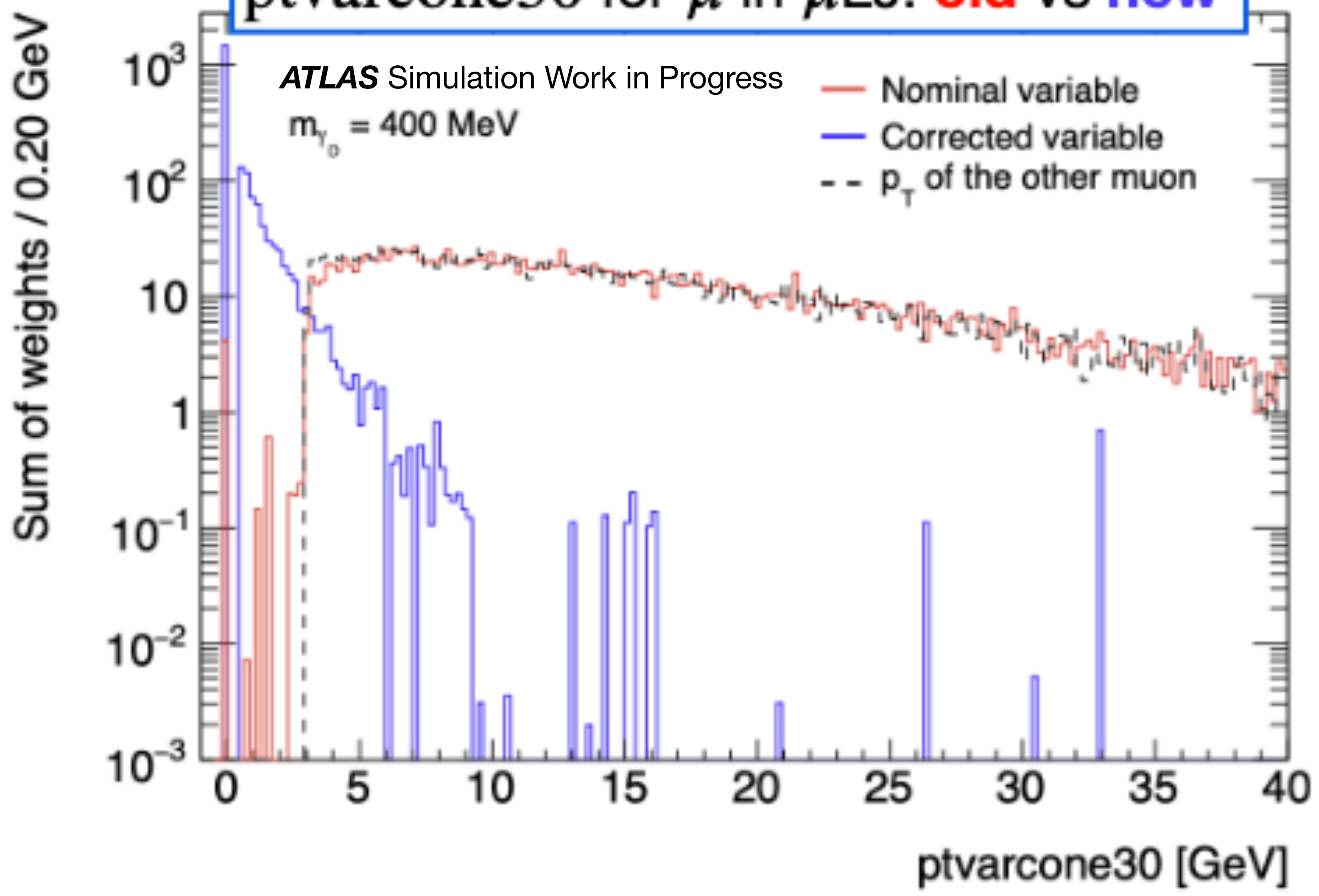

Isolation WP efficiency: **old** vs **new**

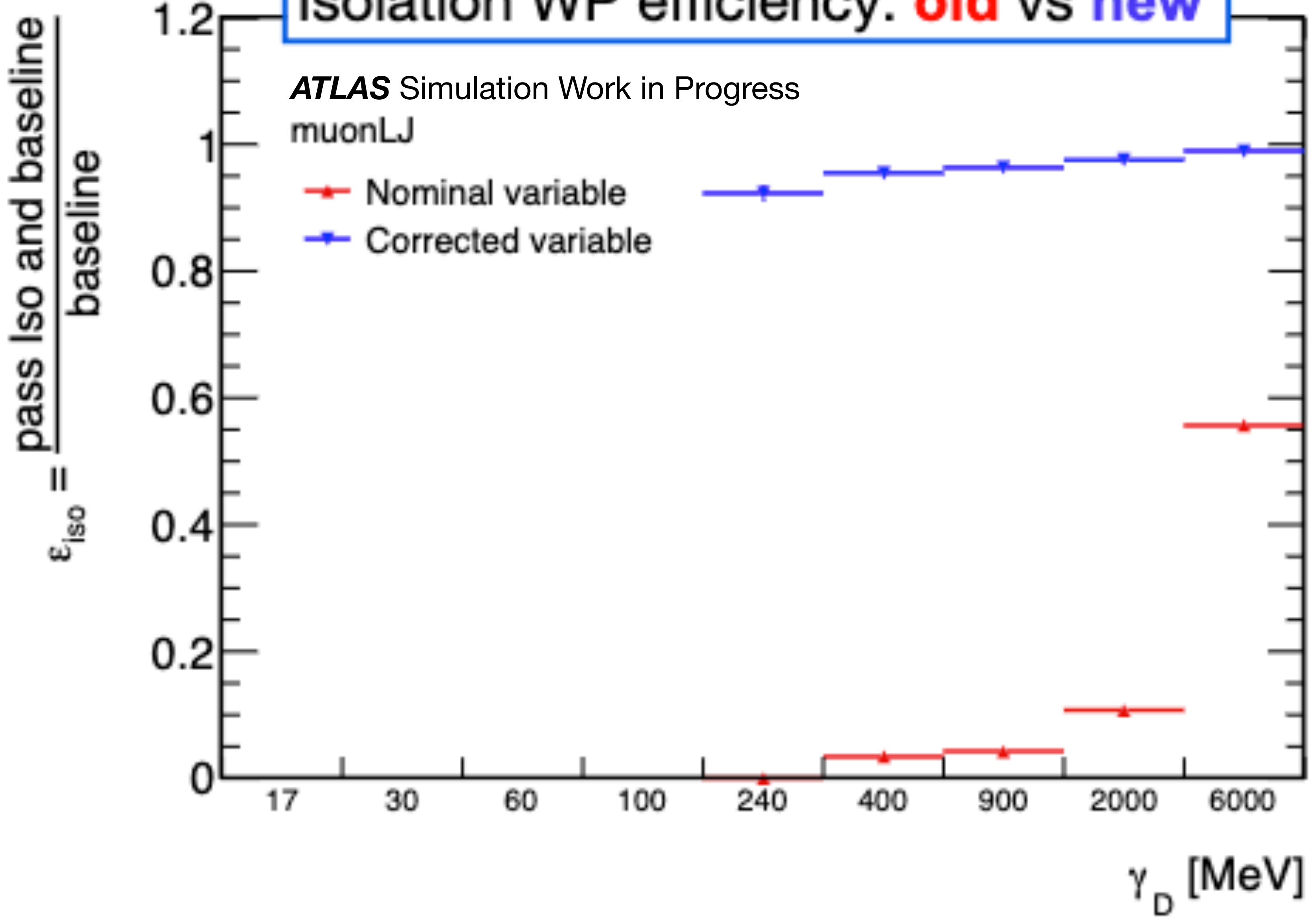

Used by HZZ analysis as well!

Efficiency increased up to 90 % !!

Strategia di triggers canale muonico

Type	Data-taking periods	Trigger
di-muon	2015	HLT_mu18_mu8noL1
	2015 - 2016 A	HLT_2mu10
	2016 A	HLT_2mu10_nomucomb
	2016 A-D3	HLT_mu20_mu8noL1
	2016 B-end - 2017 - 2018	HLT_2mu14
	2016 B-D3	HLT_2mu14_nomucomb
	2016 D4-end - 2017 - 2018	HLT_mu22_mu8noL1
tri-muon	2015 - 2016 B-D3 - 2017 - 2018	HLT_3mu6
	2015-2018 - all periods	HLT_3mu6_msonly

Table 6.1: List of muon triggers used in the μLJ–μLJ channelfor the corresponding data-taking periods.

Regione di segnale canale muonico

Cuts	$m_{\gamma_d} = 0.24$ GeV	$m_{\gamma_d} = 0.4$ GeV	$m_{\gamma_d} = 0.9$ GeV	$m_{\gamma_d} = 2$ GeV	$m_{\gamma_d} = 6$ GeV	$m_{\gamma_d} = 10$ GeV	$m_{\gamma_d} = 15$ GeV
None	337900±700	337900±700	337900±700	331200±1100	349300±1000	337800±700	337600±700
2μLJ	8760±100	11020±120	8650±100	3300±40	422±12	145±14	40±7
Trigger	5080±80	6700±90	5230±80	2482±33	400±12	139±13	40±7
Trigger matching	3460±60	4560±70	3580±70	1839±29	344±11	137±13	37±7
$q_{\mu\text{LJ}} = 0$	3460±60	4560±70	3580±70	1839±29	344±11	137±13	30±6

Table 7.1: Signal events remaining after each cut applied in the μLJ-μLJ channel. Events are generated according to the FRVZ model and are normalized assuming a branching ratio $B(\text{H} \rightarrow 2\gamma_d + \text{X}) = 0.05$.

Cuts	$m_{\gamma_d} = 0.4$ GeV	$m_{\gamma_d} = 2$ GeV	$m_{\gamma_d} = 10$ GeV	$m_{\gamma_d} = 15$ GeV	$m_{\gamma_d} = 25$ GeV
None	337800±700	337800±700	337600±700	337600±700	337800±700
2μLJ	22390±170	19780±160	3490±70	297±20	52±8
Trigger	19920±160	17850±150	3440±70	294±20	52±8
Trigger Matching	17390±150	15610±140	3350±70	289±19	50±8
$q_{\mu\text{LJ}} = 0$	17380±150	15610±140	3350±70	289±19	50±8

Table 7.2: Signal events remaining after each cut applied in the μLJ-μLJ channel. Events are generated according to the HAHM model and are normalized assuming a branching ratio $B(\text{H} \rightarrow 2\gamma_d) = 0.05$.

Regione di controllo canale muonico

ATLAS EXPERIMENT

Cuts	m_{γ_d} = 0.24 GeV	m_{γ_d} = 0.4 GeV	m_{γ_d} = 0.9 GeV	m_{γ_d} = 2 GeV	m_{γ_d} = 6 GeV	m_{γ_d} = 10 GeV	m_{γ_d} = 15 GeV
None	337900±700	337900±700	337900±700	331200±1100	349300±1000	337800±700	337600±700
1μLJ + $0e$LJ	77380±310	89480±340	83170±330	55840±270	21570±150	12530±130	3750±70
Triggers	4970±80	6550±90	6520±90	3330±40	2273±35	3220±60	1510±40
Trigger matching	585±27	1980±50	2810±60	1515±26	1372±24	2430±60	1170±40
Electron veto	581±27	1960±50	2800±60	1508±26	1361±23	2410±60	1170±40
2 signal muons	2.5±1.8	2.7±1.6	3.0±1.8	2.6±1.1	558±14	1190±40	655±28
$\Delta R_{\mu\mu} > 1.8$	2.5±1.8	1.9±1.4	1.3±1.3	1.1±0.6	0.6±0.4	39±7	240±16
$\|m^{imb}\| > 0.2$	2.5±1.8	1.9±1.4	1.3±1.3	1.1±0.6	0.6±0.4	28±6	196±15
$\Delta\phi_{\mu LJ-\mu\mu} > 2.8$	1.3±1.3	0.0±0.0	1.3±1.3	0.4±0.4	0.27±0.27	0.8±0.8	0.0±0.0
$q_{\mu LJ} = 0$	0.0±0.0	0.0±0.0	1.3±1.3	0.0±0.0	0.27±0.27	0.0±0.0	0.0±0.0

Table 7.3: Signal events remaining after each cut applied in the CR of the μLJ-μLJ channel. Events are generated according to the FRVZ model and are normalized assuming a branching ratio $B(\mathrm{H} \to 2\gamma_d + \mathrm{X}) = 0.05$.

Cuts	m_{γ_d} = 0.4 GeV	m_{γ_d} = 2 GeV	m_{γ_d} = 10 GeV	m_{γ_d} = 15 GeV	m_{γ_d} = 25 GeV
None	337800±700	337800±700	337600±700	337600±700	337800±700
1μLJ + $0e$LJ	107700±400	115500±400	53910±260	16480±150	3380±70
Trigger	9060±110	9950±110	12770±130	4800±80	1070±40
Trigger matching	3130±60	4300±70	10280±110	4100±70	875±34
Electron veto	3130±60	4290±70	10220±110	4080±70	870±33
2 signal muons	3.4±2.0	6.2±2.6	5730±80	2500±60	505±25
$\Delta R_{\mu\mu} > 1.8$	2.3±1.6	3.5±2.0	8.9±3.0	58±8	144±13
$\|\mathrm{m}^{imb}\| > 0.2$	2.3±1.6	3.5±2.0	5.8±2.4	2.3±1.6	3.3±1.7
$\Delta\phi_{\mu LJ-\mu\mu} > 2.8$	1.3±1.3	2.5±1.8	5.8±2.4	1.0±1.0	1.2±1.2
$q_{\mu LJ} = 0$	0.0±0.0	0.0±0.0	0.0±0.0	1.0±1.0	1.2±1.2

Table 7.4: Signal events remaining after each cut applied in the CR of the μLJ-μLJ channel. Events are generated according to the HAHM model and are normalized assuming a branching ratio $B(\mathrm{H} \to 2\gamma_d) = 0.05$.

Modelling del segnale canale muonico

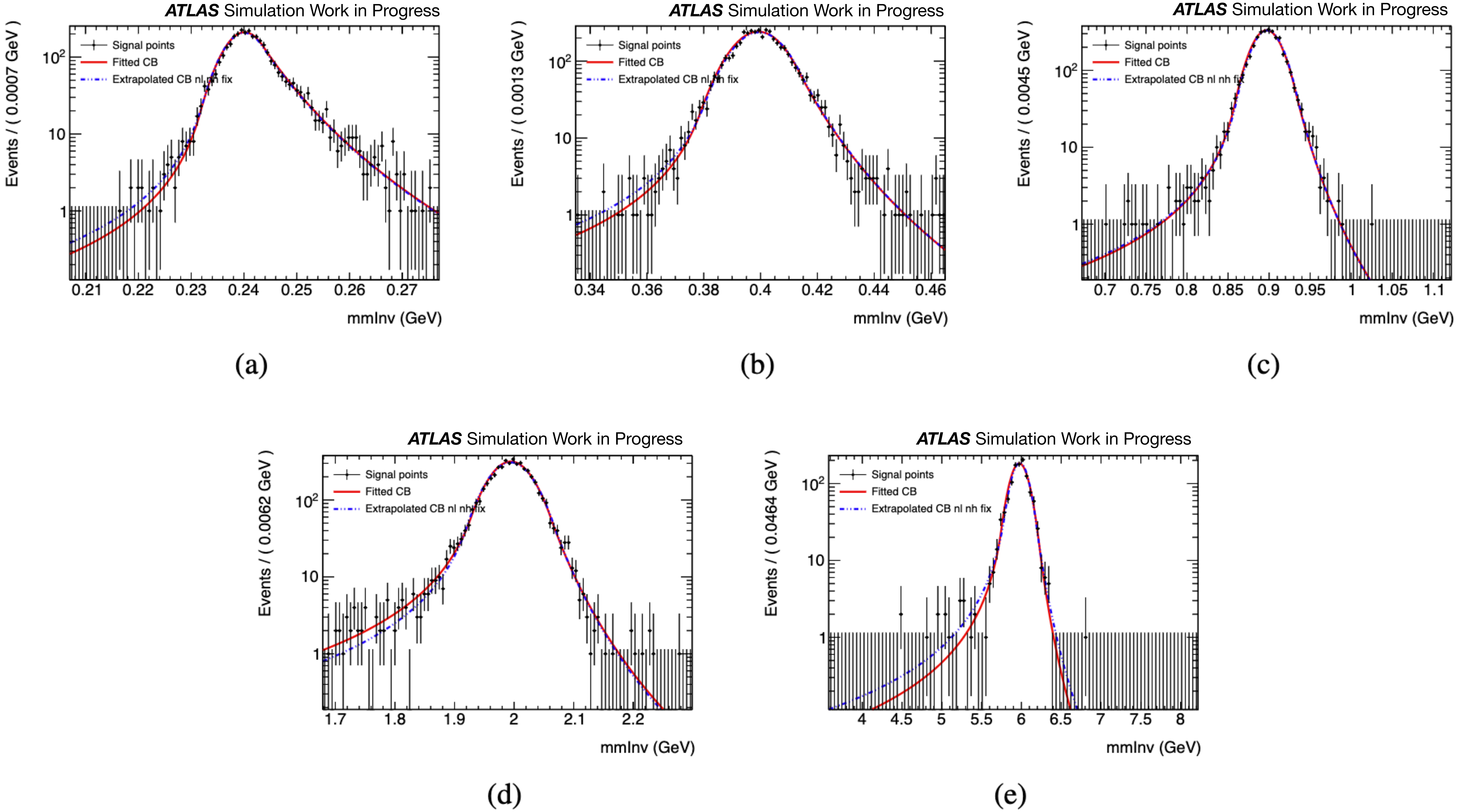

Figure 7.7: μLJ invariant mass distribution for the FRVZ model, in the μLJ-μLJ channel (dots), shown for different γ_d mass: (a) 240 MeV, (b) 400 MeV, (c) 900 MeV, (d) 2 GeV, (e) 6 GeV. The fitted pdf (red) is compared to the extrapolated one (blue).

Estrapolazione dei parametri: FRVZ canale muonico

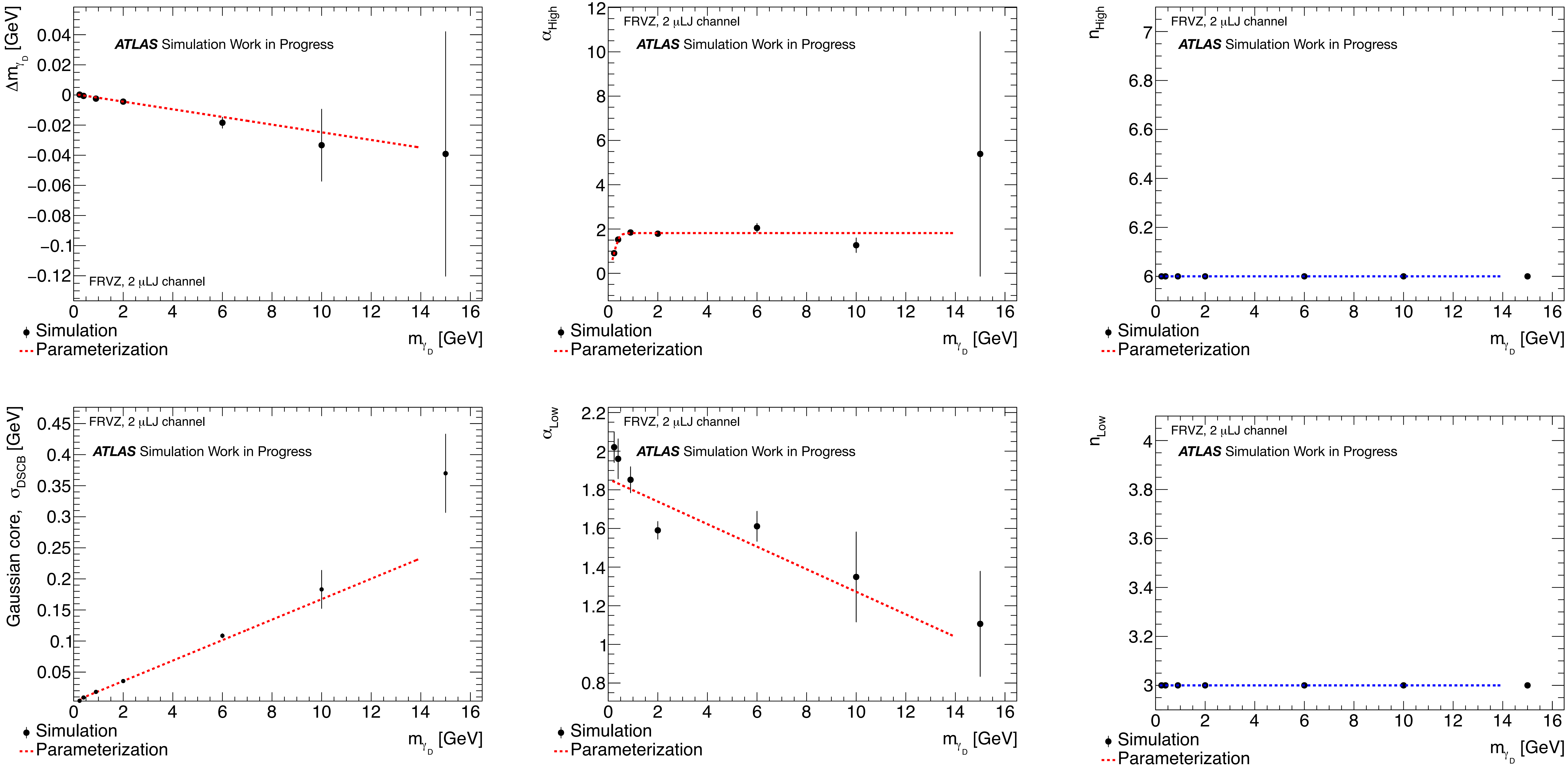

Sistematiche canale muonico

m_{γ_d} [GeV]	Muon triggers (%)	Muon isolation (%)	Momentum resolution (%)	Momentum scale (%)	Lumi (%)	PRW (%)	Total (%)
0.24	1.34	1.03	0.92	0.57	0.83	1.37	2.56
0.40	1.77	1.16	0.91	0.71	0.83	1.46	2.92
0.90	1.47	1.09	0.51	0.20	0.83	1.38	2.49
2	1.45	1.05	0.76	0.43	0.83	1.94	2.89
6	0.67	0.64	0.68	0.64	0.83	1.78	2.35
10	0.13	0.27	0.10	0.11	0.83	2.95	3.07
15	0.10	0.18	-	-	0.83	3.76	3.85

Table 6.23. Summary table of the impact of the experimental systematic uncertainties for the FRVZ signal samples in the μLJ–μLJ channel. Uncertainties below the per-mill level are not shown. PRW stands for the uncertainty associated to the PU reweighting.

m_{γ_d} [GeV]	Muon triggers (%)	Muon isolation (%)	Momentum resolution (%)	Momentum scale (%)	Lumi (%)	PRW (%)	Total (%)
0.40	0.62	0.51	0.59	0.35	0.83	0.91	1.60
2	0.58	0.51	0.39	0.17	0.83	0.94	1.51
10	0.17	0.25	0.28	0.23	0.83	0.60	1.11
15	0.1	0.14	-	-	0.83	0.41	0.91
25	0.1	0.14	-	-	0.83	1.55	1.75

Table 6.24. Summary table of the impact of the experimental systematic uncertainties for the HAHM signal samples in the μLJ–μLJ channel. Uncertainties below the per-mill level are not shown. PRW stands for the uncertainty associated to the PU reweighting.

Strategia di triggers canale elettronico

Periods	Single-electron triggers
2015	HLT_e24_lhmedium_L1EM20VH HLT_e60_lhmedium HLT_e120_lhloose
2016-2018	HLT_e26_lhtight_nod0_ivarloose HLT_e60_lhmedium_nod0 HLT_e140_lhloose_nod0

Table 6.2: Choice of lowest unprescaled single electron trigger list used in the eLJ–eLJ selection and the corresponding data-taking periods.

Periods	Di-electron triggers
2015	HLT_2e12_lhvloose_L12EM10VH
2016	HLT_2e17_lhvloose_nod0
2017 (only B5-B8)	HLT_2e24_lhvloose_nod0
2017 (except B5-B8)	HLT_2e17_lhvloose_nod0_L12EM15VHI
2018	HLT_e60_lhmedium_nod0

Table 6.3: Choice of lowest unprescaled di-electron trigger list used in the eLJ–eLJ selection and the corresponding data-taking periods. During the accidentally prescaled periods B5-B8 (runs 326834-328393 with an effective reduction of 0.6 fb-1), HLT_2e24_lhvloose_nod0 is used instead of HLT_2e17_lhvloose_nod0_L12EM15VHI.

Regione di segnale canale elettronico

ATLAS EXPERIMENT

FRVZ

m_{γ_d} [GeV]	0.017	0.03	0.06	0.1	0.24	0.4	0.9	2	6
2 eLJs	1900±22	1500±20	1100±17	830±14	210±7	54±4	8.5±1.4	1.2±0.5	7.9±1.3
Trigger Matched	1700±20	1300±18	960±15	730±13	200±7	53±4	8.5±1.4	1.2±0.5	7.5±1.2
Leading track $p_T > 5$ GeV	1600±20	1300±18	940±15	710±13	200±7	53±4	8.1±1.4	0.9±0.4	7.2±1.2
eLJ $\eta < 1.5$	1100±16	820±14	610±12	420±10	130±6	36.0±2.9	5.6±1.1	0.38±0.27	4.8±1.0
$\Delta\Phi(eLJ, eLJ) > 2$	720±13	550±12	410±10	300±9	72±4	17±2	3.2±0.9	/	4.3±1.0
Z mass veto	580±12	450±11	330±9	250±8	57±4	11.0±1.6	2.4±0.8	/	2.5±0.7
$q_{eLJ} = 0$	580±12	450±11	330±9	250±8	57±4	11.0±1.6	2.4±0.8	/	2.5±0.7
$m_{eLJ} > 20$ MeV	200±6.9	290±8.6	310±8.9	240±7.7	57±3.7	11.0±1.6	2.2±0.72	/	/
$\|m^{imb}\| < 0.8$	200±6.9	290±8.6	310±8.9	240±7.7	57±3.7	11.0±1.6	2.0±0.68	/	/

HAHM

m_{γ_d} [GeV]	0.017	0.1	0.4	2	10	15	25
2 eLJs	8400±46	3300±29	470±11	8.5 ±1.4	230 ±7.5	48 ±3.4	12 ±1.8
Trigger Matched	8300±46	3200±28	470±11	8.5 ±1.4	230 ±7.4	46 ±3.3	12 ±1.7
Leading track $p_T > 5$ GeV	8200±46	3200±28	460±11	8.2 ±1.4	220 ±7.4	44 ±3.2	11 ±1.7
eLJ $\eta < 1.5$	5500±37	1700 21	280±8.5	5.9 ±1.1	140 ±5.7	20 ±2.1	4.6 ±1.2
$\Delta\Phi(eLJ, eLJ) > 2$	4400±33	1300±18	180±6.8	2.1 ±0.69	130 ±5.6	4.8 ±1	0.68 ±0.39
Z mass veto	4200±32	1200±17	170±6.6	2 ±0.69	120 ±5.5	2.5 ±0.7	0.22 ±0.22
$q_{eLJ} = 0$	4200±32	1200±17	170±6.6	2 ±0.69	120 ±5.5	2.3 ±0.69	/
$m_{eLJ} > 20$ MeV	1800±21	1100±117	170±6.6	2 ±0.69	120 ±5.5	2.3 ±0.69	/
$\|m^{imb}\| < 0.8$	1800 ±21	1100±117	170±6.6	2 ±0.69	120 ±5.2	0.33 ±0.24	/

ABCD canale elettronico

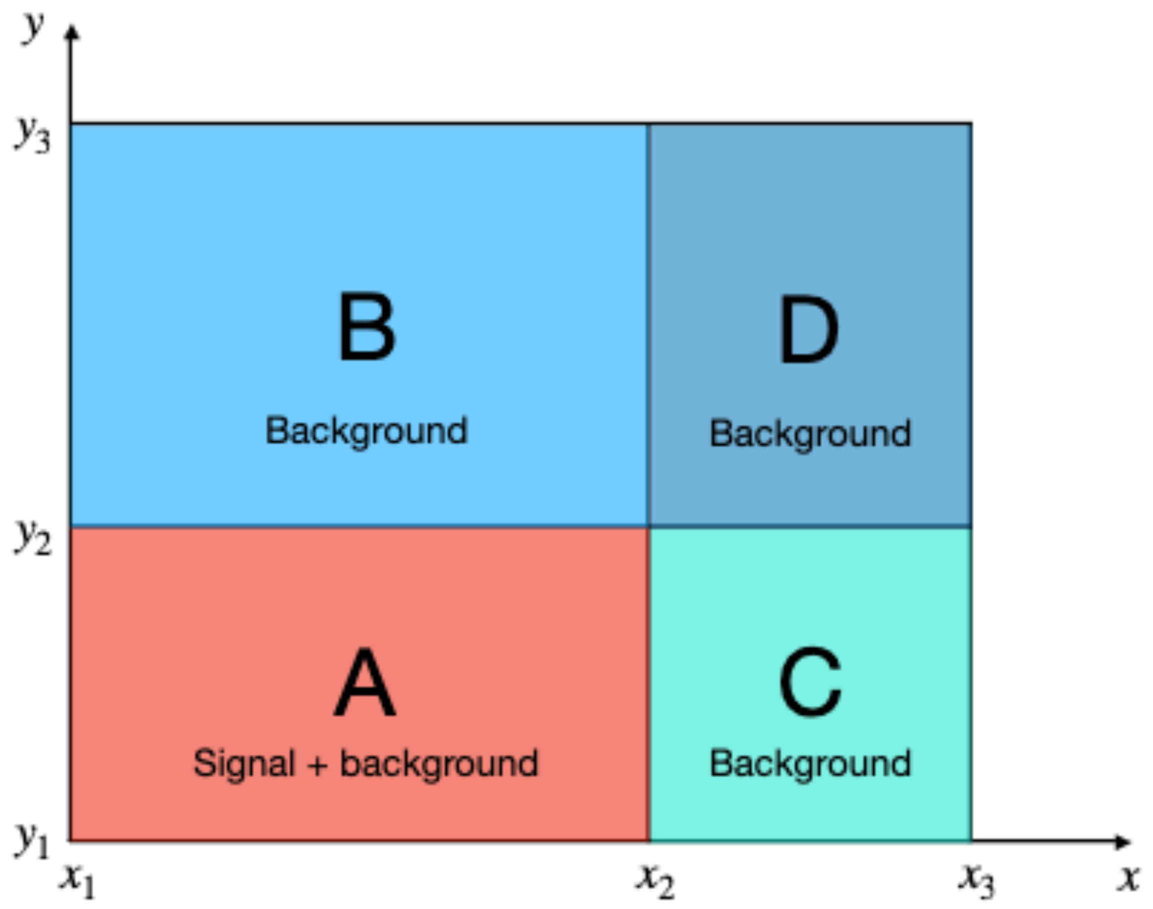

Requirement / Region	A (SR)	B	C	D
Lead e$LJ|cos(\theta_h)|$	< 0.8	< 0.8	> 0.8	> 0.8
Far eLJ R_ϕ	< 0.96	> 0.96	< 0.96	> 0.96

Region	FRVZ Signal samples								Run-2 data
	γ_d mass [GeV]	0.017	0.03	0.06	0.1	0.24	2.0	6.0	
A (SR)		17.31±1.45	12.91±1.30	8.86±1.03	4.75±0.74	2.73±0.57			
B		25.08±1.75	21.29±1.64	16.13±1.39	10.27±1.10	2.62±0.55			140
C		3.03±0.59	2.14±0.58	2.02±0.56	1.12±0.34	0±0			983
D		155.54±4.34	116.41±3.79	86.84±3.31	47.73±2.35	17.23±1.43			427
A (exp.)									322 ± 33

Table 7.13: ABCD yields in FRVZ signal and data driven estimate for background in the eLJ–eLJ channel. The signal assumes a $H \to 2\gamma_d + X$ BR of 0.5%. Uncertainties on the signal are statistical only, while the uncertainty on the number of expected events in region A is obtained from the propagation of the statistical uncertainty on regions B, C and D. Numbers are rounded following the PDG guidelines.

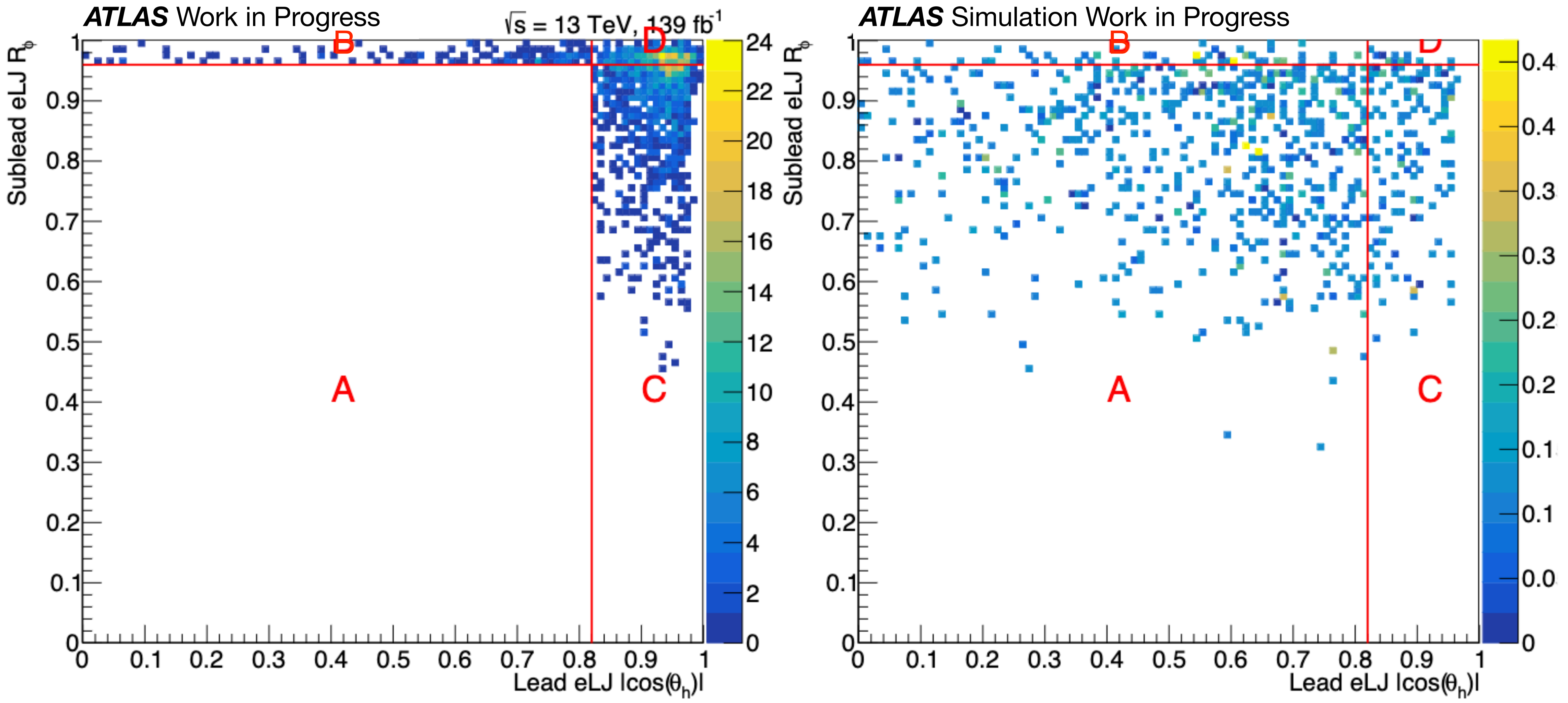

(a) (b)

Figure 7.20: ABCD plane lead p_T^{imb} and far R_ϕ for full Run 2 data and FRVZ benchmark signal sample with $m_{\gamma_d} = 0.1$ GeV.

	γ_d mass [GeV]	0.017	0.03	0.06	0.1	0.24	2.0	6.0
$S/\sqrt{B}$	A (SR)	9.03	13.98	14.80	10.93	2.34	0.29	0.07
	B	2.53	3.75	3.45	2.80	0.96	0.16	0.03
	C	1.00	1.27	1.90	1.58	0.32	0.12	0.01
	D	0.27	0.44	0.31	0.39	0.04	0.04	0.01

Table 7.14: $S/\sqrt{B}$ for regions A, B, C and D in the eLJ-eLJ channel, as predicted by the FRVZ signal model. Region A takes into account the expected number of background events, obtained with the ABCD method.

Sistematiche canale elettronico

ATLAS EXPERIMENT

m_{γ_d} [GeV]	Electron triggers (%)	Electron isolation (%)	Electron ID (%)	Electron reconstruction (%)	Energy resolution (%)	Energy scale (%)	Lumi (%)	PRW (%)	Total (%)
0.017	0.2	0.3	2.15	1.26	0.65	0.4	0.83	0.8	2.7
0.03	0.2	0.3	2.26	1.29	0.66	0.3	0.83	2.2	3.5
0.06	0.2	0.3	2.31	1.29	1.11	0.8	0.83	3.9	4.9
0.10	0.2	0.3	2.21	1.27	0.69	0.7	0.83	3.6	4.5
0.24	0.2	0.3	2.19	1.33	0.7	0.1	0.83	8.6	9.0

Table 6.25. Summary table of the impact of the experimental systematic uncertainties for the FRVZ signal samples in the eLJ–eLJ channel. Uncertainties below the per-mill level are not shown. PRW stands for the uncertainty associated to the PU reweighting.

m_{γ_d} [GeV]	Electron triggers (%)	Electron isolation (%)	Electron ID (%)	Electron reconstruction (%)	Energy resolution (%)	Energy scale (%)	Lumi (%)	PRW (%)	Total (%)
0.017	-	0.1	0.69	1.11	0.20	0.16	0.83	1.0	1.7
0.1	-	0.1	0.83	1.08	0.27	0.3	0.83	1.0	1.7
0.4	-	0.1	0.70	1.06	0.50	0.7	0.83	1.0	1.8
2	-	-	0.46	1.15	-	-	0.83	7.4	7.5

Table 6.26. Summary table of the impact of the experimental systematic uncertainties for the HAHM signal samples in the eLJ–eLJ channel. Uncertainties below the per-mill level are not shown. PRW stands for the uncertainty associated to the PU reweighting.